TÉCNICO LISBOA

An Analytical Approach to Dispersion-Induced Limitations on the Bit-Rate of Fiber-Optic Communication Systems

Pedro Miguel Monteiro Maia

Thesis to obtain the Master of Science Degree in

Electrical and Computer Engineering

Supervisors: Prof. Doctor Carlos Paiva
Prof. Doctor Filipa Isabel Rodrigues Prudêncio

Examination Committee

Chairperson: Prof. Doctor José Eduardo Charters Ribeiro da Cunha Sanguino

Supervisor: Prof. Doctor Carlos Manuel dos Reis Paiva

Member of the Committee: Prof. Doctor João Carlos Roquete Fidalgo Canto

December 2019

Declaration

I declare that this document is an original work of my own authorship and that it fulfills all the requirements of the Code of Conduct and Good Practices of the Universidade de Lisboa.

Declaração

Declaro que o presente documento é um trabalho original da minha autoria e que cumpre todos os requisitos do Código de Conduta e Boas Práticas da Universidade de Lisboa.

Abstract

The main goal of this dissertation is to optimize the bit-rate of single mode optical fibers. Denoting by B_0 the maximum value for the bit-rate and by L the fiber length, closed-form analytical expressions are derived both for the maximum bit-rate and the product of the square of the bit-rate with the length, $B_0^2 L$, to get a figure of merit for the performance of a single-channel fiber-optic communication system (considering only dispersion limitations).

Both unchirped hyperbolic secant pulses and chirped Gaussian (and super-Gaussian) pulses were considered throughout. Apart from these types of pulses, closed-form analytical expressions for pulse width evolution along the fiber involve rather cumbersome calculations. On the other hand, losses will be disregarded: they can be easily tackled, whence its effect will not be addressed herein. So, dispersion is the only problem under analysis as it imposes severe limitations. Of course, other limitations can affect this figure of merit; however, the focus will be the effects of both group-velocity dispersion and higher-order dispersion.

The main original contribution of this dissertation is to find the optimum values for the input and output pulse widths (χ_0^{opt} and χ_1^{opt} respectively) for any given value of the chirp parameter. Namely, it is shown that exists a critical value of the chirp parameter for which $\chi_0 = \chi_1$ so that, for any given point along the optical fiber, $\xi = z/L$, one has $\chi(\xi) \leq \chi_0$ for $0 \leq \xi \leq 1$.

Keywords

Fiber-Optic Communication Systems; Chirped Gaussian Pulses; Group-Velocity Dispersion; Higher-Order Dispersion; Bit-rate; Analytical Approach.

Resumo

O objetivo principal desta dissertação é otimizar o débito binário em fibras óticas monomodo. Sendo B_0 o valor máximo do débito binário e L o comprimento da fibra, são deduzidas expressões analíticas para o débito binário máximo e para o produto do débito binário ao quadrado com o comprimento, $B_0^2 L$, de forma a obter uma figura de mérito para o desempenho de um sistema de comunicação por fibra ótica de um só canal (considerando apenas limitações devido à dispersão).

Tanto impulsos secantes hiperbólicos sem trinado como impulsos Gaussianos (e super-Gaussianos) com trinado foram considerados ao longo do trabalho. Tirando estes impulsos, expressões analíticas para a evolução da largura dos impulsos ao longo da fibra envolvem cálculos bastante complicados. As perdas, por outro lado, serão desprezadas uma vez que podem facilmente ser eliminadas, logo os seus efeitos não serão tidos em conta. Sendo assim, a dispersão será o único problema a ser analisado visto que é o que impõe maiores limitações. Obviamente, que outras limitações podem afetar a figura de mérito; no entanto, o foco será nos efeitos da dispersão de velocidade de grupo e da dispersão de ordem superior.

A principal contribuição original desta dissertação é encontrar os valores ótimos da largura dos impulsos à entrada e à saída (χ_0^{opt} e χ_1^{opt}, respetivamente) para qualquer valor de trinado. Nomeadamente, é demonstrado que existe um valor de trinado crítico para o qual $\chi_0 = \chi_1$ fazendo com que, para qualquer ponto da fibra ótica, $\xi = z/L$, se verifique $\chi(\xi) \leq \chi_0$, para $0 \leq \xi \leq 1$.

Palavras-Chave

Sistemas de Comunicação por Fibra Ótica; Impulsos Gaussianos com Trinado; Dispersão de Velocidade de Grupo; Dispersão de Ordem Maior; Débito Binário; Abordagem Analítica.

Table of Contents

Abstract ..... **v**

Resumo ..... **vii**

List of Figures ..... **xi**

List of Acronyms ..... **xv**

List of Symbols ..... **xvii**

1. Introduction **1**

1.1 Historical Background 1

1.2 Motivation 3

1.3 Objectives 3

1.4 Structure 4

1.5 Original Contributions 4

2. Theoretical Background **5**

2.1 Pulse Propagation 5

2.2 Chirped Gaussian Pulses 10

2.3 Combined Effects of GVD and Chirp Parameter 14

2.4 Dispersion Compensation 15

3. Hyperbolic Secant Pulses **17**

4. Chirped Gaussian Pulses **21**

4.1 Unchirped Gaussian Pulses 23

4.2 Anomalous Dispersion Regime 26

4.3 Normal Dispersion Regime 28

4.4 Bit-Rate for Chirped Gaussian Pulses 31

5. Comparison between Hyperbolic Secant Pulses and Gaussian Pulses **33**

6. Chirped Gaussian Pulses: Effect of Higher-Order Dispersion **39**

6.1 Unchirped Gaussian Pulses 45

6.2 Critical Value of the Chirp Parameter 46

6.3 Normal Dispersion Regime 47

6.4 Anomalous Dispersion Regime 50

6.5 Maximum Bit-Rate Value 57

7. Super-Gaussian Pulses **61**

8. WDM Systems **75**

9. Conclusions and Future Work **79**

A. Modal Analysis **81**

A.1 Closed-Form Analytical Expressions 81

A.2 Numerical Results 84

B. Chirped Gaussian Pulses ($\beta 2 = 0, \beta 3 \neq 0$) **87**

B.1 Maximum Bit-Rate Value 89

References **93**

List of Figures

Figure 1.1 Optical Telegraph Network. ……..1

Figure 1.2 International Morse Code. ……2

Figure 3.1 Variation of the normalized output pulse width χ_1 with the normalized input pulse χ_0 for an unchirped Hyperbolic Secant pulse. ……18

Figure 3.2 Behavior of the pulse width along an optical fiber for an unchirped Hyperbolic Secant pulse with $\beta_2 \neq 0$ and $\beta_3 = 0$, being $\mu^{opt} = \mu(\chi_0^{opt}, \xi) = \chi/\chi_0^{opt} = 1 + \xi^2$……19

Figure 3.3 Bit-rate squared product with the length of a given optical fiber for unchirped hyperbolic secant pulses as an instrument to measure the performance of a fiber-optic communication system……..20

Figure 4.1 Variation of the normalized output pulse width χ_1 with the normalized input pulse χ_0 for an unchirped Gaussian pulse……23

Figure 4.2 Behavior of the pulse width along an optical fiber for an unchirped Gaussian pulse with $\beta_2 \neq 0$ and $\beta_3 = 0$, being $\mu^{opt} = \mu(\chi_0^{opt}, \xi) = \chi/\chi_0^{opt} = 1 + \xi^2$……..24

Figure 4.3 Bit-rate squared product with the length of a given optical fiber for unchirped Gaussian pulses as an instrument to measure the performance of a fiber-optic communication system……..25

Figure 4.4 Variation of the normalized output pulse width χ_1 with the normalized input pulse χ_0 for a chirped Gaussian pulse on the anomalous dispersion regime ($\beta_2 < 0$) and for a chosen value of $C = -2$……...26

Figure 4.5 Variation of the normalized output pulse width χ_1 with the normalized input pulse χ_0 for a chirped Gaussian pulse on the anomalous dispersion regime ($\beta_2 < 0$) and for a chosen value of $C = 2$……..27

Figure 4.6 Variation of χ_0^{opt} and χ_1^{opt} with the chirp parameter C, when $\beta_2 < 0$……..28

Figure 4.7 Variation of the normalized output pulse width χ_1 with the normalized input pulse χ_0 for a chirped Gaussian pulse on the normal dispersion regime ($\beta_2 > 0$) and for a chosen value of $C = -2$……29

Figure 4.8 Variation of the normalized output pulse width χ_1 with the normalized input pulse χ_0 for a chirped Gaussian pulse on the normal dispersion regime ($\beta_2 > 0$) and for a chosen value of $C = 2$……...29

Figure 4.9 Variation of χ_0^{opt} and χ_1^{opt} with the chirp parameter C, when $\beta_2 > 0$……30

Figure 4.10 Bit-rate squared product with the length of a given optical fiber for chirped gaussian pulses as an instrument to measure the performance of a fiber-optic communication system……..32

Figure 5.1 Variation of the normalized output pulse width χ_1 with the normalized input pulse χ_0 for an unchirped Hyperbolic Secant pulse (red curve) and for an unchirped Gaussian pulse (blue curve), being $\beta_2 \neq 0$ and $\beta_3 = 0$……35

Figure 5.2 Behavior of the pulse width along the optical fiber for an unchirped Gaussian pulse and for an unchirped Hyperbolic Secant pulse with $\beta_2 \neq 0$ and $\beta_3 = 0$, being $\mu^{opt} = \mu(\chi_0^{opt}, \xi) = 1 + \xi^2$……35

Figure 5.3 Bit-rate squared product with the length of a given optical fiber ($B_0^2 L$) for unchirped Gaussian pulses as an instrument to measure the performance of a fiber-optic communication system……37

Figure 5.4 Bit-rate squared product with the length of a given optical fiber ($B_0^2 L$) for unchirped hyperbolic secant pulses as an instrument to measure the performance of a fiber-optic communication system……37

Figure 6.1 Variation of the adimensional coefficient a with the group-velocity dispersion parameter β_2 for an optical fiber with $L = 40\ km$ and a higher-order dispersion parameter $\beta_3 = 0.1\ ps^3/km$……40

Figure 6.2 Graphical solution of the cubic equation for $C = -6$ and $a = 1$……42

Figure 6.3 Graphical solution of the cubic equation for $C = -6$ and $a = 4$……42

Figure 6.4 Variation of χ_0^{opt} with the chirp parameter C for different fixed values of a……...43

Figure 6.5 Variation of χ_0^{opt} with the adimensional coefficient a for a fixed value of the chirp parameter, $C = -6$……..44

Figure 6.6 Variation of the normalized output pulse width χ_1 with the normalized input pulse χ_0 for an unchirped Gaussian pulse with $a = 1$……45

Figure 6.7 Variation of the chirp critical value, C_{cr} with the adimensional coefficient, a……46

Figure 6.8 Variation of the normalized output pulse width χ_1 with the normalized input pulse χ_0 for a chirped Gaussian pulse on the normal dispersion regime ($\beta_2 > 0$), for a chosen value of $C = -2$ and for a chosen value of $a = 1$……47

Figure 6.9 Variation of the normalized output pulse width χ_1 with the normalized input pulse χ_0 for a chirped Gaussian pulse on the normal dispersion regime ($\beta_2 > 0$), for a chosen value of $C = 2$ and for a chosen value of $a = 1$……48

Figure 6.10 Variation of χ_0^{opt} and χ_1^{opt} with the chirp parameter C, when $\beta_2 > 0$ and for a fixed value of $a = 1$……...48

Figure 6.11 Optimum pulse width behavior of a chirped Gaussian pulse in the normal dispersion regime for $C = 4$, $C = -4$ and $C = C_{cr}$ with a fixed value of $a = 1$……49

Figure 6.12 Variation of the normalized output pulse width χ_1 with the normalized input pulse χ_0 for a chirped Gaussian pulse on the anomalous dispersion regime ($\beta_2 < 0$), for a chosen value of $C = -2$ and for a chosen value of $a = 1$……50

Figure 6.13 Variation of the normalized output pulse width χ_1 with the normalized input pulse χ_0 for a chirped Gaussian pulse on the anomalous dispersion regime ($\beta_2 < 0$), for a chosen value of $C = 2$ and for a chosen value of $a = 1$……50

Figure 6.14 Variation of χ_0^{opt} and χ_1^{opt} with the chirp parameter C, when $\beta_2 < 0$ and for a fixed value of $a = 1$……...51

Figure 6.15 Optimum pulse width behavior of a chirped Gaussian pulse in the anomalous dispersion regime for $C = -4$, $C = 4$ and $C = C_{cr}$ with a fixed value of $a = 1$……52

Figure 6.16 Variation of χ_1^{opt} with χ_0^{opt} for $a = 0$……53

Figure 6.17 Variation of χ_1^{opt} with χ_0^{opt} for $a = 0.05$……53

Figure 6.18 Variation of χ_1^{opt} with χ_0^{opt} for $a = 0.1$……..54

Figure 6.19 Variation of χ_1^{opt} with χ_0^{opt} for $a = 0.5$……..54

Figure 6.20 Variation of χ_1^{opt} with χ_0^{opt} for $a = 1$……..55

Figure 6.21 Optimum pulse width behavior for $C = C_{cr}$ across the entire journey inside an optical fiber for different a values such as $a = 0$, $a = 1$, $a = 2$ and $a = 5$……56

Figure 6.22 Variation of the bit-rate B_0 with the adimensional coefficient a for $\beta_2 = -1\ ps^2/km$ and for a fiber length $L = 40\ km$……58

Figure 6.23 Variation of the figure of merit F with the adimensional coefficient a……58

Figure 6.24 Bit-rate percentage loss introduced by β_3 on the channel and corresponding first approximation……..59

Figure 6.25 Approximation error between the expression that gives the bit-rate loss percentage and the first approximation which is a linear curve whose expression is defined by $10a$….60

Figure 7.1 Super-Gaussian pulse shape for $m = 1$, $m = 3$ and $m = 10$……..61

Figure 7.2 Variation of the normalized output pulse width χ_1 with the normalized input pulse χ_0 for a super-Gaussian pulse for a chosen value of $|C| = 2$ and for $m = 1$, $m = 2$ and $m = 3$, where $\beta_2 C > 0$……64

Figure 7.3 Variation of the normalized output pulse width χ_1 with the normalized input pulse χ_0 for a super-Gaussian pulse for a chosen value of $|C| = 2$ and for $m = 1$, $m = 2$ and $m = 3$, where $\beta_2 C < 0$……64

Figure 7.4 Optimum pulse width behavior of a super-Gaussian pulse when $\beta_2 < 0$ for $C = -4$, $C = 4$ and $C = C_{cr}$ with a fixed value of $m = 1$……65

Figure 7.5 Optimum pulse width behavior of a super-Gaussian pulse when $\beta_2 < 0$ for $C = -4$, $C = 4$ and $C = C_{cr}$ with a fixed value of $m = 3$……66

Figure 7.6 Optimum pulse width behavior of a super-Gaussian pulse when $\beta_2 < 0$ for $C = -4$, $C = 4$ and $C = C_{cr}$ with a fixed value of $m = 5$……66

Figure 7.7 Variation of χ_0^{opt} and χ_1^{opt} with the chirp parameter C, when $\beta_2 < 0$ for $m = 1$……...67

Figure 7.8 Variation of χ_0^{opt} and χ_1^{opt} with the chirp parameter C, when $\beta_2 < 0$ for $m = 3$……...68

Figure 7.9 Variation of χ_0^{opt} and χ_1^{opt} with the chirp parameter C, when $\beta_2 < 0$ for $m = 5$……...68

Figure 7.10 Variation of χ_0^{opt} and χ_1^{opt} with the chirp parameter C, when $\beta_2 < 0$ for $m = 7$……...69

Figure 7.11 Variation of the bit-rate B_0 with parameter m for $\beta_2 = -1\ ps^2/km$ and $\beta_3 = 0$ for an optical fiber length $L = 40\ km$……71

Figure 7.12 Variation of the figure of merit F with the parameter m……71

Figure 7.13 Bit-rate squared product with the length of a given optical fiber for super-Gaussian pulses with $m = 1$, as an instrument to measure the performance of a fiber-optic communication system……..72

Figure 7.14 Bit-rate squared product with the length of a given optical fiber for super-Gaussian pulses with $m = 3$, as an instrument to measure the performance of a fiber-optic communication system……..72

Figure 7.15 Bit-rate squared product with the length of a given optical fiber for super-Gaussian pulses with $m = 10$, as an instrument to measure the performance of a fiber-optic communication system……73

Figure A.1 Dielectric contrast as a function of the core radius for a fixed refractive index core value, being $n_1 = 1.45$ and for fixed cutoff wavelength values of $\lambda_c = 1.4\ \mu m$, $\lambda_c = 1.2\ \mu m$, $\lambda_c = 0.7\ \mu m$……84

Figure A.2 Maximum core radius for wavelengths inside the interval $\lambda = [1200; 1700]\ nm$. The refractive core index value is $n_1 = 1.45$, the normalized cutoff frequency is $v_c = 2.4048$ and $\Delta = 0.5\%$.....84

Figure A.3 Propagation modes for $v = 5$……...85

Figure A.4 Radial distribution of the intensity profile for the propagation modes when $v = 5$…..85

Figure A.5 Propagation modes for $v \leq 10$……...86

Figure B.1 Variation of the normalized output pulse width ϱ with the normalized input pulse r for a chirped Gaussian pulse for $\beta_2 = 0$ and $\beta_3 \neq 0$……87

Figure B.2 Behavior of the pulse width along an optical fiber for $\beta_3 \neq 0$ and $\beta_2 = 0$……..88

Figure B.3 Variation of the bit-rate B_0 with the chirp parameter C for $\beta_3 = 1\ ps^3/km$ and $\beta_2 = 0$ for an optical fiber with length $L = 40\ km$……..89

Figure B.4 Variation of the figure of merit F' with the parameter C……..90

Figure B.5 Bit-rate cubic product with the length of a given optical fiber for chirped Gaussian pulses with $C = 0$, as an instrument to measure the performance of a fiber-optic communication system considering $\beta_2 = 0$……...90

Figure B.6 Bit-rate cubic product with the length of a given optical fiber for chirped Gaussian pulses with $|C| = 2$, as an instrument to measure the performance of a fiber-optic communication system considering $\beta_2 = 0$……91

List of Acronyms

BL	Bit-Rate Distance Product
DCF	Dispersion Compensation Fiber
GVD	Group-Velocity Dispersion
HOD	Higher-Order Dispersion
LP	Linearly Polarized Propagation Modes
RMS	Root Mean Square
WDM	Wavelength-Division Multiplexing

List of Symbols

β_0	Zero order dispersion term
β_1	First order dispersion term
β_2	Second order dispersion term
β_3	Third order dispersion term
β_m	M-order dispersion term
γ	Pulse width behavior ($\beta_2 = 0$)
$\Gamma(m)$	Gamma function
Δ	Dielectric constant
η	Broadening factor
θ	Frequency phase
λ	Wavelength
μ	Pulse width behavior
μ^{opt}	Optimum pulse width behavior
ξ	Normalized distance
σ	RMS pulse width
σ_0	RMS input pulse width
σ_1	RMS output pulse width
σ_{max}	Maximum RMS pulse width
τ_g	Group-delay
ϕ	Time phase
χ	Normalized pulse width
χ_{max}	Maximum normalized pulse width
χ^{opt}	Optimum normalized pulse width
χ_0	Normalized input pulse width
χ_0^{opt}	Optimum normalized input pulse width
χ_1	Normalized output pulse width
χ_1^{opt}	Optimum normalized output pulse width
Ψ	Electromagnetic field
ω	Angular frequency
Ω	Frequency shift
r	Normalized input pulse width ($\beta_2 = 0$)
r_{opt}	Optimum normalized input pulse width ($\beta_2 = 0$)

ϱ	Normalized output pulse width ($\beta_2 = 0$)
ϱ_{opt}	Optimum normalized output pulse width ($\beta_2 = 0$)
B	Bit-rate
B_0	Maximum bit-rate
C	Chirp parameter
C_{cr}	Critical chirp parameter
C_0	Chirp parameter where the derivative of χ_1^{opt} is zero
D	Dispersion coefficient
E	Pulse energy
F	Figure of merit
F'	Figure of merit ($\beta_2 = 0$)
$J_\ell(x)$	Bessel function
$K_\ell(x)$	Modified Bessel function
L	Length of the optical fiber
m	Degree of edge sharpness
n	Refractive index
n_1	Core refractive index
n_2	Cladding refractive index
P	Normalized pulse width ($\beta_2 = 0$)
P_{opt}	Optimum normalized pulse width ($\beta_2 = 0$)
S	Dispersion slope
T_b	Allocated time-slot
T_0	Input pulse width
T_1	Output pulse width
v	Normalized frequency
v_c	Normalized cutoff frequency
v_g	Group-velocity

1. Introduction

1.1 Historical Background

The use of light for communication purposes dates back to antiquity if we interpret optical communications in a broad sense. Most civilizations have used messengers, pigeons, mirrors, flags, fire beacons, or smoke signals to convey a single piece of information (such as victory in a war). However, actual written records suggest the development of a more complex device of what we know today as the telegraph, due to Aeneas (350 BC) and Polybius (150 BC), being the latter system was able to transmit more sophisticated messages than a simple alarm signal, by encoding the 24 letters of the Greek alphabet into signals using a torch telegraph. Unfortunately, this knowledge was lost for nearly twenty centuries, meaning the communication until the end of the eighteenth century was made through signaling lamps, flags, and other semaphore devices. Only in 1792, Claude Chappe came with the idea of an "optical telegraph", allowing to transmit mechanically coded messages over long distances (approximately 100 km) using intermediate relay stations, acting as regenerators or repeaters in the modern-day language. The first line of this device was put into use in July 1794. The line had about 230 km and its purpose was to connect Paris and Lille. Claude Chappe telegraph was in use for 61 years. It has been the first and largest network using optical telegraph, in continuous operation over more than sixty years. The opto-mechanical communication systems of the nineteenth century were inherently slow. In modern-day terminology, the effective bit rate of such systems was less than 1 bit per second (B < 1 b/s). Low velocity transmission of information and the vulnerability of these systems to weather conditions and to human error motivated the search for other alternatives. Nevertheless, optical telegraphs had proven that simple signs could be used to send complex messages, therefore paving the way for electrical communication means.

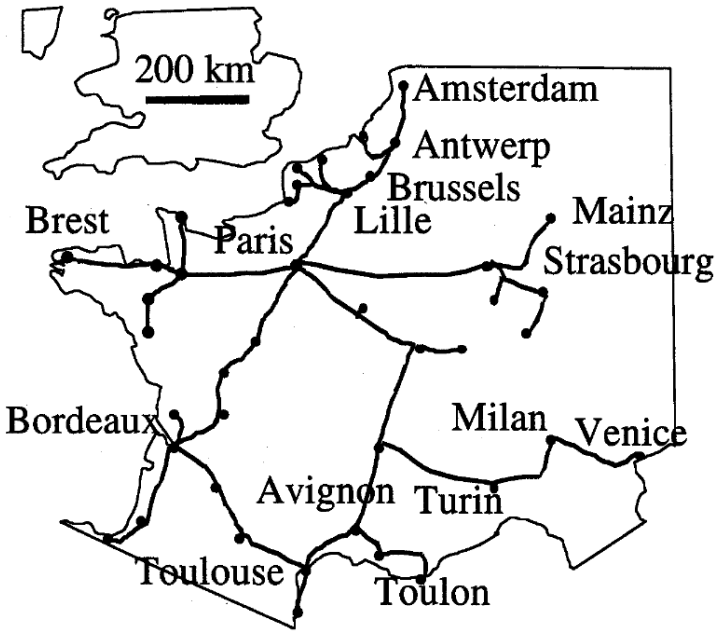

Figure 1.1 – Optical Telegraph Network

In the 1830s the electrical telegraph, or more commonly just telegraph, superseded optical semaphore telegraph. This means that the use of light was replaced by electricity and therefore began the era of electrical communications. Electrical telegraph networks permitted people and commerce to transmit messages across both continents and oceans almost instantly, with widespread social and economic impacts. With this technology, the bit rate B could be increased to approximately 10 b/s by the use of new coding techniques, such as the Morse code. Morse code is a method of transmitting text information as a series of on-off tones, lights, or clicks that can be directly understood by a skilled listener or observer without special

equipment and it was created by Samuel Morse and Alfred Vail originally to be used with the telegraph. Each Morse code symbol represents either a text character (letter or numeral) and is represented by a unique sequence of dots and dashes. The dot duration is the basic unit of time measurement in code transmission. The duration of a dash is three times the duration of a dot. Each dot or dash is followed by a short silence, equal to the dot duration. The letters of a word are separated by a space equal to three dots (one dash), and the words are separated by a space equal to seven dots. Morse code is the earliest type of digital communications, as the code is made solely from Ones and Zeros (ons and offs) and it was the only way to rapidly communicate over very long distances. In an emergency, Morse code can be sent by improvised methods that can be easily "keyed" on and off, making it one of the simplest and most versatile methods of telecommunication. The most famous "word" in Morse code is SOS and it was chosen as the international Morse code distress signal, because the three dots for S and the three dashes for O (…---…) make a clear and distinct signal.

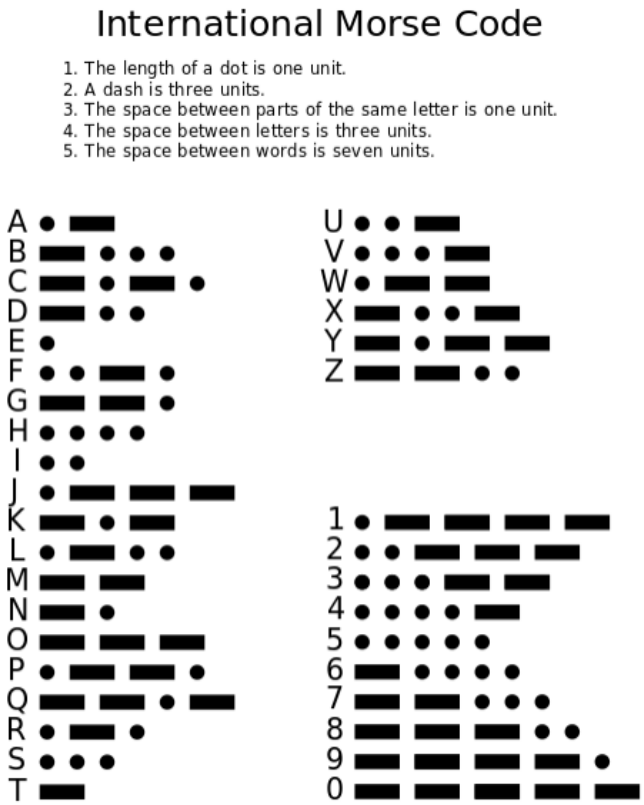

Figure 1.2 – International Morse Code

In 1842, Jean Daniel-Colladon accidentally discovered that light could be guided with water. Colladon was studying the fluid mechanics of jets of water that were emitted horizontally in the air from a nozzle in a container. However, in performing demonstrations of these jets in a lecture hall, Colladon became irritated that his audience could not clearly see what was happening to the falling water. He then hit upon the idea of directing a beam of light into the stream from the other side of the tank, using the light in the stream to illuminate its behavior. It was at that point that the phenomenon of total internal reflection was experienced for the first time, a discovery that would form the basis for a revolution in communications. In 1870, John Tyndall demonstrated that light used internal reflection to follow a specific path using a jet of water that flowed from one container to another and a beam of light. The invention of the telephone in 1876 brought a major change inasmuch as electric signals were transmitted in analog form through a continuously varying current. Analog electrical techniques were to dominate communication systems for a century or so. The development of worldwide telephone networks during the twentieth century led to many advances in the design of electrical communication systems. The use of coaxial cables in place of wire pairs increased system capacity considerably. The first coaxial-cable system, put into service in 1940, was a 3-MHz system capable of transmitting 300 voice channels or a single television channel. The bandwidth of such systems is limited by the frequency-dependent cable losses, which increase rapidly for frequencies beyond 10 MHz. This limitation led to the development of microwave communication systems in which an electromagnetic

carrier wave with frequencies in the range of 1-10 GHz is used to transmit the signal by using suitable modulation techniques. The first microwave system operating at the carrier frequency of 4 GHz was put into service in 1948. Since then, both coaxial and microwave systems have evolved considerably and are able to operate at bit rates of approximately 100 Mb/s. The most advanced coaxial system was put into service in 1975 and operated at a bit rate of 274 Mb/s. A severe drawback of such high-speed coaxial systems is their small repeater spacing (about 1 km), which makes the system relatively expensive to operate. Microwave communication systems generally allow for a larger repeater spacing, but their bit rate is also limited by the carrier frequency of such waves. A commonly used figure of merit for communication systems is the bit rate-distance product, BL, where B is the bit rate and L is the repeater spacing. It was realized during the second half of the twentieth century that an increase of several orders of magnitude in the BL product would be possible if optical waves were used as the carrier. However, neither a coherent optical source nor a suitable transmission medium was available during the 1950s. The invention of the laser and its demonstration in 1960 solved the first problem. At Hughes Research Laboratories, Theodore Maiman discovered that high gain pulsed oscillation could be achieved in synthetic ruby by optically pumping with a solid-state flash lamp. Attention was then focused on finding ways for using laser light for optical communications. Many ideas were advanced during the 1960s, the most noteworthy being the idea of light confinement using a sequence of gas lenses. It was suggested in 1966 that optical fibers might be the best choice, as they are capable of guiding the light in a manner similar to the guiding of the electrons in copper wires. The main problem was the high losses of optical fibers – fibers available during the 1960s had losses in excess of 1000 dB/km. A breakthrough occurred in 1970 when fiber losses could be reduced to below 20 dB/km in the wavelength near 1 μm. The simultaneous availability of compact optical sources and low-loss optical fibers led to a worldwide effort developing fiber-optic communication systems.

1.2 Motivation

A large demand for the development of fiber-optic communications systems started in the 1970s, since this solution had the potential to allow the transmission of information at high bit-rates and with a potentially low cost of implementation because the raw material that is used for producing optical fibers is silica, which can be easily found and extracted. Some other vantages in using optical fibers that were found during several researches along the years were that in the spectral region between 1,3 μm and 1,55 μm the attenuation was very low (between 0.5 dB/km and 0.2 dB/km), large frequency bandwidth, small size and weight, immunity to electromagnetic interferences, electrical isolation, reliability and ease of maintenance.

Nowadays, the bit-rate in an optical fiber can be up to 100 Gb/s depending on the transmission distance. However, the demand for even higher bit-rates never stops and to take a step forward in the speed with which digital information is sent along an optical fiber, the problem of dispersion-induced limitations must be overcomed if it is intended to progress technologically.

It will be crucial to tackle this issue, because every year more users are connected to the internet which requires more effort from the network to give an acceptable quality of experience to everyone connected since more information is requested by the users.

1.3 Objectives

The purpose of this dissertation is to understand how dispersion affects the bit rate on fiber-optic communication systems. It is known that exists a large demand for higher bit-rates, because in quantitative terms, data traffic is increasing every year. This means that it is more important than ever to be aware of dispersion limitations and to know how to deal with them. When travelling a fiber, pulses suffer dispersion and attenuation. Nevertheless, it will be assumed that there is no attenuation meaning that all the energy of the signals on the input of the fibers will be the same as in the output. However, the signals will broaden due to dispersion phenomena. This is a huge problem, since pulses will interfere with their neighbors causing a decrease in the quality of the information that is transmitted along the fibers. The occurrence of dispersion depends on many factors, being the most important ones the following: length of the fiber (L),

Group Velocity Dispersion - GVD (β_2), higher-order dispersion (β_3), input pulse width (T_0). The band of wavelengths to be considered in this study is the C band, which reference wavelength is: $\lambda_0 = 1550\, nm$.

To have a better understanding on how to tackle this issue, closed-form analytical expressions will be presented to have a qualitative perspective that will allow to analyze every situation that needs to be addressed. Numerical solutions will also be shown to verify the accuracy of the analytical approach. However, a numerical solution for itself only allows to see what happens in a specific situation being that the reason for developing closed-form analytical expressions that are going to give us the tools to address every case in hand.

1.4 Structure

The structure of this dissertation is the following one:

Chapter 1 is the current one and it is intended to give a general idea on the topic in which this dissertation is going to be based on.

Chapter 2 is where is given a theoretical background on the various aspects that must be understood to be capable of understating the numerical simulations presented in this thesis and the optimizations that can be achieved from the knowledge acquired from its analysis.

Chapter 3 is where it is analyzed unchirped Hyperbolic Secant pulses. The closed-form analytical expressions and corresponding numerical results obtained and presented in this chapter are valid considering no chirp, and only having group-velocity dispersion in the optical channel.

Chapter 4 is where chirped Gaussian pulses will be analyzed. In this chapter, it is only addressed the issue of having group-velocity dispersion in a fiber-optic communication system.

Chapter 5 is where it is made a comparison between the two pulses analyzed in chapters 3 and 4 (both having no chirp) and where it is justified why having chirp in pulses may be a good thing.

Chapter 6 is intended to analyze the effects of higher-order dispersion in the performance of fiber-optic communication systems, considering the pulses analyzed in chapter 4.

Chapter 7 is where it will be analyzed super-Gaussian pulses, which are a super-set pulse type of the pulses analyzed on chapter 4. It is going to be addressed how much their extra sharpness will affect the previous results.

Chapter 8 is where WDM systems are discussed in a simplified manner and some practical examples are presented regarding their potential capacity.

Chapter 9 is where the conclusions and future work are presented.

1.5 Original Contributions

Nowadays, what happens in optical communications systems is for a certain optical signal travelling along an optical fiber, it is measured its chirp value and then, according to those measures, engineers will try to minimize the impact it has on the bit rate, maybe by increasing the signal amplification or trying to get higher signal to noise ratio by changing the frequency on which they are working with, or simply by making the chirp value to be zero.

However, with the work developed in this dissertation, we will see that we do not need to go by trial and error to get the optimum bit-rate value under certain conditions. What is shown along the way, is that it is possible to optimize the chirp value an optical signal has by finding the optimum relation between the input width and the output width of the optical signal. So, it will be possible to obtain an optimum value for the chirp parameter that will allow us to maximize the bit rate on a fiber-optic communication system.

2. Theoretical Background

2.1 Pulse Propagation

The guided propagation of electromagnetic waves through an optical fiber occurs due to the physical mechanism called total internal reflection (happening in the interface between the core and the cladding) [1]. For single-mode fibers, any component $\Psi(r, \phi, z, t)$ of the optical fiber electromagnetic field as the form:

$$\Psi(r, \phi, z, t) = F(r, \phi)U(z, t)\,, \tag{2.1}$$

where $U(z, t)$ will be:

$$U(z, t) = A(z, t)\exp[i(\beta_0 z - \omega_0)t]\,. \tag{2.2}$$

Since in the course of the study that is going to be made, we are only interested to look at how the information along the optical fiber is transmitted, $U(z, t)$ will be the term of special relevance here, meaning we will not going to analyze the modal function $F(r, \phi)$ further.

At the input of the optical fiber, $z = 0$, we get:

$$U(0, t) = g(t)\exp(-i\omega_0 t)\,. \tag{2.3}$$

In this case, $g(t)$ is the modulating signal (which in fact, contains all the information to being carried) and $\omega_0 = 2\pi f$ is the (angular) frequency of the carrier. So, how may we know $U(z, t)$ knowing $U(0, t)$? To answer this question, we need to apply the Fourier transform.

Let $G(\omega)$ be the Fourier transform of the modulating signal $g(t)$, which is:

$$G(\omega) = F[g(t)] = \int_{-\infty}^{\infty} g(t)\exp\,(i\omega t)dt\,. \tag{2.4}$$

Inversely, we have:

$$g(t) = F^{-1}[G(\omega)] = \frac{1}{2\pi}\int_{-\infty}^{\infty} G(\omega)\exp\,(-i\omega t)d\omega\,. \tag{2.5}$$

Then, knowing $U(0, t) = g(t)\exp(-i\omega_0 t)$, it comes:

$$\tilde{\mathrm{U}}(0, \omega) = F[U(0, t)] = \int_{-\infty}^{\infty} U(0, t)\exp\,(i\omega t)dt = \int_{-\infty}^{\infty} g(t)\exp\,[\mathrm{i}(\omega - \omega_0)\mathrm{t}]dt\,, \tag{2.6}$$

$$\tilde{\mathrm{U}}(0, \omega) = G(\omega - \omega_0)\,. \tag{2.7}$$

But, for every given point $z \geq 0$ of the optical fiber, we get:

$$\tilde{\mathrm{U}}(z, \omega) = H(z, \omega)\tilde{\mathrm{U}}(0, \omega)\,, \tag{2.8}$$

$$H(z, \omega) = \exp[i\beta(\omega)z]\,. \tag{2.9}$$

Here, we are saying the following: the optical fiber is being operated in the linear monomodal regime and its behavior is characterized by the transfer function $H(z, \omega)$ expressed in the frequency domain and here it is assumed a propagation between the input, $z = 0$, and the point of longitudinal coordinate $z > 0$. Even more, $\beta = \beta(\omega)$ is the longitudinal propagation constant (later on, we will see how to calculate this "constant") of the fundamental mode. Therefore, it comes:

$$U(z, t) = F^{-1}[\tilde{\mathrm{U}}(z, \omega)] = \frac{1}{2\pi}\int_{-\infty}^{\infty} \tilde{\mathrm{U}}(z, \omega)\exp\,(-i\omega t)d\omega\,. \tag{2.10}$$

From (2.10), the result is:

$$U(z,t) = \frac{1}{2\pi}\int_{-\infty}^{\infty} G(\omega-\omega_0)\exp\{i[\beta(\omega)z-\omega t]\}\,d\omega\,. \tag{2.11}$$

To solve the integral from the last expression, a variable change needs to take place. For that matter, it is necessary to consider $\Omega = \omega - \omega_0$. This way, it comes that:

$$\beta(\omega) = \beta(\omega_0+\Omega)\,. \tag{2.12}$$

To get the expression of this function, we can consider a Taylor expansion (around ω_0):

$$\beta(\omega) = \beta(\omega_0+\Omega) = \sum_{m=0}^{\infty}\frac{\beta_m}{m!}\Omega^m\,. \tag{2.13}$$

with β_m being given by:

$$\beta_m = \frac{d^m\beta}{d\omega^m}\,,\omega=\omega_0\,. \tag{2.14}$$

Luckily, when the shift in frequency Ω is too small (more precisely, when $\Omega \ll \omega_0$) or when $\beta_m \approx 0$ for $m \geq 4$ (being m the order of a given term in the expansion), it is reasonable to consider just $0 \leq m \leq 3$ in the expansion. The outcome is simply:

$$\beta(\omega) = \beta(\omega_0+\Omega) \approx \beta_0 + \beta_1\Omega + \frac{1}{2}\beta_2\Omega^2 + \frac{1}{6}\beta_3\Omega^3, \tag{2.15}$$

being:

$$\beta_0 = \beta(\omega_0)\,, \tag{2.16}$$

$$\beta_1 = \beta'(\omega_0) = \frac{d\beta}{d\omega}\,;\,\omega=\omega_0\,, \tag{2.17}$$

$$\beta_2 = \beta''(\omega_0) = \frac{d^2\beta}{d\omega^2}\,;\,\omega=\omega_0\,. \tag{2.18}$$

Before saying anything else, let us clarify that β_0 is the longitudinal propagation constant corresponding to the carrier frequency itself and β_1 is the term related with the group-delay, which is something that will be defined further ahead. However, neither β_0 nor β_1 introduce changes in the pulse shape, meaning in the chapters ahead the two terms of greater relevance will be β_2 denominated as the Group-Velocity Dispersion (GVD) and β_3 being the higher-order dispersion term, because both β_2 and β_3 will have a direct influence on the bit-rate of the fiber-optic communication systems.

In the case of β_2, as the name implies, the pulses will suffer dispersion due to the different propagation velocities of the spectral components that constitute the signal, which is also something to be explored with more detail later on. As for β_3, it will also cause dispersion but in a different way. Contrary to β_2, whose dispersion effects are symmetric when analyzing the front and the tail of the pulse, i.e., the entire pulse as a whole. With β_3 in play, the dispersion effects will be asymmetric when looking to both front and tail of the pulse. This is the qualitative difference between both.

From here, we may obtain:

$$U(z,t) \approx \exp[i(\beta_0 z - \omega_0 t)] \times$$

$$\times \frac{1}{2\pi}\int_{-\infty}^{\infty} G(\Omega)\exp[-i\Omega(t-\beta_1 z)]\exp\left(i\frac{1}{2}\beta_2\Omega^2 z\right)\exp\left(i\frac{1}{6}\beta_3\Omega^3 z\right)d\,\Omega\,. \tag{2.19}$$

Having in mind (2.2), it is clear that:

$$A(z,t-\beta_1 z) =$$

$$= \frac{1}{2\pi}\int_{-\infty}^{\infty} G(\Omega)\exp[-i\Omega(t-\beta_1 z)]\exp\left(i\frac{1}{2}\beta_2\Omega^2 z\right)\exp\left(i\frac{1}{6}\beta_3\Omega^3 z\right)d\,\Omega\,. \tag{2.20}$$

Then, when making:

$$T = t - \beta_1 z\,, \tag{2.21}$$

and $\beta_3 \approx 0$, we finally get:

$$A(z,T) = \frac{1}{2\pi}\int_{-\infty}^{\infty} G(\Omega)\exp(-i\Omega T)\exp\left(i\frac{1}{2}\beta_2\Omega^2 z\right)d\,\Omega\,. \tag{2.22}$$

To sum up, when it is possible to consider $\beta_m \approx 0$ for $m \geq 3$, we have:

$$U(0,t) = g(t)\exp(-i\omega_0 t)\,, \tag{2.23}$$

$$A(0,T) = g(t)\,, \tag{2.24}$$

$$\tilde{\mathrm{A}}(0,\Omega) = F[A(0,T)] = G(\Omega) = F[g(t)] = \int_{-\infty}^{\infty} g(t)\exp(i\Omega t)\,dt\,, \tag{2.25}$$

$$\tilde{\mathrm{A}}(z,\Omega) = \tilde{\mathrm{A}}(0,\Omega)\exp\left(i\frac{1}{2}\beta_2\Omega^2 z\right), \tag{2.26}$$

$$A(z,T) = F^{-1}[\tilde{\mathrm{A}}(z,\Omega)] = \frac{1}{2\pi}\int_{-\infty}^{\infty}\tilde{\mathrm{A}}(z,\Omega)\exp(-i\Omega T)\,d\Omega\,. \tag{2.27}$$

This is what happens in most practical cases, where we can consider expression (2.27). It is only necessary to consider β_3 when $\lambda = \lambda_D$ (for which β_2 vanishes) or for very short pulses.

From (2.21), we may define the group-delay as:

$$\tau_g = \beta_1 L\,, \tag{2.28}$$

with $1/\beta_1 = L/\tau_g$ having velocity dimensions. That velocity is called group-velocity, which is in fact:

$$v_g(\omega_0) = \frac{L}{\tau_g} = \frac{1}{\beta_1} = \frac{1}{\beta'(\omega_0)}\,. \tag{2.29}$$

Now, expression (2.21) may be rewritten as:

$$T = t - \beta_1 z = t - \frac{z}{v_g(\omega_0)} = t - \frac{z}{L}\frac{L}{v_g(\omega_0)} = t - \left(\frac{z}{L}\right)\tau_g\,, \tag{2.30}$$

resulting to be, naturally, $T = t$ for $z = 0$ and $T = t - \tau_g$ for $z = L$.

We may also define the group-velocity for any given frequency ω:

$$v_g(\omega) = \frac{1}{\beta'(\omega)} = \frac{1}{\frac{d\beta}{d\omega}}. \tag{2.31}$$

Even though β_1, β_2 and τ_g were only defined for $\omega = \omega_0$, the same notation will be considered valid for any $\omega \neq \omega_0$. This will result in doing $\beta_1 = \beta'(\omega)$, $\beta_2 = \beta''(\omega)$ and $\tau_g(\omega) = L/v_g(\omega)$. Now, we may define $\beta_2(\omega)$ as being:

$$\beta_2(\omega) = \beta''(\omega) = \frac{d^2\beta}{d\omega^2} = \frac{d\beta_1}{d\omega} = \frac{d}{d\omega}\left[\frac{1}{v_g(\omega)}\right] = \frac{1}{L}\frac{d\tau_g}{d\omega}. \tag{2.32}$$

The function defined in (2.32) will be the so-called group-velocity dispersion. Therefore:

$$\beta_2(\omega) = \frac{d}{d\omega}\left[\frac{1}{v_g(\omega)}\right] = -\frac{1}{v_g^2(\omega)}\frac{dv_g}{d\omega}. \tag{2.33}$$

The last expression will be extremely important and that is why it will be analyzed more carefully in section 2.3. Sometimes, instead of using the GVD coefficient β_2, it is used the dispersion coefficient D, which may be defined as:

$$D(\lambda) = \frac{d}{d\lambda}\left(\frac{1}{v_g(\lambda)}\right) = \frac{1}{L}\frac{d\tau_g}{d\lambda}. \tag{2.34}$$

Being aware that:

$$\beta''(\omega) = \frac{1}{L}\frac{d\tau_g}{d\omega}, \tag{2.35}$$

it is possible to see that a relationship between the dispersion coefficient D and the GVD may exist. First, we need to have in consideration the following:

$$\omega = 2\pi f = \frac{2\pi c}{\lambda}, \tag{2.36}$$

from which the derivative of ω over λ is:

$$\frac{d\omega}{d\lambda} = -\frac{2\pi c}{\lambda^2}. \tag{2.37}$$

Now, D may be rewritten as:

$$D = \frac{1}{L}\frac{d\tau_g}{d\omega}\frac{d\omega}{d\lambda} = -\frac{2\pi c}{\lambda^2}\left(\frac{1}{L}\frac{d\tau_g}{d\omega}\right). \tag{2.38}$$

From expression (2.47), a simple relation between D and β_2 arises:

$$D = -\frac{2\pi c}{\lambda^2}\beta_2\,. \tag{2.39}$$

An expression for the dispersion slope S may also be introduced:

$$S = \frac{dD}{d\lambda} = \frac{4\pi c}{\lambda^3}\beta_2 + \left(\frac{2\pi c}{\lambda^2}\right)^2 \beta_3\,. \tag{2.40}$$

Next, we are going to look through two practical cases on how to define expressions for the group-delay τ_g, the dispersion coefficient D and the dispersion slope S.

First case

The first case is in the O band corresponding to the interval $1270\ nm \leq \lambda \leq 1340\ nm$ [1]. The goal is to determine the dispersion in conventional optical fibers. The starting point is the given Sellmeier equation for the group-delay:

$$\tau_g(\lambda) = A + B\lambda^2 + C\lambda^{-2}\,. \tag{2.41}$$

In the previous equation, the specific characteristics of a given optical fiber are then determined from the three constants A, B, and C. The first thing to do is to rewrite the group-delay in the following form:

$$\tau_g(\lambda) = A + B\lambda^2\left(1 + \frac{C}{B}\lambda^{-4}\right). \tag{2.42}$$

The dispersion coefficient will be then given by:

$$D(\lambda) = \frac{1}{L}\frac{d\tau_g}{d\lambda} = \frac{2B\lambda}{L}\left(1 - \frac{C}{B}\lambda^{-4}\right). \tag{2.43}$$

Therefore, it is defined a wavelength λ_D for which the GVD is nullified, i.e., such that $D(\lambda_D) = 0$. In these conditions, it comes $C/B = \lambda_D^4$. This way:

$$D(\lambda) = \frac{2B\lambda}{L}\left[1 - \left(\frac{\lambda_D}{\lambda}\right)^4\right]. \tag{2.44}$$

Even more, we obtain:

$$\tau_g(\lambda) = A + B\lambda^2\left[1 + \left(\frac{\lambda_D}{\lambda}\right)^4\right]. \tag{2.45}$$

If $\tau_g(\lambda_D) = \tau_D$, we get the following:

$$\tau_D = A + 2B\lambda_D^2 \rightarrow \tau_g(\lambda) = \tau_D + B\lambda^2\left[1 - \left(\frac{\lambda_D}{\lambda}\right)^2\right]^2. \tag{2.46}$$

Finally, if defining the dispersion slope (or, the higher-order dispersion) as:

$$S = \frac{dD}{d\lambda}, \tag{2.47}$$

we get:

$$S(\lambda) = \frac{2B}{L}\left[1 + 3\left(\frac{\lambda_D}{\lambda}\right)^4\right]. \tag{2.48}$$

Since the general case is defined by expression (2.17), if $S(\lambda_D) = S_D$ we get $S_D = 8B/L$. Therefore, the final expressions for τ_g, D and S are:

$$\begin{cases} A = \tau_D - \dfrac{\lambda_D S_D L}{4} \\ B = \dfrac{S_D L}{8} \\ C = \dfrac{\lambda_D^4 S_D L}{8} \end{cases} \rightarrow \begin{cases} \tau_g(\lambda) = \tau_D + \dfrac{S_D L}{8\lambda^2}(\lambda^2 - \lambda_D^2)^2 \\ D(\lambda) = \dfrac{\lambda S_D}{4}\left[1 - \left(\dfrac{\lambda_D}{\lambda}\right)^4\right] \\ S(\lambda) = \dfrac{S_D}{4}\left[1 + 3\left(\dfrac{\lambda_D}{\lambda}\right)^4\right] \end{cases}. \tag{2.49}$$

Second case

This second case will focus on modified dispersion fibers, on which fibers are dimensioned to have no GVD near the minimum attenuation point. In this case, we aim to the interval $1500\ nm \leq \lambda \leq 1600\ nm$ [1] and it is considered the following Sellmeier expression for the group-delay:

$$\tau_g(\lambda) = A + B\lambda + C\lambda^2\ . \tag{2.50}$$

Then, in this case:

$$D(\lambda) = \frac{1}{L}\frac{d\tau_g}{d\lambda} = \frac{B}{L}\left(1 + 2\frac{C}{B}\lambda\right). \tag{2.51}$$

So, $B/C = -2\lambda_D$, with:

$$D(\lambda) = \frac{B}{L}\left(1 - \frac{\lambda}{\lambda_D}\right) \rightarrow S(\lambda) = -\frac{B}{\lambda_D L}. \tag{2.52}$$

Therefore:

$$\begin{cases} A = \tau_D + \dfrac{\lambda_D^2 S_D L}{2} \\ B = -\lambda_D S_D L \\ C = \dfrac{S_D L}{2} \end{cases} \rightarrow \begin{cases} \tau_g(\lambda) = \tau_D + \dfrac{S_D L}{2}(\lambda - \lambda_D)^2 \\ D(\lambda) = S_D(\lambda - \lambda_D) \\ S(\lambda) = S_D \end{cases}. \tag{2.53}$$

2.2 Chirped Gaussian Pulses

A pulse is said to be Gaussian if at the input of the fiber, $z = 0$, we have a pulse of the form [2]:

$$A(0,t) = A_0 \exp\left[-\frac{1 + iC}{2}\left(\frac{t}{T_0}\right)^2\right], \tag{2.54}$$

where C is the dimensionless chirp parameter. This signal can also be written in the following form:

$$A(0,t) = A_0 \exp\left(-\frac{t^2}{2T_0^2}\right)\exp[-i\phi(t)]\ , \tag{2.55}$$

in which:

$$\phi(t) = C\frac{t^2}{2T_0^2}. \tag{2.56}$$

So, in a pulse where we have a quadratic phase ϕ in time, C is the parameter that influences the slope of the dynamic shifting of frequency $\Omega(t)$ in relation to the carrier wave and it is linear in time. In fact:

$$\Omega(t) = \frac{d\phi}{dt} = C\frac{t}{T_0^2} \rightarrow\ \omega(t) = \omega_0 + \Omega(t) = \omega_0 + C\frac{t}{T_0^2}. \tag{2.57}$$

Like expression (2.33), expression (2.57) will also be extremely important and that is why it will also be analyzed more carefully in section 2.3, and we will see how both are related. As always, it is a good idea to put $A(0,t)$ in the frequency domain. This way, it comes that [3]:

$$\tilde{A}(0,\Omega) = \int_{-\infty}^{\infty} A(0,t)\exp(i\Omega t)\,dt = A_0\sqrt{\frac{2\pi T_0^2}{1+iC}}\exp\left[-\frac{\Omega^2 T_0^2}{2(1+iC)}\right]. \tag{2.58}$$

Now, it is possible to have an expression for the spectral density, which is:

$$|\tilde{A}(0,\Omega)|^2 = A_0^2 \frac{2\pi T_0^2}{\sqrt{1+C^2}} \exp\left(-\frac{\Omega^2 T_0^2}{1+C^2}\right). \tag{2.59}$$

So, the spectral half-width at 1/*e* intensity at the maximum intensity point is:

$$\Omega_0 T_0 = \sqrt{1+C^2}\,. \tag{2.60}$$

This last expression reveals the effect of the chirp parameter over the spectral width: the existence of the chirp parameter produces a broadening of the pulse, because in its absence, the expression would be simply:

$$\Omega_0 T_0 = 1. \tag{2.61}$$

Now, to know the shape of the pulse at any given point $z \geq 0$, we must consider that the optical fiber behaves as a chirp filter. This means that we need to know the transfer function of the optical fiber. Fortunately, since the GVD is almost always much more relevant than the third order dispersion term (and for practical reasons), meaning it can be neglected ($\beta_3 \approx 0$) the transfer function can be expressed as follows:

$$H(z,\Omega) = \exp\left(i\frac{1}{2}\beta_2 \Omega^2 z\right). \tag{2.62}$$

Now it is clear that $\tilde{A}(z,\Omega)$ expression is:

$$\tilde{A}(z,\Omega) = A_0 \sqrt{\frac{2\pi T_0^2}{1+iC}} \exp\left[-\frac{\Omega^2 T_0^2}{2(1+iC)}\right] \exp\left(i\frac{1}{2}\beta_2 \Omega^2 z\right). \tag{2.63}$$

Applying the inverse Fourier transform to the expression above, we now get an expression that characterizes the pulse envelope in time at the output, which is:

$$A(z,T) = \frac{A_0 T_0}{\sqrt{2\pi(1+iC)}} \int_{-\infty}^{\infty} \exp\left[-\frac{Q(z)\Omega^2 T_0^2}{2(1+iC)}\right] \exp(-i\Omega T)\, d\Omega\,, \tag{2.64}$$

$$A(z,T) = \frac{A_0}{\sqrt{Q(z)}} \exp\left[-\frac{1+iC}{2Q(z)}\left(\frac{T}{T_0}\right)^2\right], \tag{2.65}$$

with:

$$Q(z) = 1 + (C-i)\frac{\beta_2 z}{T_0^2}\,. \tag{2.66}$$

This equation shows that a Gaussian pulse remains Gaussian on propagation, but its width, chirp, and amplitude change as dictated by the factor Q(z). The width changes with z as $T_1(z) = |Q(z)|T_0$, and chirp changes from its initial value C to become $C_1(z) = C + \frac{(1+C^2)\beta_2 z}{T_0^2}$. Changes in the pulse width are quantified through the broadening factor:

$$\eta(z) = |Q(z)| = \sqrt{\left(1 + C\frac{\beta_2 z}{T_0^2}\right)^2 + \left(\frac{\beta_2 z}{T_0^2}\right)^2} \tag{2.67}$$

Now, it is possible to define the output intensity as follows:

$$|A(z,T)|^2 = \frac{A_0^2}{\eta(z)} \exp\left[-\frac{1}{\eta(z)}\left(\frac{T}{T_0}\right)^2\right] \tag{2.68}$$

At this point, an important consideration to be made is that the pulse energy will be always constant. This is an assumption that is going to be taken as granted throughout this study, meaning that the focus is going to be only in the shape of the signal itself, always disregarding energy losses that may occur during the signal propagation. Having such idea in mind, and being E the pulse energy, it is possible to define E as:

$$E = \int_{-\infty}^{\infty} |A(z,T)|^2 dT = \sqrt{\pi} A_0^2 T_0 \tag{2.69}$$

From E expression, it is now clear that it does not depend on point z where it is calculated (lossless case).

To further continue our analysis on the propagation of pulses (in this particular case of chirped Gaussian pulses), it is now relevant to define the dispersion length, L_D, and the normalized distance, ξ. So, both can be defined as [3]:

$$\textbf{Dispersion length}: L_D = \frac{T_0^2}{|\beta_2|} \tag{2.70}$$

$$\textbf{Normalized distance}: \xi = \frac{z}{L_D} = \frac{|\beta_2| z}{T_0^2} = sgn(\beta_2)\frac{\beta_2 z}{T_0^2} \tag{2.71}$$

Now, the previous expressions that were obtained according to z can now be rewritten according to ξ:

$$Q(\xi) = \eta(\xi)\exp[-i\theta(\xi)], \theta(\xi) = \frac{\xi}{sgn(\beta_2) + C\xi} \tag{2.72}$$

$$T_1(\xi) = T_0 \eta(\xi) \tag{2.73}$$

$$C_1(\xi) = C + sgn(\beta_2)(1 + C^2)\xi \tag{2.74}$$

$$\textbf{Broadening coefficient}: \eta(\xi) = \frac{T_1(\xi)}{T_0} = \sqrt{[1 + sgn(\beta_2)C\xi]^2 + \xi^2} \tag{2.75}$$

Knowing that $A_1(\xi) = \frac{A_0}{\sqrt{\eta(\xi)}}$, we know have everything we need to know to write an expression that defines the signal at the output depending on the normalized distance. Being:

$$\tilde{A}(\xi, \Omega) = A_1(\xi)\sqrt{\frac{2\pi T_1^2(\xi)}{1 + iC_1(\xi)}}\exp\left[-\frac{\Omega^2 T_1^2(\xi)}{2[1 + iC_1(\xi)]}\right]\exp\left[i\frac{1}{2}\theta(\xi)\right] \tag{2.76}$$

and applying the same algebra from before, it comes that the signal at the output is expressed as:

$$A(\xi, T) = A_1(\xi)\exp\left\{-\frac{1+iC_1(\xi)}{2}\left[\frac{T}{T_1(\xi)}\right]^2\right\}\exp\left[i\frac{1}{2}\theta(\xi)\right]. \tag{2.77}$$

It is now important to remind that the pulse remains, along its transmission inside the optical fiber, a Gaussian pulse with a total chirp $C_1(\xi)$ which is the sum of the initial chirp C with an induced chirp. The induced chirp is proportional to the distance travelled inside the fiber. Knowing that,

$$\eta^2(\xi) = 1 + 2sgn(\beta_2)C\xi + (1 + C^2)\xi^2, \tag{2.78}$$

we can get

$$2\eta(\xi)\frac{d\eta}{d\xi} = 2sgn(\beta_2)C + 2(1 + C^2)\xi. \tag{2.79}$$

So, we get a minimum for the pulse width for:

$$\frac{d\eta}{d\xi} = 0 \Rightarrow \xi_{min} = -\frac{sgn(\beta_2)C}{1 + C^2} \Rightarrow \eta_{min} = \frac{1}{\sqrt{1 + C^2}}. \tag{2.80}$$

This condition only applies if $sgn(\beta_2)C < 0$, otherwise there is no minimum value for the width of the pulse. For unchirped pulses we get the trivial result: $\xi_{min} = 0$.

As shown before, it is possible to find closed-form analytical expressions for a chirped Gaussian pulse propagating along a fiber under the effect of GVD. However, when the effect of higher-order dispersion must be considered (through β_3) the pulse no longer remains Gaussian. In this case, a proper way to measure the pulse width is to calculate its root mean square (RMS) width $\sigma = \sigma(z)$, such that:

$$\sigma = \sqrt{\langle t^2 \rangle - \langle t \rangle^2}\,, \tag{2.81}$$

where the angle brackets denote averaging with respect to the intensity profile [2]:

$$\langle t^m \rangle = \frac{\int_{-\infty}^{\infty} t^m |A(z,t)|^2 dt}{\int_{-\infty}^{\infty} |A(z,t)|^2 dt}. \tag{2.82}$$

However, in the lossless case energy (E) does not depend on the point z. This way, it comes that [3]:

$$\langle t^m \rangle = \frac{1}{E}\int_{-\infty}^{\infty} t^m |A(z,t)|^2 dt\,. \tag{2.83}$$

The RMS width of a chirped Gaussian pulse can be simply calculated as:

$$\sigma_0 = \frac{T_0}{\sqrt{2}}. \tag{2.84}$$

As proven in [2], the broadening factor is given by:

$$\left(\frac{\sigma}{\sigma_0}\right)^2 = \left[1 + C\left(\frac{\beta_2 L}{2\sigma_0^2}\right)\right]^2 + \left(\frac{\beta_2 L}{2\sigma_0^2}\right)^2 + (1 + C^2)^2 \left(\frac{\beta_3 L}{4\sqrt{2}\sigma_0^3}\right)^2. \tag{2.85}$$

However, the last expression does not account for the source linewidth and hence is only applicable to optical sources with small spectral width (such as single-mode semiconductor lasers).

For optical sources with a large spectral width, the expression that holds true for the broadening factor is the following:

$$\left(\frac{\sigma}{\sigma_0}\right)^2 = \left[1 + C\left(\frac{\beta_2 L}{2\sigma_0^2}\right)\right]^2 + (1 + V_\omega^2)\left(\frac{\beta_2 L}{2\sigma_0^2}\right)^2 + (1 + C^2 + V_\omega^2)^2 \left(\frac{\beta_3 L}{4\sqrt{2}\sigma_0^3}\right)^2, \tag{2.86}$$

with $V_\omega = 2\sigma_\omega \sigma_0 \gg 1$. However, when considering optical sources with a small spectral width, $V_\omega \ll 1$ and therefore we recover the expression presented in (2.85).

From now on, in the next chapters we will be always assuming optical sources with small spectral width.

2.3 Combined Effects of GVD and Chirp Parameter

Both GVD and chirp parameter will cause the different frequency components of an optical pulse to travel at different velocities. This fact alone may not mean much, but what we want to see is if there is a way to take advantage of such effects when it comes to optimize the bit-rate in a fiber-optic communication system.

To begin, let us first look at how GVD alters the velocity of the different frequency components of an optical pulse. To start, we need to remind the expression given in (2.33) which is:

$$\beta_2(\omega) = \frac{d}{d\omega}\left[\frac{1}{v_g(\omega)}\right] = -\frac{1}{v_g^2(\omega)}\frac{dv_g}{d\omega}. \tag{2.87}$$

To make things clear, if $dv_g/d\omega < 0$ then $\beta_2(\omega) > 0$ and one can say we are working in the normal-dispersion regime. In this regime, high-frequency (blue-shifted) components of an optical pulse travel slower than low-frequency (red-shifted) components of the same pulse, i.e., it occurs a shift to the red at the front of the pulse and a shift to the blue at its tail. On the other hand, if $dv_g/d\omega > 0$ then $\beta_2(\omega) < 0$ and one may say we are working in the anomalous-dispersion regime. In this regime, high-frequency (blue-shifted) components of an optical pulse travel faster than low-frequency (red-shifted) components of the same pulse, i.e., it occurs a shift to the blue at the front of the pulse and a shift to the red at its tail, which is the opposite of what happens in the normal-dispersion regime.

Now, since we want to know how both GVD and chirp parameter will work together it is necessary to clarify how the chirp parameter will influence the group-velocity of the different frequency components of an optical pulse. To begin with, we need to have in mind expression (2.57), which is:

$$\Omega(t) = \frac{d\phi}{dt} = C\frac{t}{T_0^2}. \tag{2.88}$$

From expression (2.88), if $C > 0$ the frequency-shift will have a positive dependence with time. Then, for $C > 0$, high-frequency (blue-shifted) components of an optical pulse travel slower than low-frequency (red-shifted) components of the same pulse, i.e., it occurs a shift to the red at the front of the pulse and a shift to the blue at its tail. If $C < 0$ the frequency-shift will have a negative dependence with time. Then, if we consider $C < 0$, high-frequency (blue-shifted) components of an optical pulse travel faster than low-frequency (red-shifted) components of the same pulse, i.e., it occurs a shift to the blue at the front of the pulse and a shift to the red at its tail.

From the analysis of (2.87) and (2.88), some observations must be made. The first thing that gets our attention is that the effects on the velocity of the different frequency components produced by GVD are the same as the ones of the chirp parameter if their signals are equal, i.e., if they are both positive or both negative. However, if their signals are not equal, the effects produced by both are the opposite.

Then, in a fiber-optic communication system where $\beta_2 C > 0$, it is expected to experience pulse broadening since both GVD and chirp parameter are both increasing the difference in the velocity of the different frequency components, which is not an ideal scenario when it comes to optimization of bit-rate in a fiber-optic communication system.

However, in a fiber-optic communication system where $\beta_2 C < 0$, we may experience pulse compression since now the combined effects of GVD and chirp parameter are now counteracting each other. Then, this may contribute to reduce the difference between the velocity of the higher-frequency components and the lower-frequency components. This way, it will be ideal that $\beta_2 C < 0$ to allow for the possibility of an effective bit-rate optimization in a fiber-optic communication system.

In the next chapters, we will see how having $\beta_2 C > 0$ instead of $\beta_2 C < 0$ will affect the size of the optical pulses and therefore the maximum bit-rate possible in a fiber-optic communication system.

2.4 Dispersion Compensation

Before moving on, it is necessary to remind what is already done to improve the performance of a fiber-optic communication system, which is something called dispersion compensation. How to achieve it? First, we need to have in mind that an optical fiber may be seen as a passive optical filter, as shown in expression (2.62), where (considering $\beta_3 \approx 0$):

$$H(z,\Omega) = \exp\left(i\frac{1}{2}\beta_2\Omega^2 z\right). \tag{2.89}$$

However, the goal here is to get a transfer function whose value is:

$$H(z,\Omega) = 1\,, \tag{2.90}$$

such that the pulse shape is the same at the input and at the output of the optical fiber, as it is possible to confirm with expression (2.26) from which we would get:

$$\tilde{A}(z,\Omega) = \tilde{A}(0,\Omega)\,. \tag{2.91}$$

In order to achieve the result presented in expression (2.90), we need to implement a dispersion-compensating fiber (DCF), which will allow to have $\beta_2 = 0$ and therefore $D = 0$. Both transfers functions, corresponding to the optical fiber itself and to the DCF will have the same form as presented in expression (2.89). What will differ is the β_2 value for each one. Then, β_{21} will correspond to the GVD of the optical fiber itself and β_{22} to the GVD of the DCF. From here, it is possible to define the condition that must be verified to achieve dispersion compensation, which is the following:

$$\exp\left(i\frac{1}{2}\beta_{21}\Omega^2 L_1\right)\exp\left(i\frac{1}{2}\beta_{22}\Omega^2 L_2\right) = 1\,, \tag{2.92}$$

$$\exp\left[i\frac{1}{2}(\beta_{21}L_1 + \beta_{22}L_2)\Omega^2\right] = 1\,, \tag{2.93}$$

being L_1 the optical fiber length and L_2 the DCF length. Now, to fulfill the condition in (2.93), the term inside the exponential must be zero. Such thing is only possible if the following condition is met [2]:

$$\beta_{21}L_1 + \beta_{22}L_2 = 0\,. \tag{2.94}$$

Considering β_3 the analysis is very similar, which means we would end up with the following condition:

$$\beta_{31}L_1 + \beta_{32}L_2 = 0 \tag{2.95}$$

The difference is that to perform dispersion compensation considering β_3, both conditions presented in (2.94) and (2.95) would have to be met, whereas in the case where $\beta_3 \approx 0$, it would be enough to ensure that (2.94) was verified. If we want to express the last two conditions in terms of D and S, then both would be expressed as such [2]:

$$\begin{cases} D_1L_1 + D_2L_2 = 0\,. \\ S_1L_1 + S_2L_2 = 0\,. \end{cases} \tag{2.96}$$

In theory, this is a simple way to address the dispersion issue. However, it is done at the cost of having to implement a link with a greater length, $L = L_1 + L_2$, instead of just being $L = L_1$. This strategy is different from the one that is being presented in this dissertation since it is suggested an approach where bit-rate optimization occurs at the signal source, while with the technique presented in this section, optimization is done after the signal travels the entire link distance which is the sum of the optical fiber length with the DCF length.

3. Hyperbolic Secant Pulses

A Hyperbolic Secant pulse, at $z = 0$, assumes the form [4]:

$$A(0,t) = A_0 \operatorname{sech}\left(\frac{t}{T_0}\right) \exp\left[-i\frac{C}{2}\left(\frac{t}{T_0}\right)^2\right]. \tag{3.1}$$

However, in this study, we will always consider Hyperbolic Secant pulses without chirp, meaning the chirp parameter will be: $C = 0$. If that is the case, the previous expression may be rewritten as:

$$A(0,t) = A_0 \operatorname{sech}\left(\frac{t}{T_0}\right). \tag{3.2}$$

This approach is taken, because there is no expression in the literature for the broadening factor of Hyperbolic Secant pulses with chirp. Fortunately, there is indeed an expression for the broadening factor of unchirped Hyperbolic Secant pulses which is the following [4]:

$$\frac{\sigma^2}{\sigma_0^2} = 1 + \left(\frac{\pi\beta_2 z}{6\sigma_0^2}\right)^2, \tag{3.3}$$

being the RMS width of the pulse [4]:

$$\sigma_0 = \frac{\pi}{\sqrt{12}} T_0 . \tag{3.4}$$

To facilitate our analysis of the broadening factor, the same will be written using normalized variables. But first, let us see some auxiliary steps before we do that:

$$\sigma^2 = \sigma_0^2 + \left(\frac{\pi\beta_2 z}{6\sigma_0^2}\right)^2, \tag{3.5}$$

$$\frac{\sigma^2}{|\beta_2|L} = \frac{\sigma_0^2}{|\beta_2|L} + \left(\frac{\pi}{6}\right)^2 \frac{|\beta_2|L}{\sigma_0^2}\left(\frac{z}{L}\right)^2. \tag{3.6}$$

Now, knowing that the normalized pulse width is [3]:

$$\chi = \frac{\sigma^2}{|\beta_2|L}, \tag{3.7}$$

then:

$$\begin{cases} z = 0 \rightarrow \sigma = \sigma_0 \rightarrow \chi_0 = \dfrac{\sigma_0^2}{|\beta_2|L} \\ z = L \rightarrow \sigma = \sigma_1 \rightarrow \chi_1 = \dfrac{\sigma_1^2}{|\beta_2|L} \end{cases}. \tag{3.8}$$

The normalized distance, as seen before, is written as:

$$0 \leq \xi = \frac{z}{L} \leq 1. \tag{3.9}$$

From this point, the broadening factor may be rewritten as:

$$\chi = \chi_0 + \left(\frac{\pi}{6}\right)^2 \frac{\xi^2}{\chi_0}. \tag{3.10}$$

As such, the pulse width behavior will be defined as:

$$\mu = \mu(\chi_0, \xi) = \frac{\chi}{\chi_0} = 1 + \left(\frac{\pi}{6}\right)^2 \left(\frac{\xi}{\chi_0}\right)^2. \tag{3.11}$$

Now, to define what χ_1 and μ_1 will look like, we first state the following:

$$\begin{cases} \xi = 0 \rightarrow \chi = \chi_0 \rightarrow \mu = \mu_0 = 1 \\ \xi = 1 \rightarrow \chi = \chi_1 \rightarrow \mu = \mu_1 \end{cases}. \tag{3.12}$$

Having the previous considerations in mind, χ_1 and μ_1 will be rewritten as follows:

$$\chi_1 = \chi_0 + \left(\frac{\pi}{6}\right)^2 \frac{1}{\chi_0}, \tag{3.13}$$

$$\mu_1 = 1 + \left(\frac{\pi}{6}\right)^2 \left(\frac{1}{\chi_0}\right)^2. \tag{3.14}$$

Now, it is important for us to know what the optimum values are for χ_0 and χ_1. To get there, we must first do the following calculation:

$$\frac{d\chi_1}{d\chi_0} = 1 - \left(\frac{\pi}{6}\right)^2 \frac{1}{\chi_0^2} = 0 \rightarrow \chi_0^{opt} = \frac{\pi}{6}. \tag{3.15}$$

Then, the optimum value for χ_1 will be simply:

$$\chi_1^{opt} = \frac{\pi}{3}. \tag{3.16}$$

From here, we may finally get the optimum broadening factor and the optimum pulse width behavior, being both written as follows:

$$\chi^{opt} = \frac{\pi}{6}(1 + \xi^2), \tag{3.17}$$

$$\mu^{opt} = 1 + \xi^2. \tag{3.18}$$

Therefore:

$$\mu_1^{opt} = 2. \tag{3.19}$$

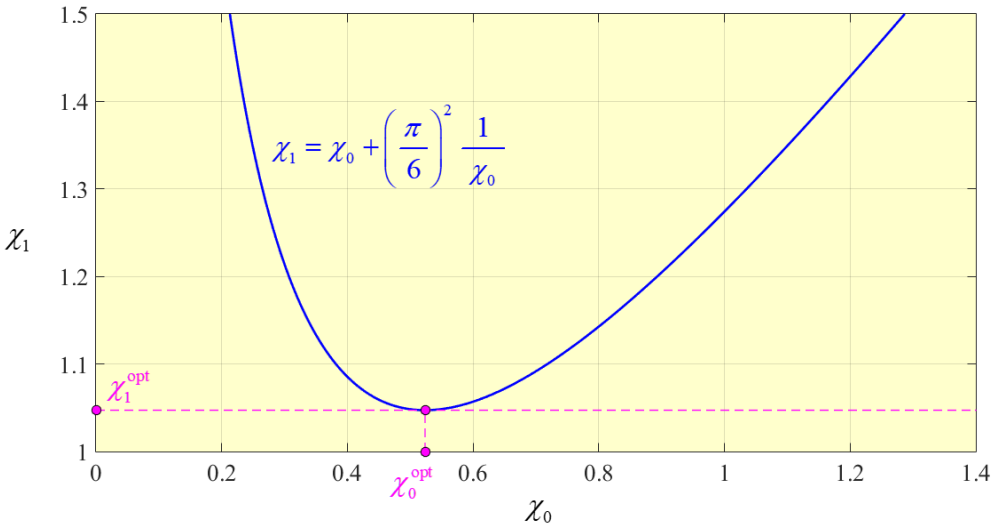

Figure 3.1 - Variation of the normalized output pulse width χ_1 with the normalized input pulse χ_0 for an unchirped Hyperbolic Secant pulse. From the graph we see a minimum for which $\chi_0^{opt} = \pi/6$ and $\chi_1^{opt} = \pi/3$.

In order to confirm the values obtained for χ_0^{opt} and χ_1^{opt}, the expression in which χ_1 depends on χ_0 was plotted and the result stands in figure (3.1). The obtained curve shows that in fact exists an optimum input pulse width that will allow to minimize the output pulse width meaning that also exists an optimum output pulse width. Since $\chi_0^{opt} \approx 0.52$ and $\chi_1^{opt} \approx 1.04$, the graph confirms what was deducted from the analytical expressions. This means we can trust in these values and therefore they will be taken as granted.

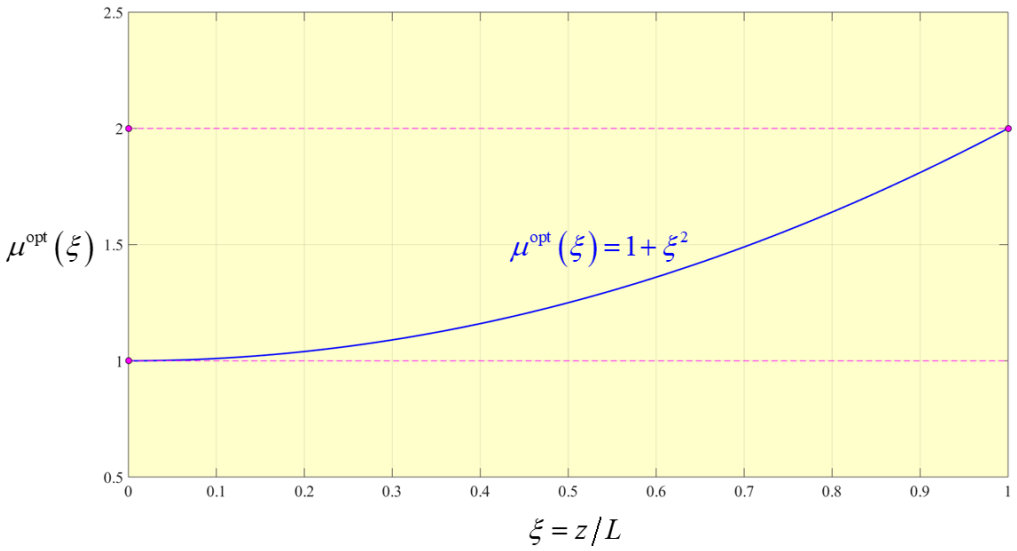

Figure 3.2 – Behavior of the pulse width along an optical fiber for an unchirped Hyperbolic Secant pulse with $\beta_2 \neq 0$ and $\beta_3 = 0$, being $\mu^{opt} = \mu(\chi_0^{opt}, \xi) = \chi/\chi_0^{opt} = 1 + \xi^2$. The pulse width grows monotonically through the entire journey inside the optical fiber.

From figure (3.2), it is possible to observe that the pulse width grows monotonically through the entire journey inside the optical fiber. Even more, the growth rate of the pulse width increases with the distance traveled inside the optical fiber. We can also state that the pulse width has a size which is exactly the double at the output in comparison with the pulse width at the input of the optical fiber, which is exactly what the analytical expressions predicted.

To obtain the maximum value for the bit-rate, first we need to have in mind the given practical rule of thumb [1]:

$$\sigma_{max} \leq \frac{T_b}{4} = \frac{1}{4B} \rightarrow B \leq B_0 = \frac{1}{4\sigma_{max}}. \tag{3.20}$$

Since the point in the optical fiber where the pulse width is the largest is at its output, $\sigma_{max} = \sigma_1$. With that information, it is possible to get an expression that will give us the optimized bit-rate value:

$$B_0 = \frac{1}{4\sigma_{max}} = \frac{1}{4}\sqrt{\frac{3}{\pi|\beta_2|L}} \approx \frac{0.2443}{\sqrt{|\beta_2|L}}. \tag{3.21}$$

But even more important than knowing the B_0 value is to know the product $B_0^2 L$ that will allow us to obtain a figure of merit, which will permit to better evaluate the performance of the fiber-optic communication system. Having a high bit-rate only for short distances will not be good enough for a transoceanic network and that is why this parameter is so important. The bit-rate squared product with the length of the optical fiber is given by:

$$B_0^2 L = \frac{F}{|\beta_2|}, with\ F = \frac{3}{16\pi} \approx 0.0597\,. \tag{3.22}$$

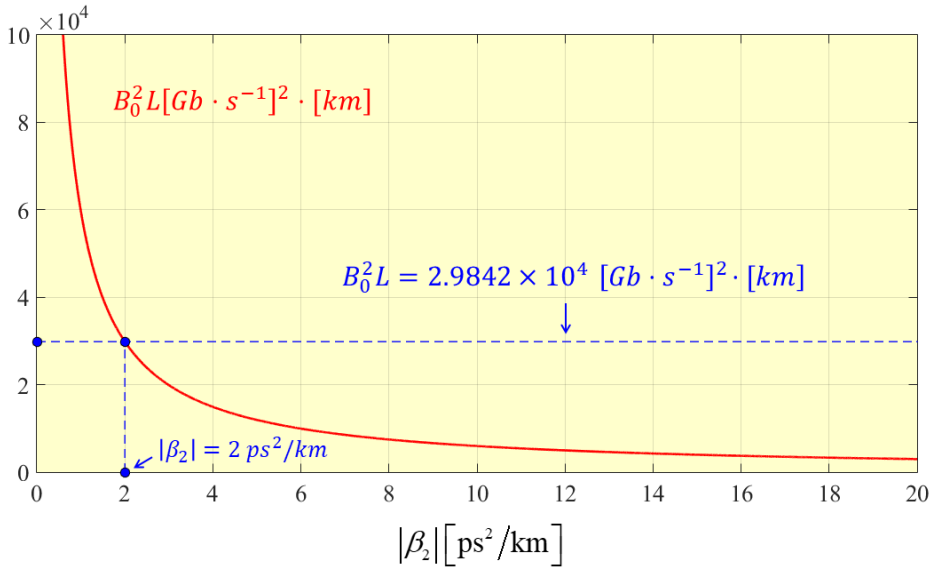

Figure 3.3 – Bit-rate squared product with the length of a given optical fiber for unchirped hyperbolic secant pulses as an instrument to measure the performance of a fiber-optic communication system. It is possible to see a decay in the performance for higher β_2 values.

Looking at figure (3.3), we may see now why having dispersion on the system is a bad thing. The greater β_2 is, the worse is the performance of a fiber-optic communication system. Naively, one could think that it may be possible to have an infinite growth on the bit-rate value by diminishing the length of the optical-fiber of course. However, we must not forget that we are not considering the effects of the higher-order dispersion term β_3, which is something that is going to be discussed on chapter 6. It is also possible to see a marked point on the graph for $|\beta_2| = 2\ ps^2/km$. This point will serve as a way to compare the performance of a fiber-optic communication system considering other types of pulses, being the exact value measured for $B_0^2 L$ not so important for itself but as way to later on discuss how fiber-optic communication system behaves in the presence of other pulses.

4. Chirped Gaussian Pulses

A chirped Gaussian pulse, at $z = 0$, assumes the form [2]:

$$A(0,t) = A_0 \exp\left[-\frac{1+iC}{2}\left(\frac{t}{T_0}\right)^2\right]. \tag{4.1}$$

Then, the corresponding broadening factor expression for this kind of pulse (if $\beta_3 = 0$) is given by [2]:

$$\frac{\sigma^2}{\sigma_0^2} = \left(1 + C\frac{\beta_2 z}{2\sigma_0^2}\right)^2 + \left(\frac{\beta_2 z}{2\sigma_0^2}\right)^2, \tag{4.2}$$

To facilitate our analysis of the broadening factor, the same will be written using normalized variables. But first, let us see some auxiliary steps before we do that:

$$\sigma^2 = \left(\sigma_0 + C\frac{\beta_2 z}{2\sigma_0}\right)^2 + \left(\frac{\beta_2 z}{2\sigma_0}\right)^2, \tag{4.3}$$

$$\sigma^2 = \sigma_0^2 + C\beta_2 z + (1+C^2)\left(\frac{\beta_2 z}{2\sigma_0}\right)^2, \tag{4.4}$$

$$\frac{\sigma^2}{|\beta_2|L} = \frac{\sigma_0^2}{|\beta_2|L} + sgn(\beta_2)C\left(\frac{z}{L}\right) + \frac{1}{4}(1+C^2)\frac{|\beta_2|L}{\sigma_0^2}\left(\frac{z}{L}\right)^2. \tag{4.5}$$

Now, knowing that the normalized pulse width is:

$$\chi = \frac{\sigma^2}{|\beta_2|L}, \tag{4.6}$$

then:

$$\begin{cases} z = 0 \rightarrow \sigma = \sigma_0 \rightarrow \chi_0 = \dfrac{\sigma_0^2}{|\beta_2|L} \\ z = L \rightarrow \sigma = \sigma_1 \rightarrow \chi_1 = \dfrac{\sigma_1^2}{|\beta_2|L} \end{cases}. \tag{4.7}$$

The parameter p is introduced as follows:

$$p = \frac{1}{4}(1+C^2) \geq \frac{1}{4}. \tag{4.8}$$

The normalized distance, as seen before, is written as:

$$0 \leq \xi = \frac{z}{L} \leq 1. \tag{4.9}$$

From this point, the broadening factor may be rewritten as:

$$\chi = \chi_0 + sgn(\beta_2)C\xi + \frac{p}{\chi_0}\xi^2. \tag{4.10}$$

As such, the pulse width behavior will be defined as:

$$\mu = \mu(sgn(\beta_2), C, \chi_0, \xi) = \frac{\chi}{\chi_0} = 1 + \left[sgn(\beta_2)C + p\left(\frac{\xi}{\chi_0}\right)\right]\left(\frac{\xi}{\chi_0}\right). \tag{4.11}$$

Now, to define what χ_1 and μ_1 will look like, we first state the following:

$$\begin{cases} \xi = 0 \rightarrow \chi = \chi_0 \rightarrow \mu = \mu_0 = 1 \\ \xi = 1 \rightarrow \chi = \chi_1 \rightarrow \mu = \mu_1 \end{cases}. \tag{4.12}$$

Having the previous considerations in mind, χ_1 and μ_1 will be rewritten as follows:

$$\chi_1 = \chi_0 + sgn(\beta_2)C + \frac{p}{\chi_0}, \tag{4.13}$$

$$\mu_1 = 1 + \left[sgn(\beta_2)C + \frac{p}{\chi_0}\right]\left(\frac{1}{\chi_0}\right). \tag{4.14}$$

Now, it is important for us to know what the optimum values are for χ_0 and χ_1. To get there, we must first do the following calculation:

$$\frac{d\chi_1}{d\chi_0} = 1 - \frac{p}{\chi_0^2} = 0 \rightarrow \chi_0^{opt} = \sqrt{p} = \frac{1}{2}\sqrt{1 + C^2}\,. \tag{4.15}$$

Then, the optimum value for χ_1 will be simply:

$$\chi_1^{opt} = sgn(\beta_2)C + \sqrt{1 + C^2}\,. \tag{4.16}$$

From here, we may finally get the optimum broadening factor and the optimum pulse width behavior, being both written as follows:

$$\chi^{opt} = sgn(\beta_2)C\xi + \frac{1}{2}(1 + \xi^2)\sqrt{1 + C^2}\,, \tag{4.17}$$

$$\mu^{opt} = 1 + 2\frac{sgn(\beta_2)C}{\sqrt{1 + C^2}}\xi + \xi^2\,. \tag{4.18}$$

Therefore:

$$\mu_1^{opt} = 2\left(1 + \frac{sgn(\beta_2)C}{\sqrt{1 + C^2}}\right). \tag{4.19}$$

To optimize the bit-rate in a fiber-optic communication system that works with chirped Gaussian pulses, we need to find a chirp parameter that will make the output pulse width to be equal to the input pulse width. Such value will be called as the critical value of the chirp parameter. Since $\mu_0 = 1$, we need to find the solution of the following equation:

$$\mu_1^{opt}(C = C_{cr}) = 1\,. \tag{4.20}$$

After solving the previous equation, we obtain for C_{cr} the given equation:

$$C_{cr} = -\frac{1}{\sqrt{3}}sgn(\beta_2)\,. \tag{4.21}$$

From here, we may now know what values we will get for χ_0^{opt} and χ_1^{opt} if $C = C_{cr}$. So, by making $C = C_{cr}$ in (4.15) and (4.16), we find that regardless of the signal of β_2, the outcome is the following:

$$\chi_0^{opt} = \chi_1^{opt} = \frac{1}{\sqrt{3}}. \tag{4.22}$$

This result in (4.22) was expected to happen since in (4.20) was defined a condition that forced the output width to be equal to the input width. Going back to (4.6), and knowing from (4.22) that $\sigma_{max} = \sigma_0 = \sigma_1$, using the result obtained in (4.22) we can obtain an expression that will define σ_{max}:

$$\sigma_{max} = 3^{-1/4}\sqrt{|\beta_2|L}\,. \tag{4.23}$$

This last result will be important to define the bit-rate value of chirped Gaussian pulses.

4.1 Unchirped Gaussian Pulses

In this section, it is going to be shown how an unchirped Gaussian pulse behaves according to the width of the input pulse behavior and how even when we find an optimized value for the mentioned with, it still occurs pulse broadening along the journey inside the optical fiber.

Since the case when $C = 0$ is being analyzed, some expressions will be worth mention because their form will change in comparison with the cases where chirp is verified. First, the expression that relates the dependence of the output pulse width with the input pulse width takes the following form:

$$\chi_1 = \chi_0 + \frac{1}{4\chi_0}\,. \tag{4.24}$$

Then, by using the same process as done to find χ_0^{opt} and χ_1^{opt} for chirped Gaussian pulses, the values for χ_0^{opt} and χ_1^{opt} are:

$$\chi_0^{opt} = 0.5\,, \tag{4.25}$$

$$\chi_1^{opt} = 1\,. \tag{4.26}$$

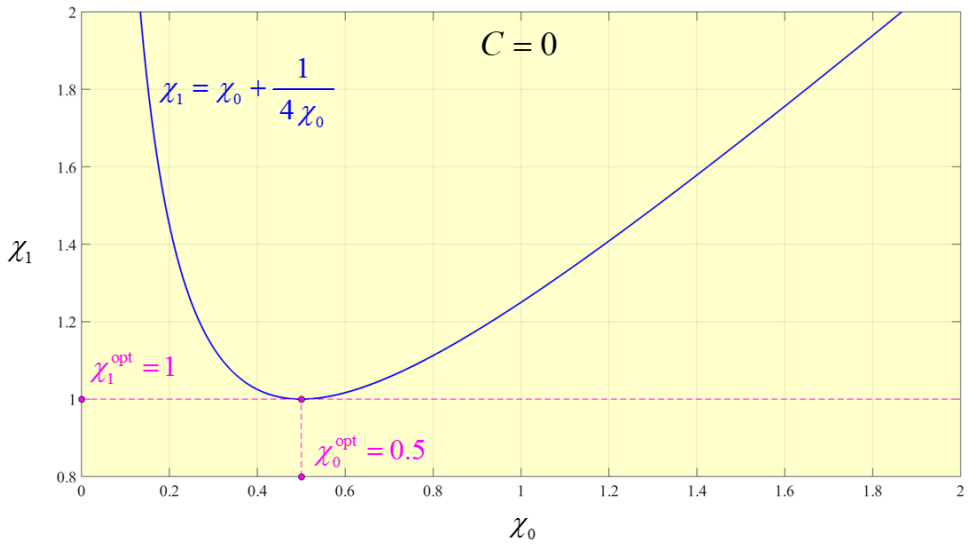

Figure 4.1 - Variation of the normalized output pulse width χ_1 with the normalized input pulse χ_0 for an unchirped Gaussian pulse. From the graph we see a minimum for which $\chi_0^{opt} = 0.5$ and $\chi_1^{opt} = 1$.

In order to confirm the values obtained for χ_0^{opt} and χ_1^{opt}, the expression in which χ_1 depends on χ_0 was plotted and the result stands in figure (4.1). The obtained curve shows that in fact exists an optimum input pulse width that will allow to minimize the output pulse width meaning that also exists an optimum output pulse width. Since $\chi_0^{opt} = 0.5$ and $\chi_1^{opt} = 1$, the graph confirms what was deducted from the analytical expressions. This means we can trust in these values and therefore they will be taken as granted.

Another expression that is worth mentioning is the one that defines μ^{opt}. Now, considering $C = 0$, μ^{opt} will take the following form:

$$\mu^{opt} = 1 + \xi^2 \,, \tag{4.27}$$

which is the same as the one for an unchirped Hyperbolic Secant pulse. However, a full comparison of both pulses will be made in another chapter since know we are interested in analyzing only the unchirped Gaussian pulse itself.

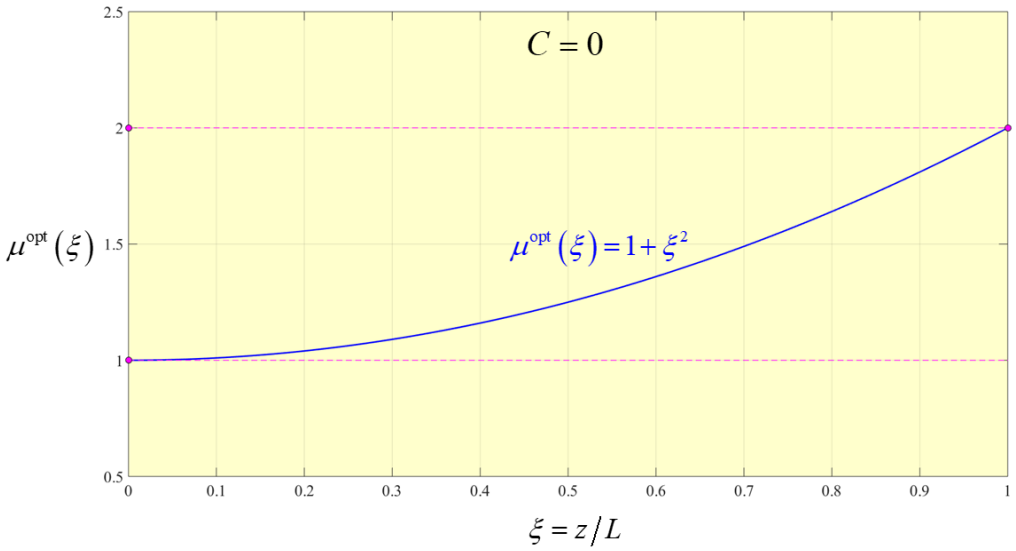

Figure 4.2 – Behavior of the pulse width along an optical fiber for an unchirped Gaussian pulse with $\beta_2 \neq 0$ and $\beta_3 = 0$, being $\mu^{opt} = \mu(\chi_0^{opt}, \xi) = \chi/\chi_0^{opt} = 1 + \xi^2$. The pulse width grows monotonically through the entire journey inside the optical fiber.

From figure (4.2), it is possible to observe that the pulse width grows monotonically through the entire journey inside the optical fiber. Even more, the growth rate of the pulse width increases with the distance traveled inside the optical fiber. We can also state that the pulse width has a size which is exactly the double at the output in comparison with the pulse width at the input of the optical fiber, which is exactly what the analytical expressions predicted.

Now that we now $\sigma_{max} = \sigma_1$ from figure (4.2), we may present the bit-rate expression for unchirped Gaussian pulses, which is this one:

$$B_0 = \frac{1}{4\sigma_{max}} = \frac{1}{4\sqrt{|\beta_2|L}} = \frac{0.25}{\sqrt{|\beta_2|L}}. \tag{4.28}$$

Once again, even more important is to know the product $B_0^2 L$ to get a figure of merit which will allow to better analyze the performance of a fiber-optic communication system giving us a more accurate perception about the performance of such system for different distances. Without further delay, the product $B_0^2 L$ is as follows:

$$B_0^2 L = \frac{F}{|\beta_2|} \,, with\ F = \frac{1}{16} = 0.0625 \,. \tag{4.29}$$

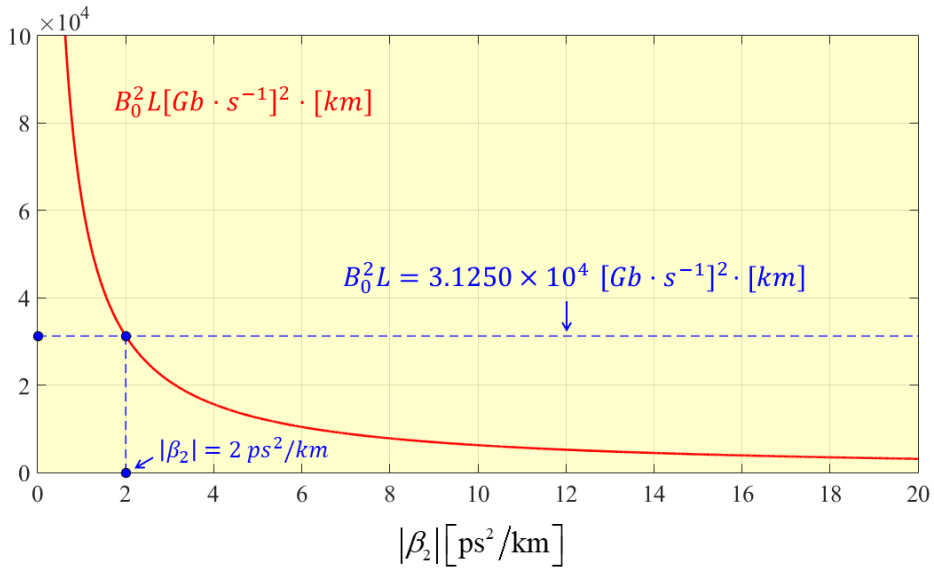

Figure 4.3 - Bit-rate squared product with the length of a given optical fiber for unchirped Gaussian pulses as an instrument to measure the performance of a fiber-optic communication system. It is possible to see a decay in the performance for higher β_2 values.

Looking at figure (4.3), we may see that the performance of a fiber-optic communication system improves when using unchirped gaussian pulses instead of unchirped hyperbolic secant pulses. Such claim can be made since according to the marked value of $|\beta_2| = 2\ ps^2/km$, the bit-rate squared product with the length of a given optical fiber is greater than the one obtained in figure (3.3). Once again, it looks feasible to have systems with infinite bit-rate but the reason behind this behavior is the same as the one explained for figure (3.3), i.e, it is assumed $\beta_3 = 0$. However, the performance of such systems may be greatly improved if instead of just getting rid of the chirp present in the pulse, we proceed to optimize it. In section 4.4, we will see how positive it may be for the system performance to operate with an optimized chirp parameter value.

4.2 Anomalous Dispersion Regime

In this section, chirped Gaussian pulses whose β_2 value is negative are going to be analyzed. We will also see in the next section than the analysis on the normal dispersion regime will be very similar, but instead β_2 will hold a positive value.

Let us recover some relevant expressions before we proceed further on our study. The first expression relevant that we need to remember is the one on which is shown the dependence of the input pulse width with the output pulse width:

$$\chi_1 = sgn(\beta_2)C + \chi_0 + \frac{1+C^2}{4\chi_0}. \tag{4.30}$$

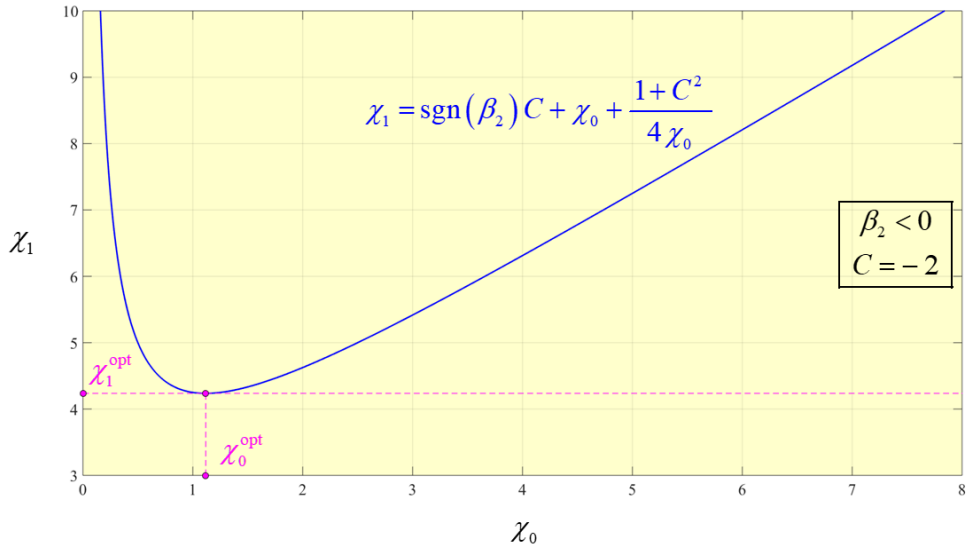

Figure 4.4 - Variation of the normalized output pulse width χ_1 with the normalized input pulse χ_0 for a chirped Gaussian pulse on the anomalous dispersion regime ($\beta_2 < 0$) and for a chosen value of $C = -2$. In this example, it is also possible to state that $\beta_2 C > 0$.

From figure (4.4), we can see that for any χ_0 value it always corresponds a higher value of χ_1. This holds true whenever $\beta_2 C > 0$ since both effects from β_2 and C act together to make the pulse broaden along the journey inside the optical fiber. However, if $\beta_2 C < 0$ we may observe pulse compression which is something we will see in figure (4.4).

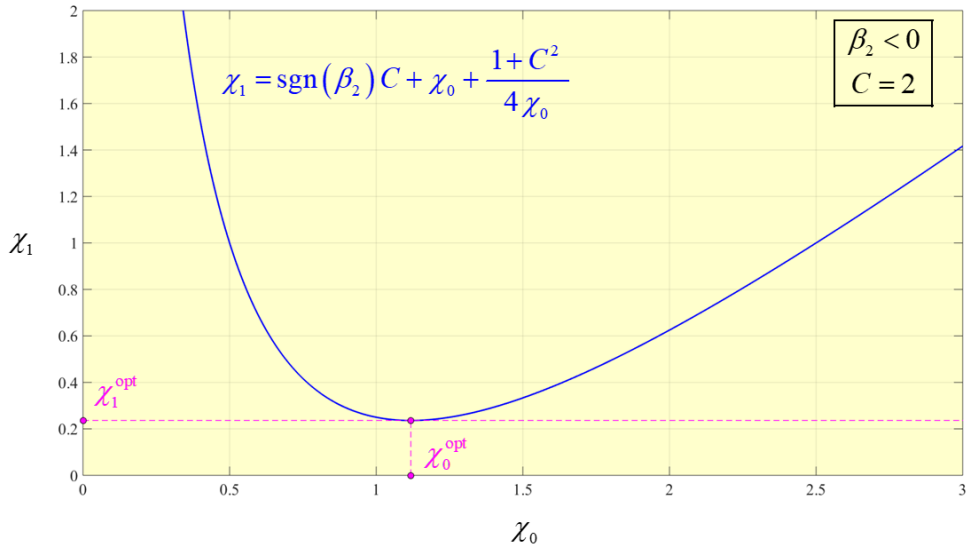

Figure 4.5 - Variation of the normalized output pulse width χ_1 with the normalized input pulse χ_0 for a chirped Gaussian pulse on the anomalous dispersion regime ($\beta_2 < 0$) and for a chosen value of $C = 2$. In this example, it is also possible to state that $\beta_2 C < 0$.

As it is possible to see in figure (4.5), for the concrete example shown there, for $0.5 < \chi_0 < 2.5$ it is possible to see that $\chi_1 < \chi_0$ and the opposite happens for $\chi_0 < 0.5$ and $\chi_0 > 2.5$. Those results mean that for some values of χ_0, pulse compression occurs meaning that the output pulse width will be lower than the input pulse width. This may happen because $\beta_2 C < 0$ meaning that the effects caused by β_2 and C may counteract each other causing the pulses to compress along their journey inside the optical fiber.

Now, if we pay close attention to the figures (4.4) and (4.5) we will see that for each C value it corresponds a given χ_0^{opt} and χ_1^{opt}. Needless to say that a figure showing how those values are affected by the chirp parameter is much needed at this point to see how is going to be found a chirp value (C_{cr}) that will optimize the pulse width.

However, before jumping into that, we need to remind two important expressions that will help us to understand, from a graphical point of view, how it is obtained the critical chirp value for a chirped Gaussian pulse travelling in the anomalous dispersion regime, meaning $\beta_2 < 0$. Having this said, let us bring back the expressions that define χ_0^{opt} and χ_1^{opt}:

$$\chi_0^{opt} = \frac{1}{2}\sqrt{1 + C^2}\,, \tag{4.31}$$

$$\chi_1^{opt} = sgn(\beta_2)C + \sqrt{1 + C^2}\,. \tag{4.32}$$

Both expressions will help us find C_{cr} since their intersection will be the key to get the value we need to know.

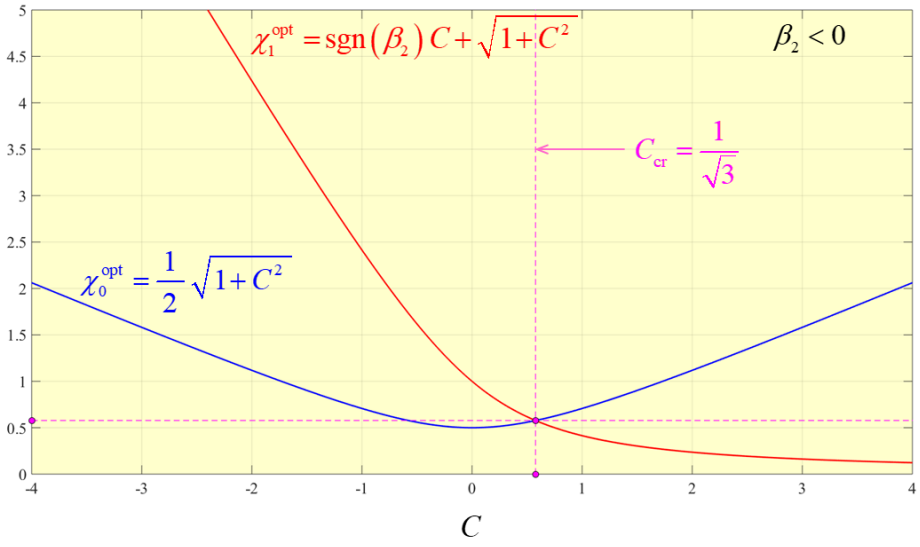

Figure 4.6 – Variation of χ_0^{opt} and χ_1^{opt} with the chirp parameter C, when $\beta_2 < 0$. As shown, the intersection of both curves gives us the critical chirp value, $C_{cr} = 1/\sqrt{3}$ for which we optimize the pulse width.

Looking into figure (4.6), we can look at it as the big picture of all we have analyzed before. Now we can clearly see that if $\beta_2 C > 0$ the pulse always undergoes broadening, being in this regime both β_2 and C holding negative values. On the contrary, if $\beta_2 C < 0$ and for chirp values greater than C_{cr} we confirm that pulses suffer compression. Naively, we could think that having no chirp could be better. But, after analyzing figure (4.6), it is clear that such conclusion does not hold true because even though χ_0^{opt} has its minimum value at $C = 0$, χ_1^{opt} for $C = 0$ is higher than the one for $C = C_{cr} = 1/\sqrt{3}$. This means that having no chirp is far from being the optimal solution, despite popular belief.

4.3 Normal Dispersion Regime

In this section, chirped Gaussian pulses whose β_2 is positive are going to be analyzed. As we will see in a moment, many similarities are going to be found with the previous dispersion regime we discussed in the last section. However, we will also find that the value for the chirp parameter will be different and see how different and give a brief note about it.

Once again, some expressions are needed before jumping straight into the full analysis of the matter. Luckily, expressions (4.30), (4.31) and (4.32) are also valid in this regime.

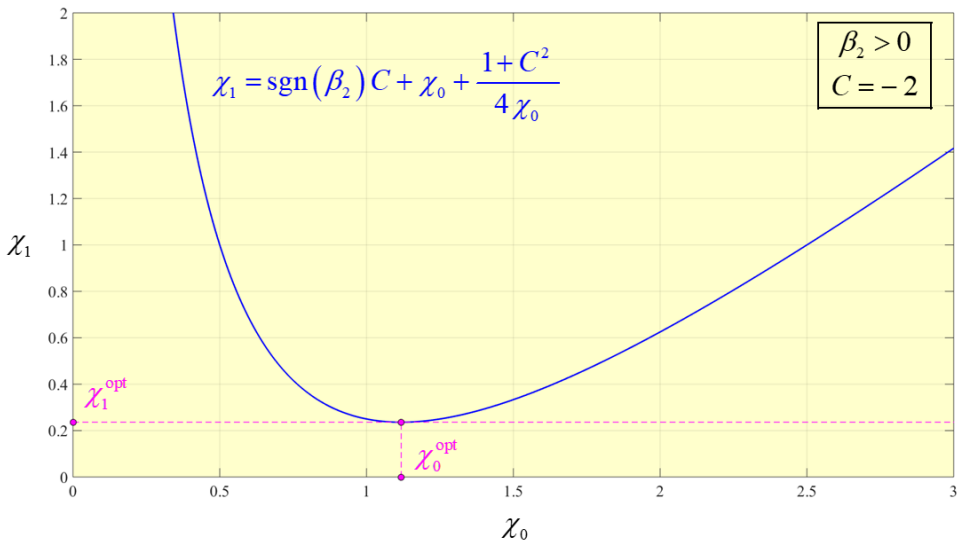

Figure 4.7 - Variation of the normalized output pulse width χ_1 with the normalized input pulse χ_0 for a chirped Gaussian pulse on the normal dispersion regime ($\beta_2 > 0$) and for a chosen value of $C = -2$. In this example, it is also possible to state that $\beta_2 C < 0$.

Analyzing figure (4.7) carefully, we find the curve obtained to be the same as the one presented in figure (4.5). However, since we now are discussing the normal dispersion regime where $\beta_2 > 0$, to have this result to happen, the chirp parameter had to be negative, i.e, $C < 0$. Once again, we can observe that pulse compression may occur since $\beta_2 C < 0$ is the case where this can happen, as already discussed early.

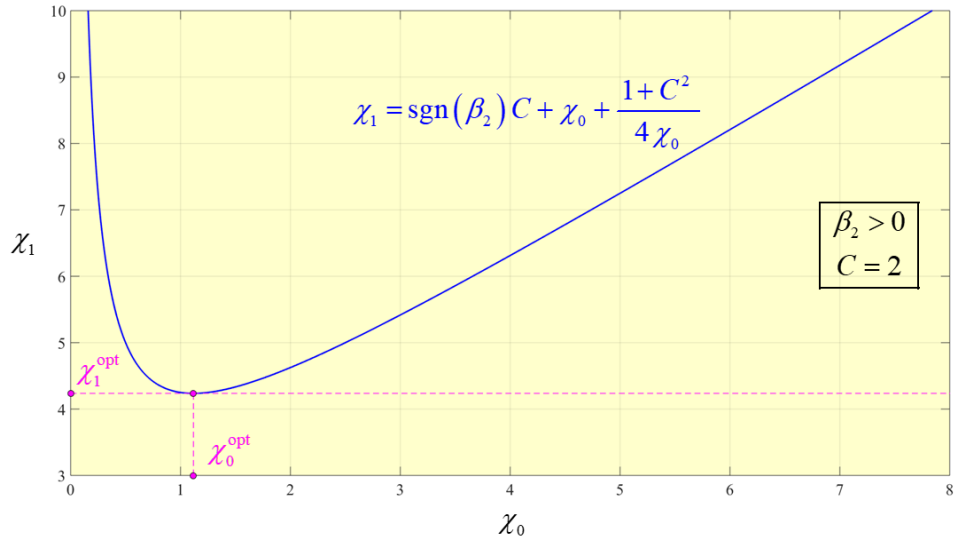

Figure 4.8 - Variation of the normalized output pulse width χ_1 with the normalized input pulse χ_0 for a chirped Gaussian pulse on the normal dispersion regime ($\beta_2 > 0$) and for a chosen value of $C = 2$. In this example, it is also possible to state that $\beta_2 C > 0$.

Analyzing figure (4.8) carefully, we find the curve obtained to be the same as the one presented in figure (4.4). However, since we now are discussing the normal dispersion regime where $\beta_2 > 0$, to have this result to happen, the chirp parameter had to be positive, i.e, $C > 0$. Once again, we can observe that since the product $\beta_2 C > 0$, the pulse will always undergo broadening, as already discussed earlier.

Now, to find the optimum value of the chirp parameter, the same process is going to applied meaning that the expressions (4.31) and (4.32) are going to be plotted and its intersection will give us the value we need but now for the normal dispersion regime.

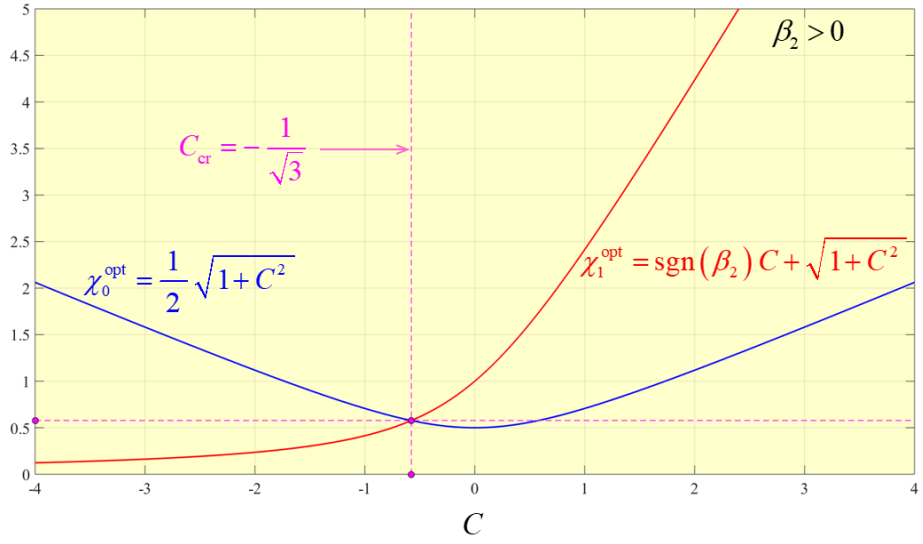

Figure 4.9 – Variation of χ_0^{opt} and χ_1^{opt} with the chirp parameter C, when $\beta_2 > 0$. As shown, the intersection of both curves gives us the critical chirp value, $C_{cr} = -1/\sqrt{3}$ for which we optimize the pulse width.

Analyzing figure (4.9) carefully, we may notice that the curve corresponding to χ_1^{opt} is symmetric to the one obtained in figure (4.6) and since the curve corresponding to χ_0^{opt} is equal to the one plotted in figure (4.6), the result of C_{cr} is going to be equal in module but with an opposite signal, meaning C_{cr} is also symmetric relative to one that belongs to the anomalous dispersion regime. Having this said, we obtain for the normal dispersion regime, $C_{cr} = -1/\sqrt{3}$.

Looking into figure (4.9), we can also see that if $\beta_2 C > 0$ the pulse always undergoes broadening, being in this regime both β_2 and C holding positive values. On the contrary, if $\beta_2 C < 0$ and for chirp values smaller than C_{cr} we confirm that pulses suffer compression. However, the chirp values for which this happens in the normal dispersion regime are all symmetric to the ones in the anomalous dispersion regime.

4.4 Bit-Rate for Chirped Gaussian Pulses

After a clear understanding on how to optimize chirped Gaussian pulses, regardless of the dispersion regime, we saw from expression (4.22) that $\chi_0^{opt} = \chi_1^{opt} = 1/\sqrt{3}$ which means that $\sigma_{max} = \sigma_0 = \sigma_1$. Furthermore, being aware of this fact it was also possible to reach an expression for σ_{max} by doing the following on expression (4.6):

$$\frac{1}{\sqrt{3}} = \frac{\sigma_{max}^2}{|\beta_2|L}, \tag{4.33}$$

since the optimized χ value is $1/\sqrt{3}$ as already seen.

From here, we get the expression presented in (4.23) which now reveals to be crucial to being able to deduct an expression that will give us B_0, which is good practice to remind at this point:

$$\sigma_{max} = 3^{-1/4}\sqrt{|\beta_2|L}\,. \tag{4.34}$$

Now, we know everything we need to write an expression that will define B_0:

$$B_0 = \frac{1}{4\sigma_{max}} = \frac{\sqrt[4]{3}}{4}\frac{1}{\sqrt{|\beta_2|L}} \approx \frac{0.3290}{\sqrt{|\beta_2|L}}. \tag{4.35}$$

At this point, you may be asking yourselves why there is no dependence on the chirp parameter from the expression above. Well, it is logic that was supposed to happen since we found a chirp value which was $C = C_{cr}$ that allowed to optimize σ_{max}. Then, the expression obtained in (4.35) is already the result of such optimization, meaning it is right the way it is. So far, an optimized chirped Gaussian pulse is the one that will give us a higher bit-rate in a single channel, because if we recall expressions (3.21) and (4.28) and comparing them with (4.35), we see the denominator of all of them is the same, but the numerator of expression (4.35) is the highest of the three expressions taken into account. This allows to declare that having chirp in our channel, as long as it is optimized, is actually better than having no chirp at all.

Once again, even more important is to know the product $B_0^2 L$ to get a figure of merit which will allow to better analyze the performance of a fiber-optic communication system giving us a more accurate perception about the performance of such system for different distances. Without further delay, the product $B_0^2 L$ is as follows:

$$B_0^2 L = \frac{F}{|\beta_2|}\,, with\ F = \frac{\sqrt{3}}{16} \approx 0.1083\,. \tag{4.36}$$

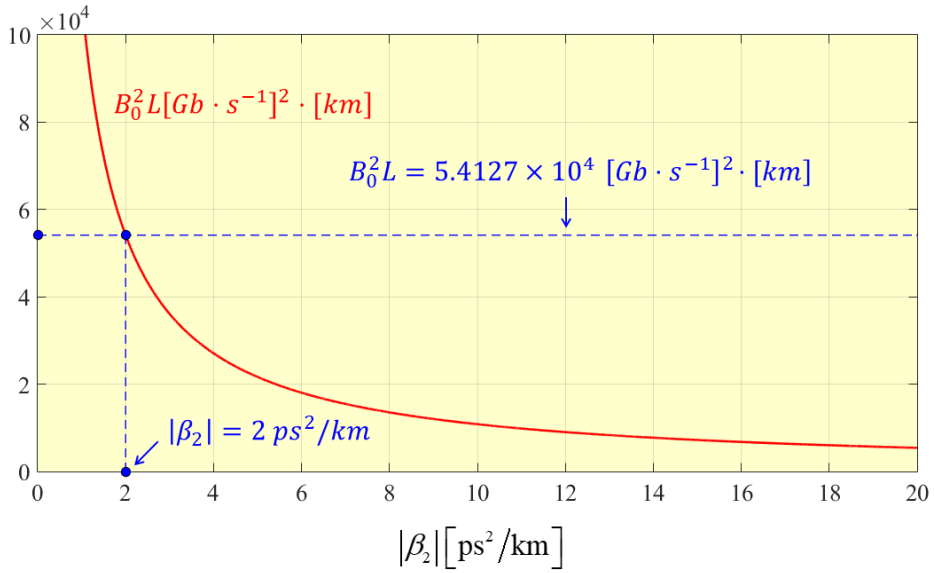

Figure 4.10 - Bit-rate squared product with the length of a given optical fiber for chirped gaussian pulses as an instrument to measure the performance of a fiber-optic communication system. It is possible to see a decay in the performance for higher β_2 values.

Analyzing figure (4.10), comparing with figures (3.3) and (4.3) we may see the benefits of doing an optimization by finding the critical chirp parameter value. It is now clear that for chirped gaussian pulses whose chirp value parameter is $C = C_{cr}$, the performance of fiber-optic communication systems is improved in such conditions. Looking at the chosen example $|\beta_2| = 2\ ps^2/km$, we may see an increase in the bit-rate squared product with the length of a given optical fiber comparing with the cases where we simply did $C = 0$, instead of $C = C_{cr}$. Therefore, we may conclude that having chirp on the system is actually an advantage rather than being a problem.

5. Comparison between Hyperbolic Secant Pulses and Gaussian Pulses

As we already know a Gaussian pulse is a specific case of the chirped Gaussian pulses in which $C = 0$. If so, we may write the incident field as:

$$A(0,t) = A_0 \exp\left(-\frac{t^2}{2T_0}\right). \tag{5.1}$$

The optical field corresponding to unchirped Hyperbolic Secant pulses as the following form:

$$A(0,t) = A_0 \operatorname{sech}\left(\frac{t}{T_0}\right). \tag{5.2}$$

From the previous expressions, it may seem that both pulses are way different from each other. However, if we look at the broadening factor of both pulses, we will see that their behavior is not so different. So, let us consider the broadening factor of both pulses [4]:

$$(1): \left(\frac{\sigma_1}{\sigma_0}\right)^2 = 1 + \left(\frac{\beta_2 L}{2\sigma_0^2}\right)^2, \tag{5.3}$$

$$(2): \left(\frac{\sigma_1}{\sigma_0}\right)^2 = 1 + \left(\frac{\pi\beta_2 L}{6\sigma_0^2}\right)^2. \tag{5.4}$$

Note: from now on, (1) will refer to expressions related to unchirped Gaussian pulses and (2) will refer to expressions related to unchirped Hyperbolic secant pulses.

Just by looking at both expressions, it is possible to see that the only tangible difference is the constant factor, being it equal to 0.5 for unchirped Gaussian pulses and for unchirped Hyperbolic Secant pulses equal to $\pi/6 \approx 0.52$. From here, we could conclude that a "sech" pulse broadens almost at the same rate and exhibits the same qualitative behavior as a Gaussian pulse (assuming $C = 0$ and $\beta_3 = 0$) when the comparison is made on the basis of their RMS width. But, to be sure that we are not getting ahead of ourselves it is going to be made the full analysis of both broadening behaviors, being such analysis supported via numerical solutions and corresponding analytical expressions.

To start, let us write the broadening factor expressions using normalized variables:

$$(1): \chi(\xi) = \chi_0 + \frac{1}{4\chi_0}\xi^2, \tag{5.5}$$

$$(2): \chi(\xi) = \chi_0 + \frac{\pi^2}{36\chi_0}\xi^2. \tag{5.6}$$

Considering $\xi = 1$, the expressions above may be written as follows:

$$(1): \chi_1 = \chi_0 + \frac{1}{4\chi_0}, \tag{5.7}$$

$$(2): \chi_1 = \chi_0 + \frac{\pi^2}{36\chi_0}. \tag{5.8}$$

Now, to find the optimum value for α, we need to know when the value of the derivative $\frac{d\chi}{d\alpha}$ is equal to zero:

$$(1): \frac{d\chi_1}{d\chi_0} = 1 - \frac{1}{4{\chi_0}^2} = 0 \rightarrow \chi_0^{opt} = \frac{1}{2}, \tag{5.9}$$

$$(2): \frac{d\chi_1}{d\chi_0} = 1 - \frac{\pi^2}{36{\chi_0}^2} = 0 \rightarrow \chi_0^{opt} = \frac{\pi}{6} \approx 0.52\,. \tag{5.10}$$

As this point, we clearly see that the optimum input pulse width in both cases is very close. However, we still do not know how it is going to be the width behavior along an optical fiber for both cases. To assure that both cases will remain to be very similar, the following expressions will show how the pulses are going to behave at any given point of an optical fiber. To start, let us find the optimum output pulse width:

$$(1): \chi_1^{opt} = \chi_1\left(\chi_0^{opt}\right) = 1\,, \tag{5.11}$$

$$(2): \chi_1^{opt} = \chi_1\left(\chi_0^{opt}\right) = \frac{\pi}{3} \approx 1.04\,. \tag{5.12}$$

This information gives us the clue that the width behavior for both cases may be very similar. But to absolutely sure, let us look at the expressions that define χ^{opt}:

$$(1): \chi^{opt}(\xi) = \frac{1}{2}(1 + \xi^2), \tag{5.13}$$

$$(2): \chi^{opt}(\xi) = \frac{\pi}{6}(1 + \xi^2). \tag{5.14}$$

Finally, knowing χ_0^{opt} and $\chi^{opt}(\xi)$ from both cases, we may finally write the expressions that will define the pulse width behavior for any given point in the optical fiber:

$$(1): \mu^{opt}(\xi) = \frac{\chi^{opt}(\xi)}{\chi_0^{opt}} = 1 + \xi^2\,, \tag{5.15}$$

$$(2): \mu^{opt}(\xi) = \frac{\chi^{opt}(\xi)}{\chi_0^{opt}} = 1 + \xi^2\,. \tag{5.16}$$

As it is now obvious to see, the pulse width behavior of a Gaussian pulse (assuming $C = 0$ and $\beta_3 = 0$) is the same as the one for a Hyperbolic Secant pulse (considering $C = 0$ and $\beta_3 = 0$).

However, we are not done yet here. There is still more that may be seen from the pulse width behavior results. By calculating $\mu(\xi)$ when $\xi = 0$ and $\xi = 1$, we get the following results:

$$\mu_0 = \mu(0) = 1, \tag{5.17}$$

$$\mu_1 = \mu(1) = 2. \tag{5.18}$$

This means that even in the optimum case, the output pulse width will be twice as much as the input pulse width. The outcome will be the bit-rate being half at the output of the optical fiber in relation to the input of the optical fiber. But, if you remember, if we had chirp in our Gaussian pulse, we could find an optimum chirp value that would give us a way to have exactly the same pulse width at the input and at the output of the optical fiber. With that being said, a huge remark can be made. According to what is common practice, which is nullifying the chirp value of the Gaussian pulses, we realized that doing such practice is far from being the best solution for optimizing the bit-rate value in fiber-optic communication systems. Actually, we do need chirp to truly optimize the bit-rate value of fiber-optic communication systems, which is much different from what it is done nowadays when it comes to deal with Gaussian pulses that present chirp.

To have a visual understanding of the topics discussed before, it will be shown the relation between the output and the input pulse width as well as the behavior of the pulse width along the optical fiber.

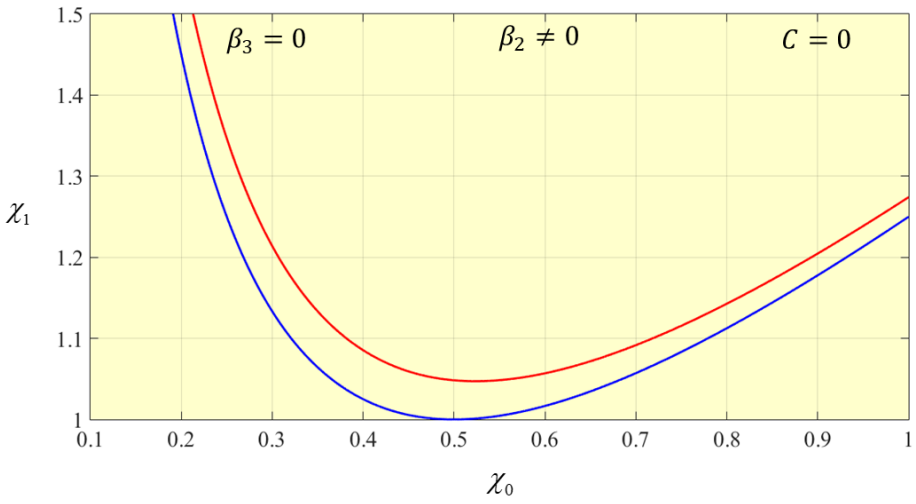

Figure 5.1 - Variation of the normalized output pulse width χ_1 with the normalized input pulse χ_0 for an unchirped Hyperbolic Secant pulse (red curve) and for an unchirped Gaussian pulse (blue curve), being $\beta_2 \neq 0$ and $\beta_3 = 0$.

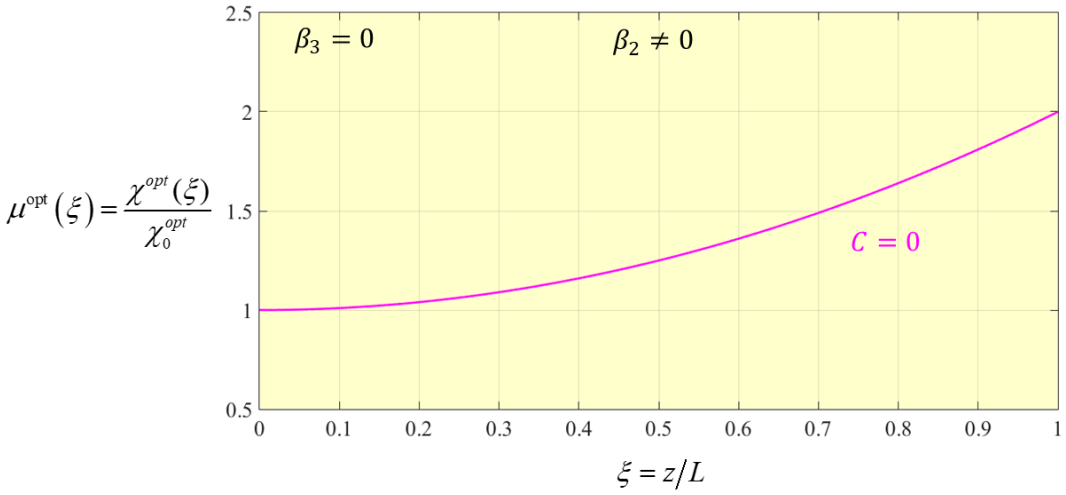

Figure 5.2 - Behavior of the pulse width along the optical fiber for an unchirped Gaussian pulse and for an unchirped Hyperbolic Secant pulse with $\beta_2 \neq 0$ and $\beta_3 = 0$, being $\mu^{opt} = \mu(\chi_0^{opt}, \xi) = 1 + \xi^2$. The pulse width grows monotonically through the entire journey inside the optical fiber.

As it is possible to analyze from figures (5.1) and (5.2), the behavior characteristics for the pulse width are very similar for both cases. In figure (5.1), the blue curve represents the dependence of the output width with the input width for Gaussian pulses (with $C = 0$ and $\beta_3 = 0$) and the red curve represents the dependence of the output width with the input width for Hyperbolic Secant pulses. The curve shape is practically the same in both pulses. The only tiny difference is in the optimum values of the input and output pulse widths, derived from the constant terms being slightly different, but almost the same in practice. However, the similarity between both situations turns out to be completely obvious when we analyze the pulse width behavior along the optical fiber for both pulses. What is seen in figure (5.2) is that the pulse width behavior is exactly the same. That is the reason why figure (5.2) as only one curve. Once more, we can see that no further optimization is possible due to the fact that chirp is not present in any of the pulses, meaning that the maximum bit-rate value for a fiber-optic communication system would be in both cases determined by the pulse width at the output of the optical fiber. Needless to say, this solution is far from being the best one since we do not have any way to reduce the pulse width at the output of the optical fiber, as it is possible if we do have chirp and manage to control its value.

To evaluate the maximum bit-rate value for an unchirped hyperbolic secant pulse, we first must remember the practical rule of thumb applied in fiber-optic communication systems:

$$\sigma_{max} \leq \frac{T_b}{4} = \frac{1}{4B} \rightarrow B \leq B_0 = \frac{1}{4\sigma_{max}}. \tag{5.19}$$

As seen before, for an unchirped hyperbolic secant pulse, $\sigma_{max} = \sigma_1$ which is the width of the signal at the output of the optical fiber. From expression (3.7), it comes that:

$$\chi = \frac{\sigma_1^2}{|\beta_2|L}. \tag{5.20}$$

Knowing from expression (5.12) that:

$$\chi_{opt} = \frac{\pi}{3}, \tag{5.21}$$

we may now obtain the following:

$$\frac{\pi}{3} = \frac{\sigma_{max}^2}{|\beta_2|L}. \tag{5.22}$$

Solving (5.22), we get:

$$\sigma_{max} = \sqrt{\frac{\pi|\beta_2|L}{3}}. \tag{5.23}$$

From here, it is now possible to obtain B_0 by calculating the following:

$$(2): B_0 = \frac{1}{4\sigma_{max}} = \frac{1}{4}\sqrt{\frac{3}{\pi|\beta_2|L}} \approx \frac{0.2443}{\sqrt{|\beta_2|L}}. \tag{5.24}$$

Using a process like the one described for obtaining B_0 for an unchirped hyperbolic secant pulse, we can obtain B_0 for an unchirped gaussian pulse:

$$(1): B_0 = \frac{1}{4\sigma_{max}} = \frac{1}{4\sqrt{|\beta_2|L}} = \frac{0.250}{\sqrt{|\beta_2|L}}. \tag{5.25}$$

From both cases, we may define a figure of merit from the optical fiber digital behavior which is the product $B_0^2 L$. So, from expressions (5.24) and (5.25) it comes that the product $B_0^2 L$ for an unchirped Gaussian pulse and for an unchirped hyperbolic secant pulse, respectively, are:

$$(1): B_0^2 L = \frac{A_G}{|\beta_2|}, with\ A_G = \frac{1}{16}.$$

$$(2): B_0^2 L = \frac{A_H}{|\beta_2|}, with\ A_H = \frac{3}{16\pi}.$$

Let us now look at the influence β_2 has in the value of the product $B_0^2 L$.

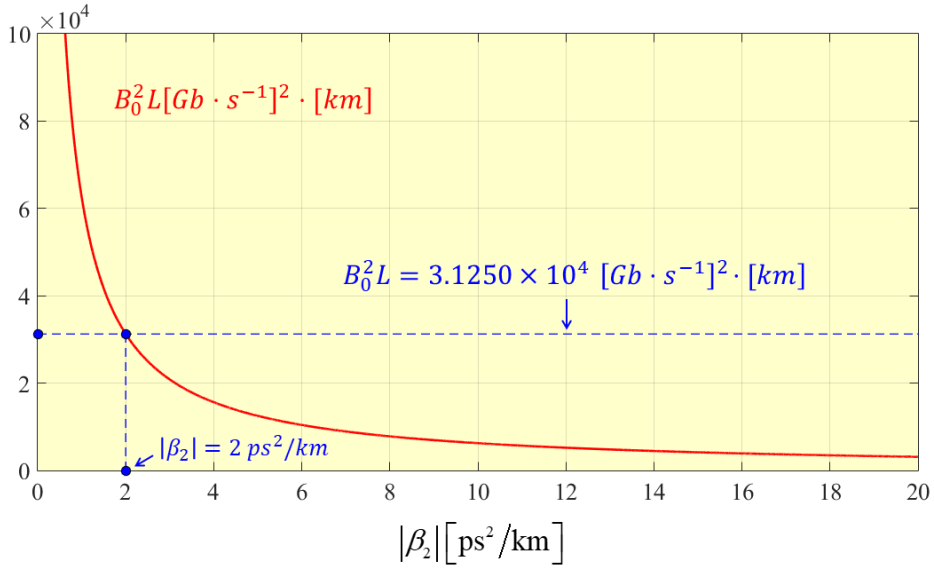

Figure 5.3 - Bit-rate squared product with the length of a given optical fiber ($B_0^2 L$) for unchirped Gaussian pulses as an instrument to measure the performance of a fiber-optic communication system.

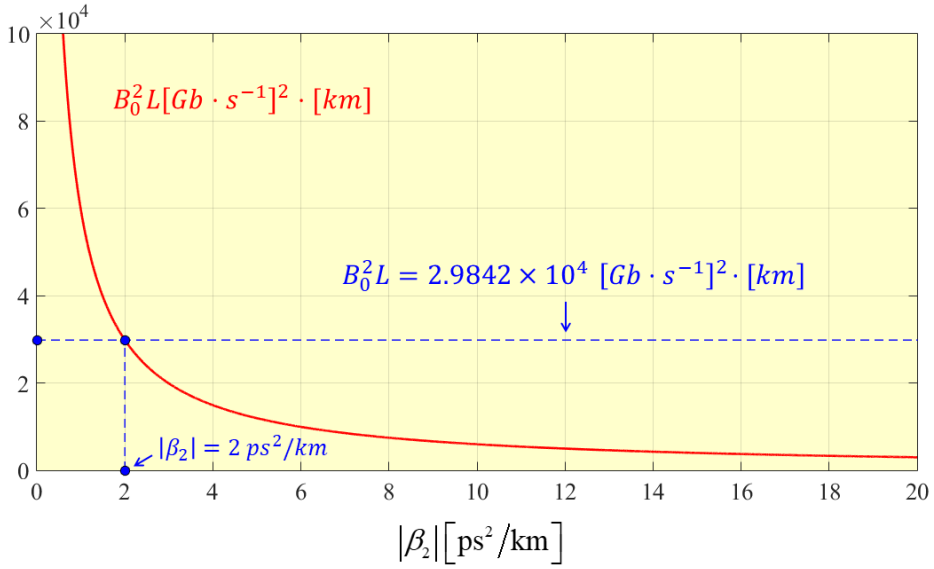

Figure 5.4 – Bit-rate squared product with the length of a given optical fiber ($B_0^2 L$) for unchirped hyperbolic secant pulses as an instrument to measure the performance of a fiber-optic communication system.

Now, looking at the behavior of the product $B_0^2 L$ in figures (5.3) and (5.4), we may see that the product $B_0^2 L$ has the same dependence on β_2 for both cases. However, due to the fact that $A_G > A_H$, we may conclude that for any given distance L, B_0 will always be higher if the chosen pulse is an unchirped Gaussian rather than if it is an unchirped Hyperbolic Secant one. This means the performance of a fiber-optic communication system will be better if instead of transmitting unchirped Hyperbolic secant pulses, we choose to transmit information using unchirped Gaussian pulses.

6. Chirped Gaussian Pulses: Effect of Higher-Order Dispersion

In this chapter, the effect of the higher-order dispersion (β_3) will now be considered in the analysis of the pulse width behavior of chirped Gaussian pulses and corresponding influence on the bit-rate value of a fiber-optic communication system. As a reminder, a chirped Gaussian pulse, at $z = 0$, assumes the form [2]:

$$A(0,t) = A_0 \exp\left[-\frac{1+iC}{2}\left(\frac{t}{T_0}\right)^2\right]. \tag{6.1}$$

The RMS width of a chirped Gaussian pulse assumes the following form [2]:

$$\sigma_0 = \frac{T_0}{\sqrt{2}}. \tag{6.2}$$

Then, the corresponding broadening factor expression for this kind of pulse is given by [2]:

$$\frac{\sigma^2}{\sigma_0^2} = \left(1 + C\frac{\beta_2 z}{2\sigma_0^2}\right)^2 + \left(\frac{\beta_2 z}{2\sigma_0^2}\right)^2 + (1+C^2)^2\left(\frac{\beta_3 z}{4\sqrt{2}\sigma_0^3}\right)^2. \tag{6.3}$$

However, before going into further analysis it will be useful to rewrite the last expression using normalized variables. As such, some steps must be made first which are the ones below:

$$\begin{aligned}\frac{\sigma^2}{|\beta_2|L} = \frac{\sigma_0^2}{|\beta_2|L} + sgn(\beta_2)C\left(\frac{z}{L}\right) + \frac{1}{4}(1+C^2)\frac{|\beta_2|L}{\sigma_0^2}\left(\frac{z}{L}\right)^2 \\ + \frac{1}{32}(1+C^2)^2\frac{\beta_3^2}{|\beta_2|^3 L}\left(\frac{|\beta_2|L}{\sigma_0^2}\right)^2\left(\frac{z}{L}\right)^2.\end{aligned} \tag{6.4}$$

Introducing a new adimensional coefficient called a, which is:

$$a^2 = \frac{\beta_3^2}{|\beta_2|^3 L}, \tag{6.5}$$

it will be useful to rewrite the broadening factor expression. But, before we proceed on writing our normalized broadening factor expression, some considerations are important to have in mind. In the last chapters, we always considered $\beta_3 = 0$, which by default leads to $a = 0$ and we would recover the expression presented in (4.5) which was:

$$\frac{\sigma^2}{|\beta_2|L} = \frac{\sigma_0^2}{|\beta_2|L} + sgn(\beta_2)C\left(\frac{z}{L}\right) + \frac{1}{4}(1+C^2)\frac{|\beta_2|L}{\sigma_0^2}\left(\frac{z}{L}\right)^2. \tag{6.6}$$

However, from now on we will always consider in this chapter [3]:

$$a^2 = \frac{\beta_3^2}{|\beta_2|^3 L} \neq 0 \; where \; \beta_2 \neq 0. \tag{6.7}$$

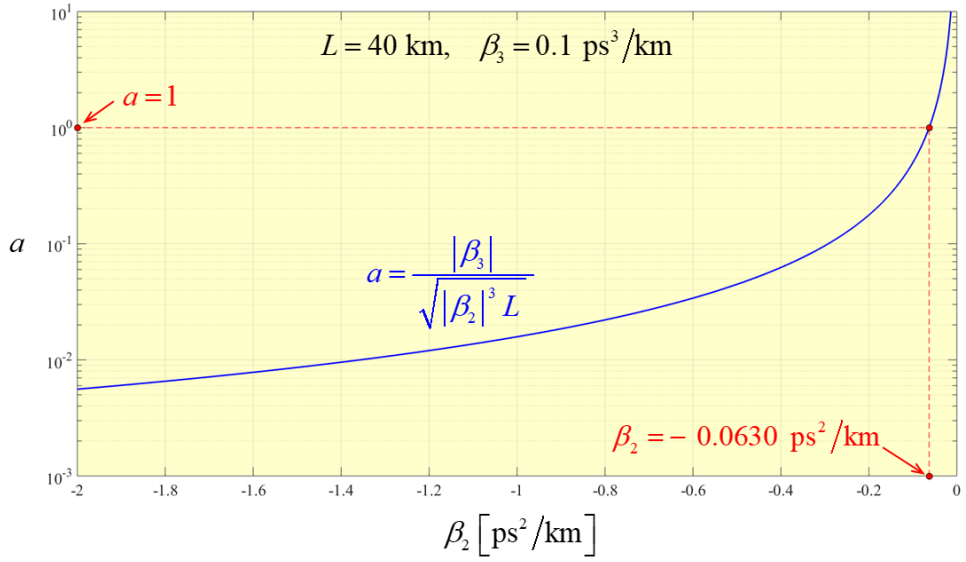

Figure 6.1 – Variation of the adimensional coefficient a with the group-velocity dispersion parameter β_2 for an optical fiber with $L = 40\ km$ and a higher-order dispersion parameter $\beta_3 = 0.1\ ps^3/km$. As it is possible to observe, the fewer the presence of β_2 (as it approaches zero), the greater is the influence of β_3 in the width of the signal.

In figure (6.1), it is presented a concrete example with a fixed value of L and β_3 where we can observe how the value of the adimensional coefficient changes according to β_2. As we can see, with the decreasing of β_2 in module, we see a faster increase of a as β_2 approaches 0. If β_2 is very small (tending to 0), this means that the influence of β_3 in the width of the signal will dominate over the influence of β_2. Having this said, this means that a high value of the adimensional coefficient ($a > 1$) tells the influence of β_3 is greater than the one coming from β_2 in the pulse width of the signal. As such, it is now clear why it is going to be important to discuss the effects of β_3 in chirped Gaussian pulses shape and resulting bit-rate.

Now that we have the motivation to proceed with the normalization of the broadening factor with $\beta_3 \neq 0$, let us remind the normalized variables introduced in (4.6), (4.7) and (4.9):

$$\chi = \frac{\sigma^2}{|\beta_2|L}, \tag{6.8}$$

$$\begin{cases} z = 0 \rightarrow \sigma = \sigma_0 \rightarrow \chi_0 = \dfrac{\sigma_0^2}{|\beta_2|L} \\ z = L \rightarrow \sigma = \sigma_1 \rightarrow \chi_1 = \dfrac{\sigma_1^2}{|\beta_2|L} \end{cases}, \tag{6.9}$$

$$0 \leq \xi = \frac{z}{L} \leq 1\,. \tag{6.10}$$

And, of course, we shall not forget the p parameter introduced in (4.8) which stays the same:

$$p = \frac{1}{4}(1 + C^2) \geq \frac{1}{4}. \tag{6.11}$$

As such, the broadening factor may now be rewritten as:

$$\chi = \chi_0 + sgn(\beta_2)C\xi + \frac{p}{\chi_0}\left(1 + a^2\frac{p}{2\chi_0}\right)\xi^2 . \tag{6.12}$$

Then, the pulse width behavior will be defined as:

$$\mu = \frac{\chi}{\chi_0} = 1 + sgn(\beta_2)C\left(\frac{\xi}{\chi_0}\right) + p\left(1 + a^2\frac{p}{2\chi_0}\right)\left(\frac{\xi}{\chi_0}\right)^2 . \tag{6.13}$$

Now, recalling how χ_1 and μ_1 were defined in (4.12), we may now write them as:

$$\chi_1 = \chi_0 + sgn(\beta_2)C + \frac{p}{\chi_0}\left(1 + a^2\frac{p}{2\chi_0}\right), \tag{6.14}$$

$$\mu_1 = 1 + \left[sgn(\beta_2)C + \frac{p}{\chi_0}\left(1 + a^2\frac{p}{2\chi_0}\right)\right]\left(\frac{1}{\chi_0}\right). \tag{6.15}$$

Now, it is important for us to know what the optimum values are for χ_0 and χ_1. To get there, we must first do the following calculation:

$$\frac{d\chi_1}{d\chi_0} = 1 - \frac{p}{\chi_0^2} - a^2\frac{p^2}{\chi_0^3} = 0 . \tag{6.16}$$

However, the equation that comes out from the previous expression is the following cubic equation:

$$\chi_0^3 - p\chi_0 - a^2p^2 = 0 . \tag{6.17}$$

The best way to solve the cubic equation that was previously deducted is graphically. As such, we must first rewrite it in a way we can get two curves that will intersect at some point to find a meaningful solution:

$$\chi_0^3 = p(\chi_0 + a^2p) , \tag{6.18}$$

$$\frac{\chi_0^4}{p} = \chi_0(\chi_0 + a^2p) . \tag{6.19}$$

If we define $x = \chi_0$, the left side of (6.19) will look like this:

$$y = \frac{x^2}{\sqrt{p}} . \tag{6.20}$$

Then, the whole (6.19) equation may be written as:

$$y^2 = x(x + a^2p) . \tag{6.21}$$

At this point, the expressions defining the two curves we need to plot to find a solution for χ_0^{opt} are the ones defined in (6.20) and (6.21). So, all we have to do is to find a solution for the given equation:

$$\frac{x^2}{\sqrt{p}} = \sqrt{x(x + a^2p)} , \tag{6.22}$$

from which we will have a solution which is a point $P(x_0, y_0)$, whose x_0 value will be equal to χ_0^{opt}.

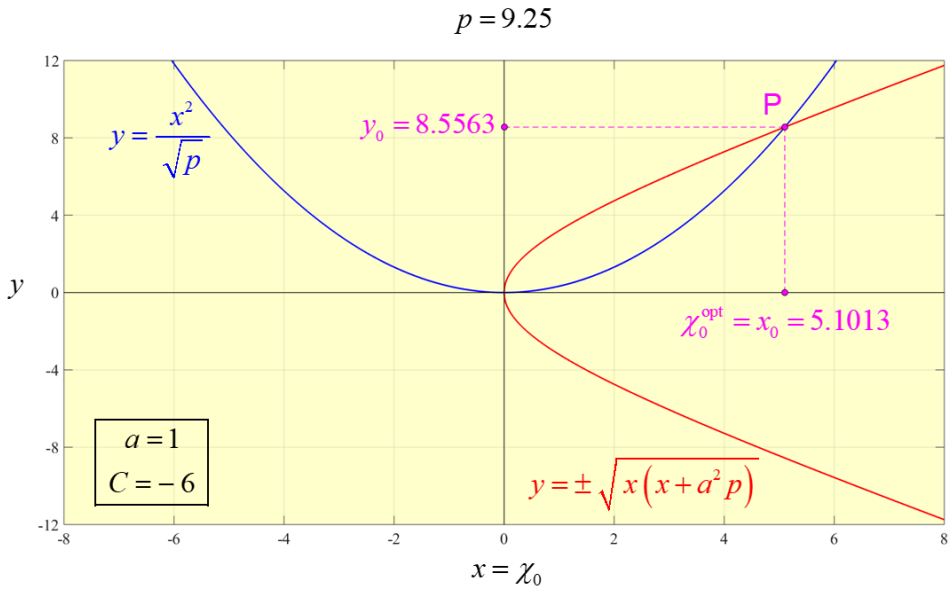

Figure 6.2 – Graphical solution of the cubic equation presented in (6.17) for $C = -6$ and $a = 1$. As observed the two curves intersect each other twice. However, P is the only solution that matters since the other one, which is $O(0,0)$ has no physical meaning.

Analyzing figure (6.2), two solutions for the cubic equation shown in (6.17) arise. However, the intersection at the origin if taken as a valid solution would mean it was possible to have pulses whose width was zero, or another to say it is nonexistent. Well, that is not possible physically speaking since it would mean the possibility of having infinite bit-rate values and as we already know, such thing is impossible due to the dispersion effects we are discussing in the course of this study.

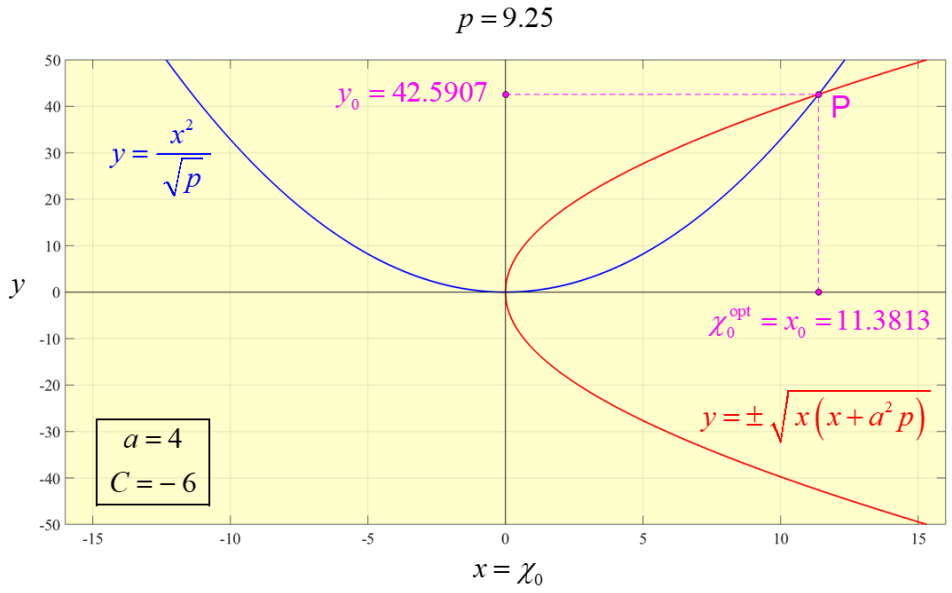

Figure 6.3 – Graphical solution of the cubic equation presented in (6.17) for $C = -6$ and $a = 4$. As observed the two curves intersect each other twice. However, P is the only solution that matters since the other one, which is $O(0,0)$ has no physical meaning.

Analyzing figure (6.3), we may notice that χ_0^{opt} is more than double than the one obtained in figure (6.2). This is no surprise since in figure (6.3) we are assuming that the influence of β_3 in the pulse width behavior is much greater than the on assumed in figure (6.2). So, the examples shown in those figures confirm why we must not disregard the effects of the higher-order dispersion parameter since it may influence the width of the signal severely, making it much wider than if there was no β_3.

Now that we understood how to graphically solve the cubic equation presented in (6.17), it is now time to show the analytical approach. The first thing we need to know is to have in mind the transition coefficient, which is this one [3]:

$$a_{tr} = \frac{2\sqrt{3}}{3}[3(1+C^2)]^{\frac{1}{4}}. \tag{6.23}$$

Then, after calculating a_{tr} depending on the value of the chirp parameter of the signal we may need to consider, χ_0^{opt} will have one of the two following forms:

$$\begin{cases} a \le a_{tr} \rightarrow \chi_0^{opt} = 2\sqrt{\frac{p}{3}}\cos\left[\frac{1}{3}cos^{-1}\left(\frac{9a^2}{2}\sqrt{\frac{p}{3}}\right)\right] \\ a \ge a_{tr} \rightarrow \chi_0^{opt} = 2\sqrt{\frac{p}{3}}\cosh\left[\frac{1}{3}cosh^{-1}\left(\frac{9a^2}{2}\sqrt{\frac{p}{3}}\right)\right] \end{cases}. \tag{6.24}$$

To ensure things are clear, for every given C value it will correspond a value for a_{tr}. Then, depending on how great the influence of β_3 is, the value of the adimensional parameter will vary accordingly, i.e, in the same way. So, a being lower or higher than a_{tr} will decide which of the two expressions in (6.24) will define χ_0^{opt}.

As a remark, if we do $a = 0$ it is possible to recover the expression of χ_0^{opt} shown in (4.15) where it is assumed $\beta_3 = 0$:

$$\chi_0^{opt} = 2\sqrt{\frac{p}{3}}\cos\left(\frac{\pi}{6}\right) = \sqrt{p} = \frac{1}{2}\sqrt{1+C^2}. \tag{6.25}$$

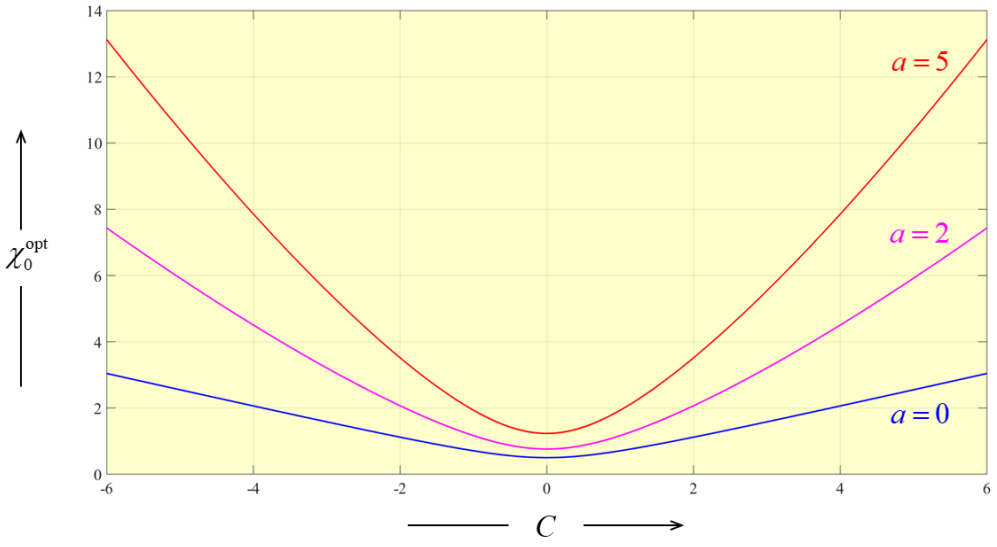

Figure 6.4 – Variation of χ_0^{opt} with the chirp parameter C for different fixed values of a. As a increases, the optimum input pulse width also increases for every C value. The graph shows a symmetric behavior due to the way a_{tr} and p are defined.

Looking at figure (6.4) we see that regardless of what the value of chirp parameter C is, bigger a values will always make χ_0^{opt} to be higher. This means that a strong presence of β_3 will mean a need of a higher input pulse width which negatively influences the bit-rate value of fiber-optic communication systems. Another fact worth mentioning is the symmetrical shape of the curve. This is due to the way a_{tr} and p are defined, since in both expressions the chirp parameter C is squared and of course the higher is the chirp parameter value in module, the higher will be χ_0^{opt}.

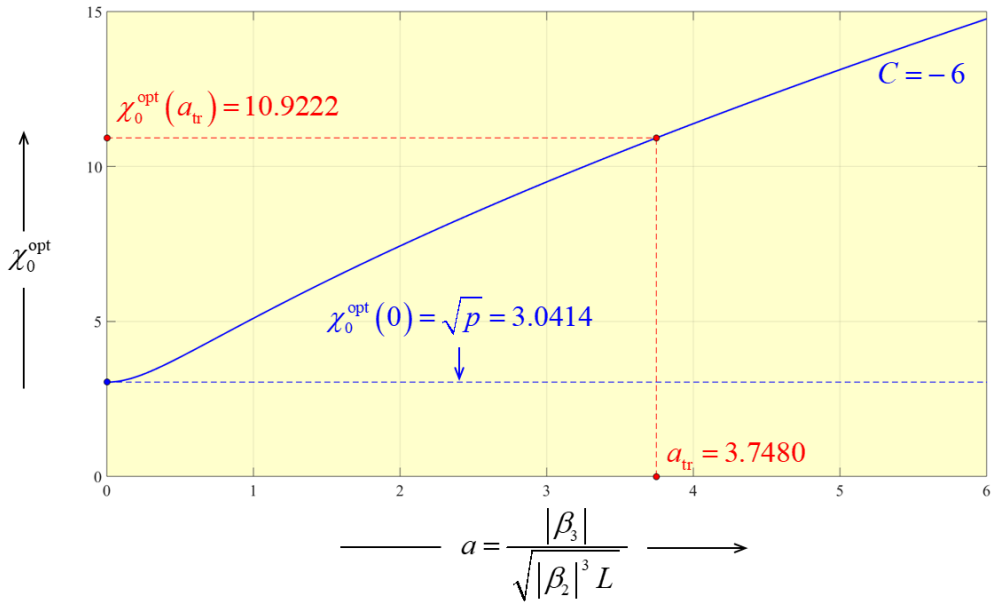

Figure 6.5 - Variation of χ_0^{opt} with the adimensional coefficient a for a fixed value of the chirp parameter, $C = -6$. As it is possible to observe, the higher the value of a the higher will be χ_0^{opt} for that fixed chirp parameter value.

Looking at figure (6.5), we can see it as another way to confirm the analysis done in figure (6.4). From a different perspective, we may see that a higher value for the adimensional coefficient a will always translate into a greater χ_0^{opt} value for a given C value. As such, we may confirm how enormous may be the effect of β_3 in the optimum input pulse width. Even more, as figure (6.5) shows there is a huge gap between the values of $\chi_0^{opt}(0)$ and $\chi_0^{opt}(a_{tr})$. The latter is more than 3.5 times larger than the first one, meaning the potential bit-rate would differ in the same proportion, which is obviously a huge difference.

6.1 Unchirped Gaussian Pulses

In this section, we are going to analyze the specific case when a Gaussian pulse has no chirp, $C = 0$. Firstly, we calculate the expression for χ_1 defined in (6.14) but now with no chirp:

$$\chi_1 = \chi_0 + \frac{1}{4\chi_0}\left(1 + a^2\frac{1}{8\chi_0}\right). \tag{6.26}$$

If we also did $a = 0$, we would recover the expression obtained in (4.24) when considering no effects of third-order dispersion in the pulse width of the signals.

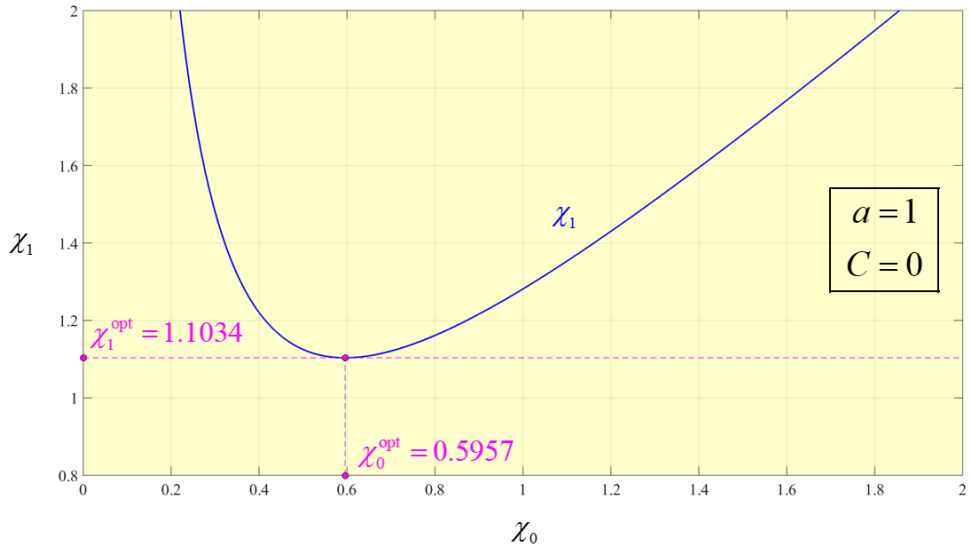

Figure 6.6 - Variation of the normalized output pulse width χ_1 with the normalized input pulse χ_0 for an unchirped Gaussian pulse with $a = 1$. From the graph we see a minimum for which $\chi_0^{opt} = 0.5957$ and $\chi_1^{opt} = 1.1034$.

Comparing figure (6.6) with figure (6.1), we see that both χ_0^{opt} and χ_1^{opt} increased. Since the only parameter that differ from both graphs is the adimensional coefficient a, we therefore conclude once more that the presence of β_3 will be prejudicial for the bit-rate in fiber-optic communication systems, even when there is no chirp present in Gaussian pulses propagating across an optical fiber.

6.2 Critical Value of the Chirp Parameter

In this section, it will be shown how to get the critical value of the chirp parameter, C_{cr}. Firstly, if we recall the process explicated in (4.20) we know that we need to have in mind the expression that defines μ_1^{opt}. Since we know already μ_1 from (6.15), we may write μ_1^{opt} as:

$$\mu_1^{opt} = 1 + \left[sgn(\beta_2)C + \frac{p}{\chi_0^{opt}}\left(1 + a^2\frac{p}{2\chi_0^{opt}}\right)\right]\left(\frac{1}{\chi_0^{opt}}\right), \tag{6.27}$$

being χ_0^{opt} defined according to the expressions shown in (6.24).

Furthermore, since p has a dependence in C there is going to be a critical p value, p_{cr} which will be:

$$p_{cr} = \frac{1}{4}(1 + C_{cr}^2)\,. \tag{6.28}$$

So, as done in (4.20), we need to do the same process but now for (6.27). This means we will need to solve the following equation:

$$sgn(\beta_2)C_{cr} + \frac{p_{cr}}{\chi_0^{opt}}\left(1 + a^2\frac{p_{cr}}{2\chi_0^{opt}}\right) = 0\,. \tag{6.29}$$

Rearranging equation (6.29), we can make it look nicer just like this:

$$32\left(\chi_0^{opt}\right)^2 sgn(\beta_2)C_{cr} + 8\chi_0^{opt}[1 + (sgn(\beta_2)C_{cr})^2] + a^2(1 + (sgn(\beta_2)C_{cr})^2)^2 = 0 \tag{6.30}$$

Solving the last equation will give us the value of C_{cr}. However, in that equation, the optimum value χ_0^{opt} is itself a function of C_{cr}. Being aware of such fact, there is only one way to make it easier to get the value of C_{cr} which is by doing a numerical simulation. Trying to solve the last equation analytically would be a tremendous effort.

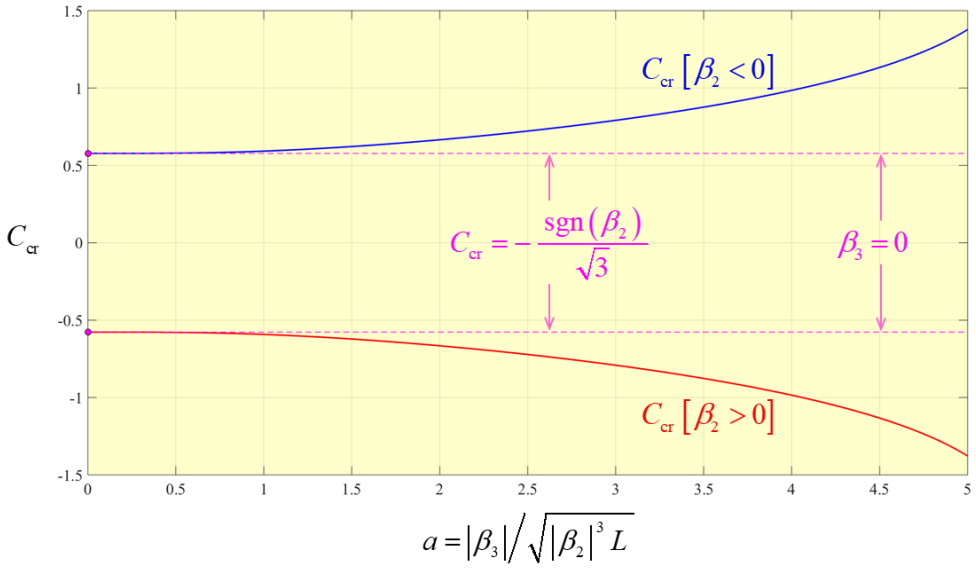

Figure 6.7 – Variation of the chirp critical value, C_{cr} with the adimensional coefficient, a. As it can be observed, the chirp critical value always increases in module for higher values of the adimensional coefficient, regardless of the dispersion regime we may consider.

Analyzing figure (6.7), we see that the chirp critical value will have to be higher if the effects of the third-order dispersion parameter, β_3 are greater than in cases which is not (a equal or close to 0 for example). This means that the presence of chirp will need to higher in order to optimize the bit-rate on the fiber-optic communication systems. Another thing worth mentioning is the symmetry of the chirp critical values curve for both dispersion regimes. The symmetry tells us that the rate of growth in the value of the chirp critical values is the same, being the only difference in the values of C_{cr} their signal which is the opposite between the two dispersion regimes.

6.3 Normal Dispersion Regime

In this section, we will analyze chirped Gaussian pulses whose β_2 is positive. We will detect some similarities with figures (4.7), (4.8) and (4.9) but also important differences from the case where $\beta_3 = 0$.

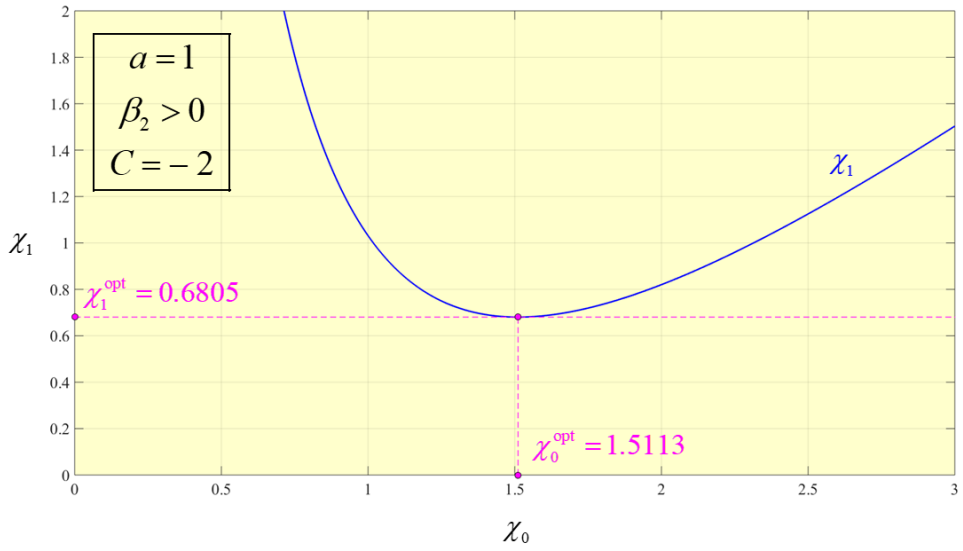

Figure 6.8 - Variation of the normalized output pulse width χ_1 with the normalized input pulse χ_0 for a chirped Gaussian pulse on the normal dispersion regime ($\beta_2 > 0$), for a chosen value of $C = -2$ and for a chosen value of $a = 1$. In this example, it is also possible to state that $\beta_2 C < 0$.

Looking at figure (6.8), we may notice that like in figure (4.7), pulse compression may still occur. However, the optimum values of χ_0^{opt} and χ_1^{opt} presented in figure (6.8) are now bigger than the ones observed in figure (4.7). The reason behind this is the presence of β_3 in the channel. As such, the consequence will be wider pulse widths and subsequently higher optimum χ_0^{opt} and χ_1^{opt} values to optimize the performance of fiber-optic communication systems.

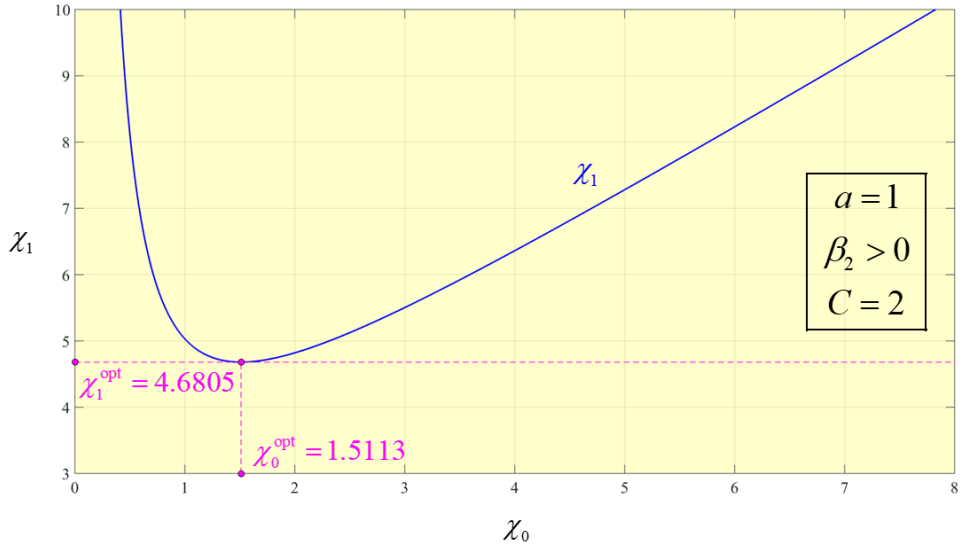

Figure 6.9 - Variation of the normalized output pulse width χ_1 with the normalized input pulse χ_0 for a chirped Gaussian pulse on the normal dispersion regime ($\beta_2 > 0$), for a chosen value of $C = 2$ and for a chosen value of $a = 1$. In this example, it is also possible to state that $\beta_2 C > 0$.

Looking at figure (6.9), we may notice that like figure (4.8), pulse broadening will always occur. However, the optimum values of χ_0^{opt} and χ_1^{opt} presented in figure (6.9) are now bigger than the ones observed in figure (4.8). The reason behind this is the presence of β_3 in the channel. As such, the consequence will be wider pulse widths and subsequently higher optimum χ_0^{opt} and χ_1^{opt} values to optimize the performance of fiber-optic communication systems.

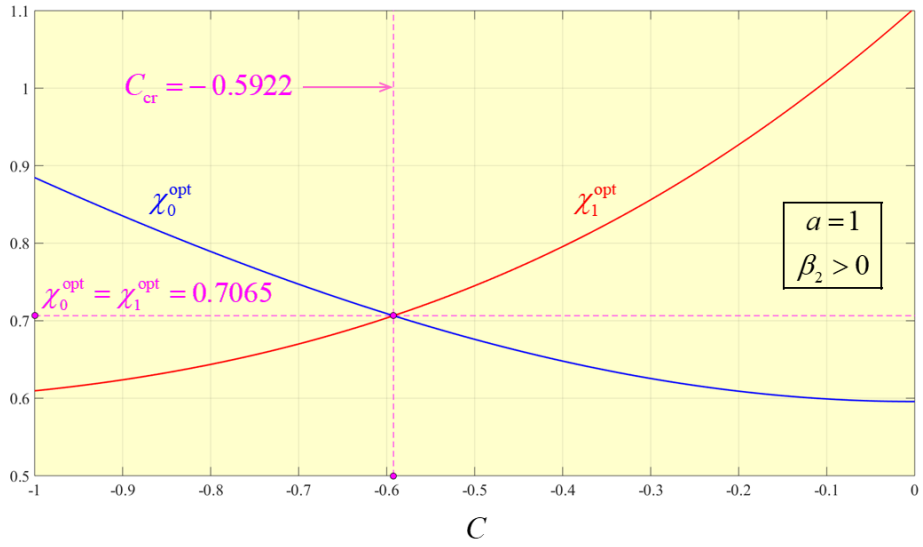

Figure 6.10 - Variation of χ_0^{opt} and χ_1^{opt} with the chirp parameter C, when $\beta_2 > 0$ and for a fixed value of $a = 1$. As shown, the intersection of both curves gives us the critical chirp value, $C_{cr} = -0.5922$ for which we optimize the pulse width.

Analyzing figure (6.10), we may notice that the behavior of both curves corresponding to χ_0^{opt} and χ_1^{opt} is very similar to the one seen in figure (4.9). In other words, for values lower than C_{cr}, the graph shows that Gaussian pulses with those chirp values will experience compression and the opposite will happen to the ones with a higher chirp value than C_{cr}. However, due to the effect of higher-order dispersion β_3, the value of χ_0^{opt} and χ_1^{opt} is slightly higher than the one corresponding to figure (4.9) and C_{cr} is also a bit higher than the one when β_3 is neglected.

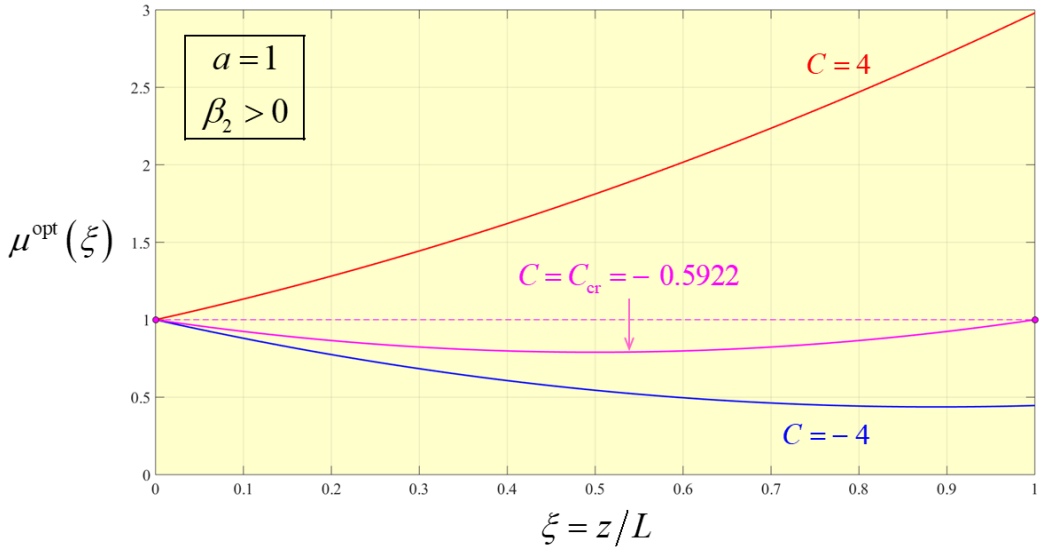

Figure 6.11 – Optimum pulse width behavior of a chirped Gaussian pulse in the normal dispersion regime for $C = 4$, $C = -4$ and $C = C_{cr}$ with a fixed value of $a = 1$. As predicted, when $C = C_{cr}$ the pulse width is the same at the input as it is at the output of the optical fiber. For $C = 4$, the pulse always broadens since $\beta_2 C > 0$ and for $C = -4$ the pulse experiences compression because $\beta_2 C < 0$.

Analyzing figure (6.11), we can see how the pulse width behaves along its entire journey inside an optical fiber. For $C = 4$, the pulse width increases continuously and if such pulse was being used to make the transmission of information, the bit-rate would be determined by the output pulse width since it would be the largest one in that case. For $C = -4$, the pulse width decreases continuously meaning that contrary to the case when $C = 4$, it would be the input pulse width to determine the bit-rate value of the system since now it would be the largest one. However, for $C = C_{cr}$ the bit-rate could be calculated by either taking the input pulse width or the output pulse width, since they would be the equal. The case $C = C_{cr}$ is the best to implement in practice because it is more feasible in practice to have a fiber-optic communication system with a lower value for the chirp parameter, even though in terms of bit-rate, the case when $C = -4$ could also do the job, but it would be harder to implement and it does not matter if the pulse in the middle of the journey is not as large as when $C = C_{cr}$ since the input pulse width is equal in both cases and the highest one when $C = -4$. A final note to make here, is that the behavior of the pulse width observed for $C = C_{cr}$ is the confirmation of the results shown in figure (6.7) since it predicted that for $a = 1$ the critical chirp value would be the one shown in figure (6.11) which is the one making the input pulse width being equal to the output pulse width.

6.4 Anomalous Dispersion Regime

In this section, we will analyze chirped Gaussian pulses whose β_2 is negative. We will detect some similarities with figures (4.4), (4.5) and (4.6) but also important differences from the case where $\beta_3 = 0$.

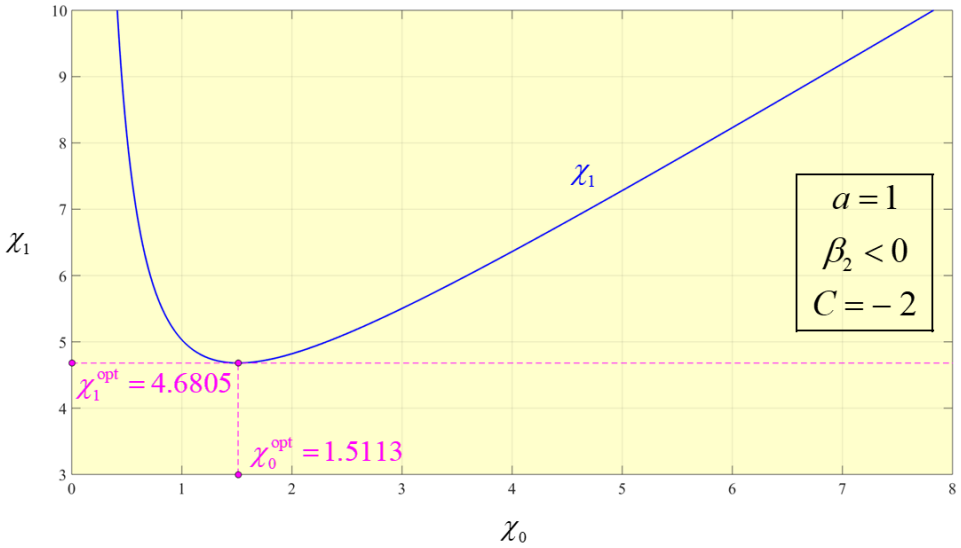

Figure 6.12 - Variation of the normalized output pulse width χ_1 with the normalized input pulse χ_0 for a chirped Gaussian pulse on the anomalous dispersion regime ($\beta_2 < 0$), for a chosen value of $C = -2$ and for a chosen value of $a = 1$. In this example, it is also possible to state that $\beta_2 C > 0$.

Looking at figure (6.12), we may notice that like figure (4.4), pulse broadening will always occur. However, the optimum values of χ_0^{opt} and χ_1^{opt} presented in figure (6.12) are now bigger than the ones observed in figure (4.4). The reason behind this is the presence of β_3 in the channel. As such, the consequence will be wider pulse widths and subsequently higher optimum χ_0^{opt} and χ_1^{opt} values to optimize the performance of fiber-optic communication systems.

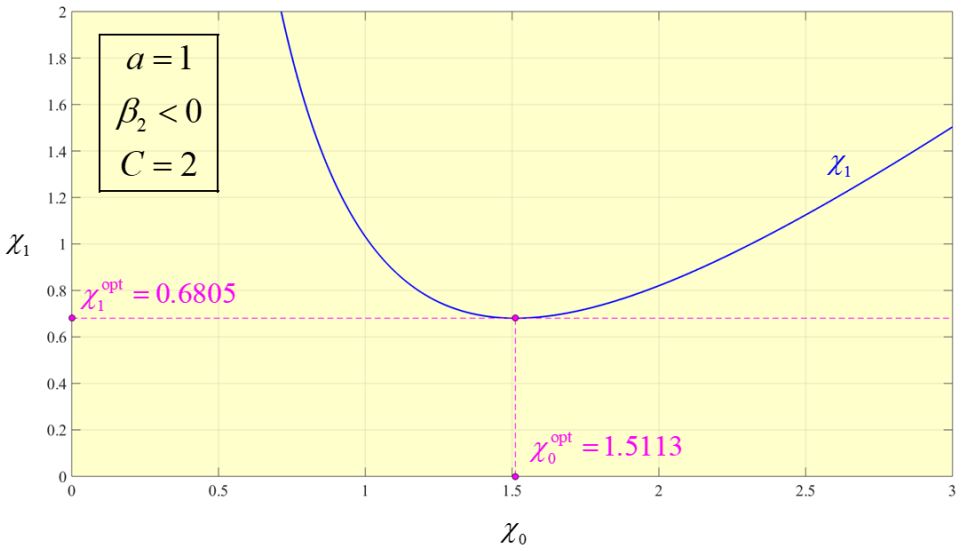

Figure 6.13 - Variation of the normalized output pulse width χ_1 with the normalized input pulse χ_0 for a chirped Gaussian pulse on the anomalous dispersion regime ($\beta_2 < 0$), for a chosen value of $C = 2$ and for a chosen value of $a = 1$. In this example, it is also possible to state that $\beta_2 C < 0$.

Looking at figure (6.13), we may notice that like in figure (4.5), pulse compression may still occur. However, the optimum values of χ_0^{opt} and χ_1^{opt} presented in figure (6.13) are now bigger than the ones observed in figure (4.5). The reason behind this is the presence of β_3 in the channel. As such, the consequence will be wider pulse widths and subsequently higher optimum χ_0^{opt} and χ_1^{opt} values to optimize the performance of fiber-optic communication systems.

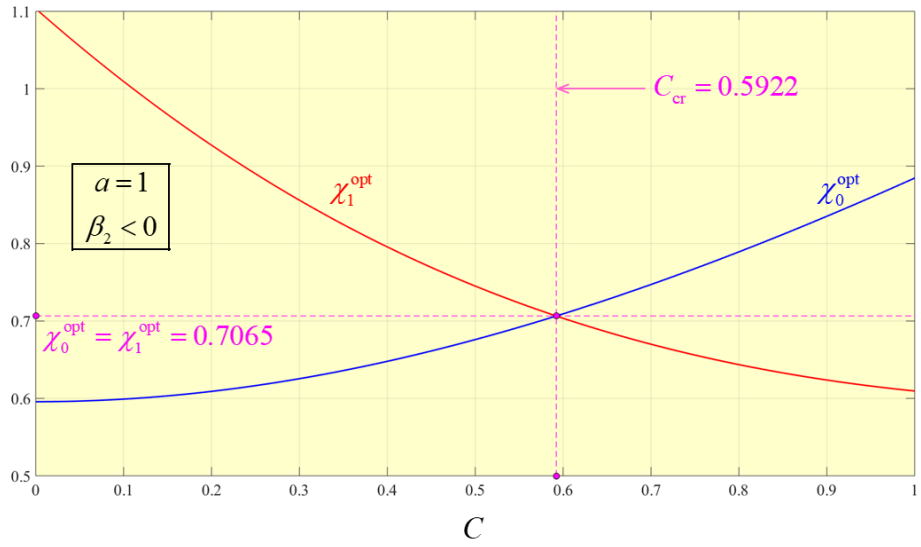

Figure 6.14 - Variation of χ_0^{opt} and χ_1^{opt} with the chirp parameter C, when $\beta_2 < 0$ and for a fixed value of $a = 1$. As shown, the intersection of both curves gives us the critical chirp value, $C_{cr} = 0.5922$ for which we optimize the pulse width.

Analyzing figure (6.14), we may notice that the behavior of both curves corresponding to χ_0^{opt} and χ_1^{opt} is very similar to the one seen in figure (4.6). In other words, for values higher than C_{cr}, the graph shows that Gaussian pulses with those chirp values will experience compression and the opposite will happen to the ones with a lower chirp value than C_{cr}. However, due to the effect of higher-order dispersion β_3, the value of χ_0^{opt} and χ_1^{opt} is slightly higher than the one corresponding to figure (4.6) and C_{cr} is also a bit higher than the one when β_3 is neglected. Worth noticing that the critical value of the chirp parameter is symmetric to the one presented in the normal dispersion regime.

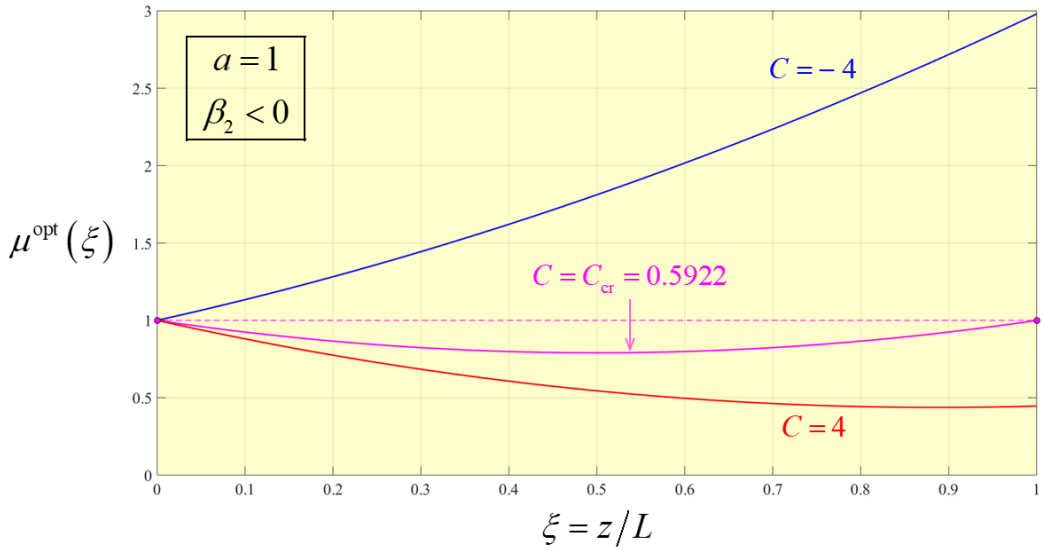

Figure 6.15 - Optimum pulse width behavior of a chirped Gaussian pulse in the anomalous dispersion regime for $C = -4$, $C = 4$ and $C = C_{cr}$ with a fixed value of $a = 1$. As predicted, when $C = C_{cr}$ the pulse width is the same at the input as it is at the output of the optical fiber. For $C = -4$, the pulse always broadens since $\beta_2 C > 0$ and for $C = 4$ the pulse experiences compression because $\beta_2 C < 0$.

Analyzing figure (6.15), we can see how the pulse width behaves along its entire journey inside an optical fiber. For $C = -4$, the pulse width increases continuously and if such pulse was being used to make the transmission of information, the bit-rate would be determined by the output pulse width since it would be the largest one in that case. For $C = 4$, the pulse width decreases continuously meaning that contrary to the case when $C = -4$, it would be the input pulse width to determine the bit-rate value of the system since now it would be the largest one. However, for $C = C_{cr}$ the bit-rate could be calculated by either taking the input pulse width or the output pulse width, since they would be the equal. The case $C = C_{cr}$ is the best to implement in practice because it is more feasible in practice to have a fiber-optic communication system with a lower value for the chirp parameter, even though in terms of bit-rate, the case when $C = 4$ could also do the job, but it would be harder to implement and it does not matter if the pulse in the middle of the journey is not as large as when $C = C_{cr}$ since the input pulse width is equal in both cases and the highest one when $C = 4$. A final note to make here, is that the behavior of the pulse width observed for $C = C_{cr}$ is the confirmation of the results shown in figure (6.7) since it predicted that for $a = 1$ the critical chirp value would be the one shown in figure (6.15) which is the one making the input pulse width being equal to the output pulse width.

So far, we have seen in figures (6.12) and (6.13) how to get χ_0^{opt} and χ_1^{opt} for a given C value and fixed value of a; in figure (6.14) how to find the critical chirp parameter value C_{cr} for a given a value and in figure (6.15) it was confirmed that the obtained C_{cr} in figure (6.14) allowed to obtain the same pulse width at the input and at the output of the optical fiber. But now, for a fixed value of a and different C values, we will see how χ_1^{opt} is related with χ_0^{opt}.

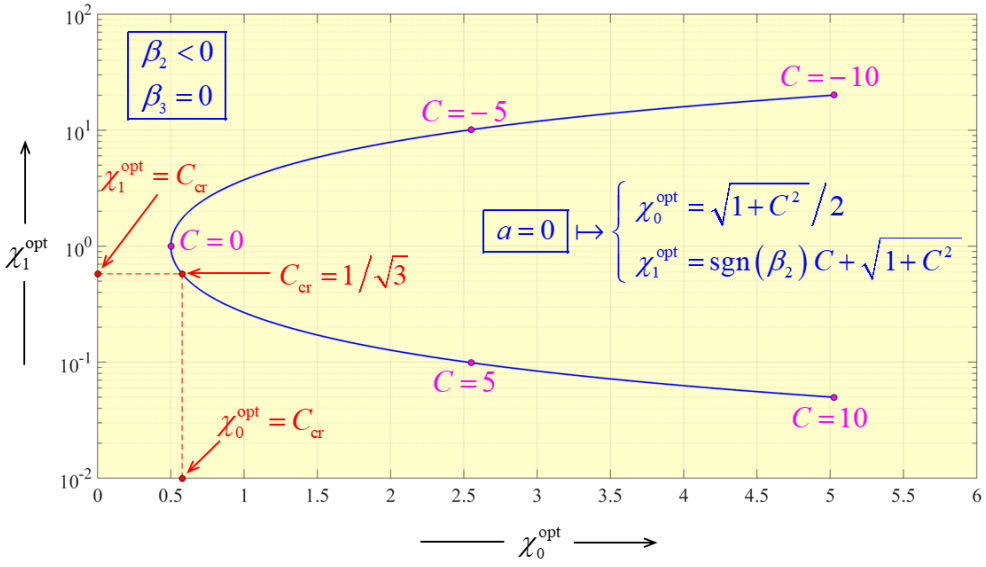

Figure 6.16 – Variation of χ_1^{opt} with χ_0^{opt} for $a = 0$. Besides the symmetrical behavior present in the plotted curve, another important fact worth mentioning is that the value obtained for $C = C_{cr}$ is the same as the ones obtained for χ_1^{opt} and χ_0^{opt}. To sum up what was said, $C_{cr} = \chi_1^{opt} = \chi_0^{opt}$.

Analyzing figure (6.16), we can see if $a = 0$ (meaning no β_3 on the system), that the curve is symmetric in relation to $C = 0$. As a result, χ_1^{opt} values between chirp values whose signal is contrary will be inverse to each other. However, a curious fact of extreme relevance is that for $C = C_{cr}$, the obtained values for $\chi_1^{opt}$and χ_0^{opt} will hold the same value as the one found for the chirped critical value, meaning that the following expression will be true: $C_{cr} = \chi_1^{opt} = \chi_0^{opt}$. However, we will see that in presence of β_3, such fact will no longer be valid.

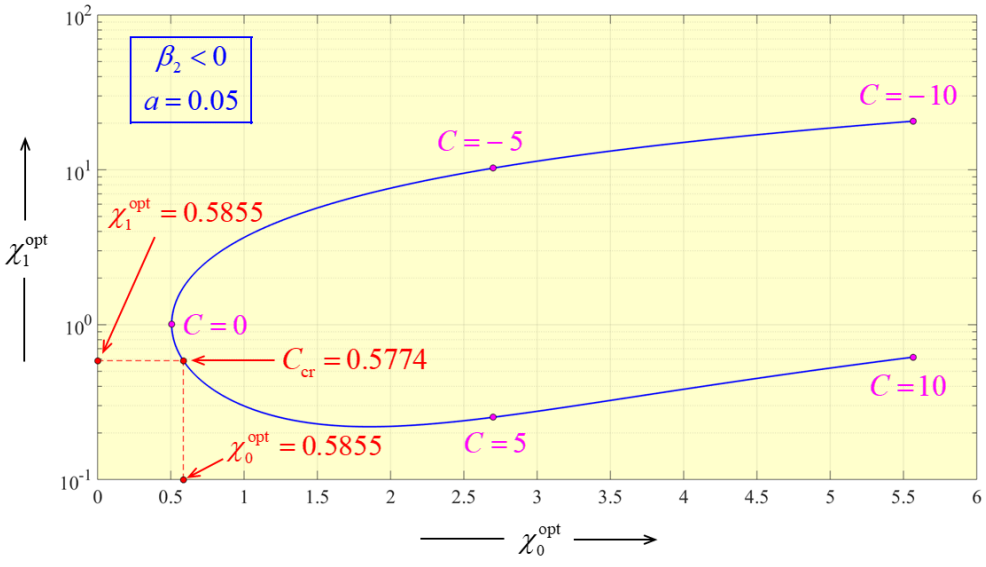

Figure 6.17 – Variation of χ_1^{opt} with χ_0^{opt} for $a = 0.05$. Besides the non-symmetrical behavior present in the plotted curve, another important fact worth mentioning is that the value obtained for $C = C_{cr}$ is no longer the same as the ones obtained for χ_1^{opt} and χ_0^{opt}. To sum up what was said, $C_{cr} \neq \chi_1^{opt} = \chi_0^{opt}$.

Looking at figure (6.17), we see that there is no more symmetric behavior as shown in figure (6.16) due to the effect of third-order dispersion on the pulse width. Even more important, the values χ_1^{opt} and χ_0^{opt} obtained for $C = C_{cr}$ are higher than C_{cr} itself. So, besides the fact that C_{cr} for $a = 0.05$ is bigger than the one for $a = 0$, χ_1^{opt} and χ_0^{opt} for $a = 0.05$ are even higher in comparison with , χ_1^{opt} and , χ_1^{opt} for $a = 0$. Briefly, with β_3 in play we now see that $C_{cr} < \chi_1^{opt} = \chi_0^{opt}$.

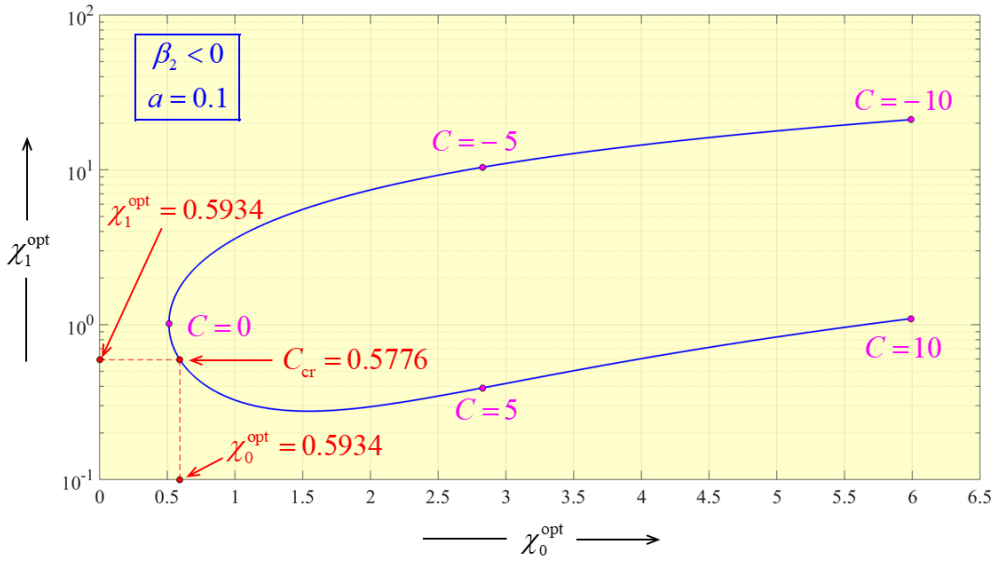

Figure 6.18 – Variation of χ_1^{opt} with χ_0^{opt} for $a = 0.1$. Besides the non-symmetrical behavior present in the plotted curve, another important fact worth mentioning is that the value obtained for $C = C_{cr}$ is not the same as the ones obtained for χ_1^{opt} and χ_0^{opt}. To sum up what was said, $C_{cr} \neq \chi_1^{opt} = \chi_0^{opt}$.

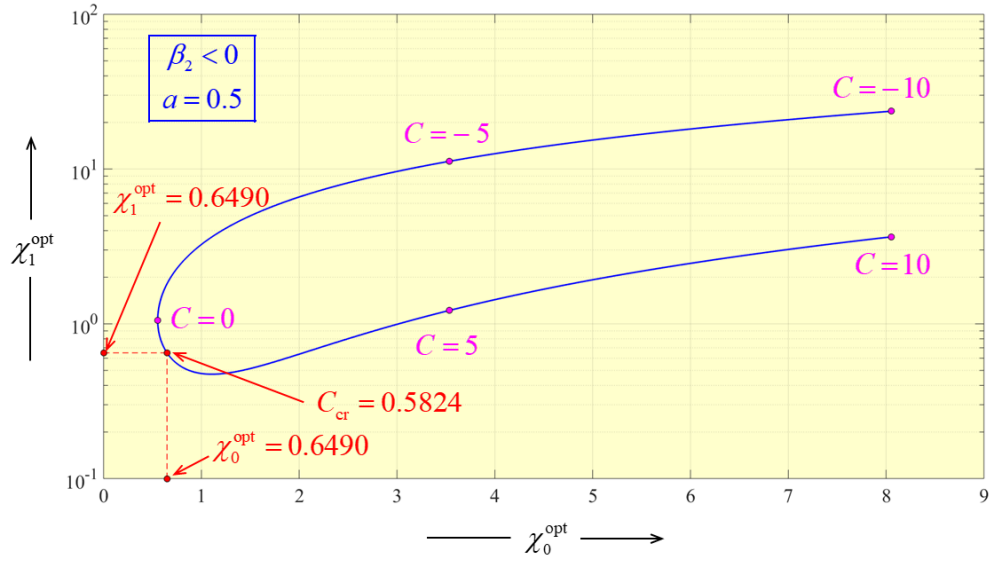

Figure 6.19 – Variation of χ_1^{opt} with χ_0^{opt} for $a = 0.5$. Besides the non-symmetrical behavior present in the plotted curve, another important fact worth mentioning is that the value obtained for $C = C_{cr}$ is not the same as the ones obtained for χ_1^{opt} and χ_0^{opt}. To sum up what was said, $C_{cr} \neq \chi_1^{opt} = \chi_0^{opt}$.

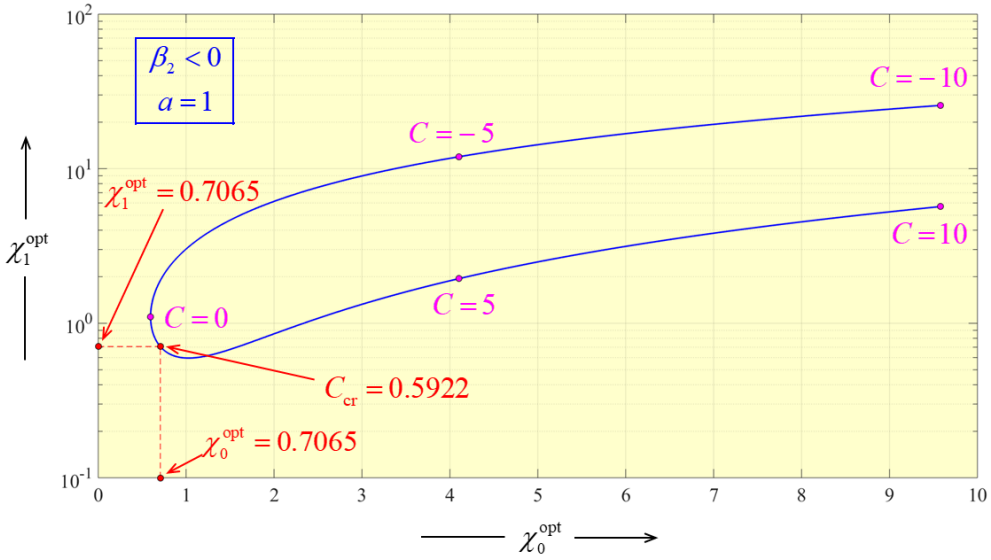

Figure 6.20 – Variation of χ_1^{opt} with χ_0^{opt} for $a = 1$. Besides the non-symmetrical behavior present in the plotted curve, another important fact worth mentioning is that the value obtained for $C = C_{cr}$ is not the same as the ones obtained for χ_1^{opt} and χ_0^{opt}. To sum up what was said, $C_{cr} \neq \chi_1^{opt} = \chi_0^{opt}$.

Analyzing figures (6.18), (6.19) and (6.20), besides seeing an even bigger difference between the value of C_{cr} and the corresponding values of χ_1^{opt} and χ_0^{opt}, we can also see that increasing the value of a, i.e, the presence of β_3 in the system, that for bigger values of C, the pulse width behavior tends to be closer to the one corresponding to its symmetric. So, if we kept increasing the value of a, we would see that if the presence of chirp in the channel was high enough, that the signal of C would not make a difference in the pulse width behavior.

Getting back at figure (6.15), we saw for a fixed a value the pulse width behavior for different C values. Something as useful would be to compare the pulse width behavior for the optimum situation. As such, we need to remind expression (6.13), which gave us the pulse width behavior. However, we are now going to rewrite it but considering $C = C_{cr}$, $\chi_0 = \chi_0^{opt}$ and $p = p_{cr}$:

$$\mu_{cr}^{opt} = 1 + sgn(\beta_2) C_{cr} \left(\frac{\xi}{\chi_0^{opt}}\right) + p_{cr} \left(1 + a^2 \frac{p_{cr}}{2\chi_0^{opt}}\right) \left(\frac{\xi}{\chi_0^{opt}}\right)^2 . \tag{6.31}$$

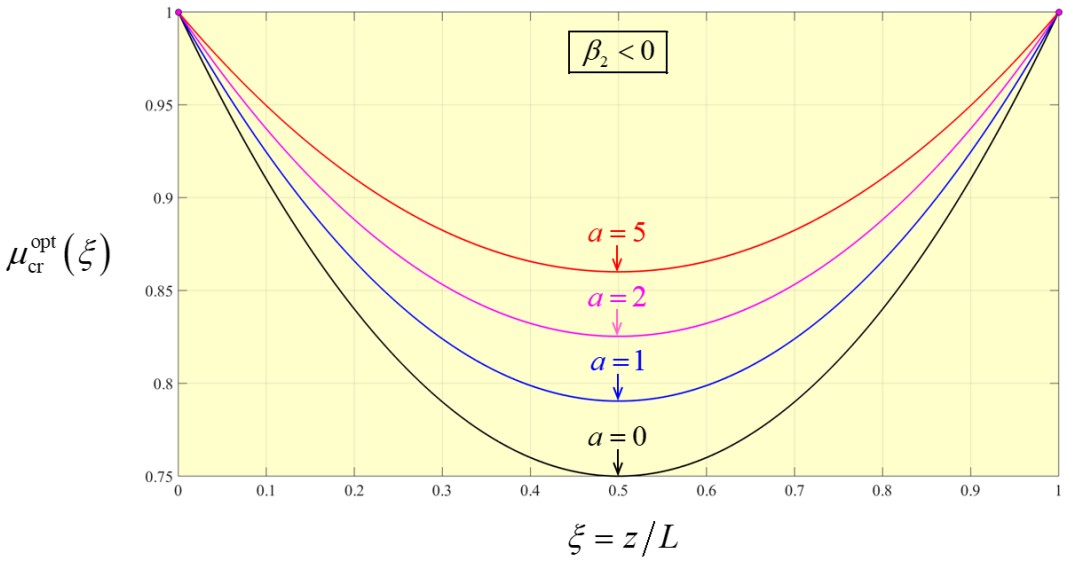

Figure 6.21 – Optimum pulse width behavior for $C = C_{cr}$ across the entire journey inside an optical fiber for different a values such as $a = 0$, $a = 1$, $a = 2$ and $a = 5$. As it is possible to see, although we still get the same width at the input and at the output of the optical fiber, the pulse compresses less for the higher values of the adimensional coefficient a.

Looking at figure (6.21), we notice that despite the fact we still can find a value of C for which we can still get the same pulse width at the input and at the output of the optical fiber even when the effect of the third-order dispersion is tremendous, the width compression experienced by the pulse across its journey throughout the optical fiber is less for the greater values of a. However, do not get fooled by this figure alone because as seen in figures (6.16), (6.17), (6.18), (6.19) and (6.20), increasing the value of a will result in greater values for χ_0^{opt} and χ_1^{opt}.

With all the information we have until now, we may predict that in the next section, where we will be looking at how to calculate the bit-rate considering the effect of the third-order dispersion parameter and how to measure the system performance through the product of bit-rate squared with the length of the optical-fiber, that for greater a values the system bit-rate and corresponding performance will be worse than if there was no β_3 on the fiber-optic communication system.

6.5 Maximum Bit-Rate Value

Now that we know how the effect of the higher-order dispersion parameter β_3 influences the pulse width of a signal travelling inside the optical-fiber, it is time to show what consequences it will have on the maximum bit-rate of an optical-fiber. From expression (6.8), σ_{max} may be written as follows:

$$\sigma_{max} = \sqrt{|\beta_2|L}\sqrt{\chi_{max}}\,. \tag{6.32}$$

Defining τ_0 as:

$$\tau_0 = \sqrt{|\beta_2|L}\,, \tag{6.33}$$

σ_{max} will be simply:

$$\sigma_{max} = \tau_0\sqrt{\chi_{max}}\,. \tag{6.34}$$

χ_{max} is the maximum width for any given value for the adimensional parameter a but considering $C = C_{cr}$. Having in mind the rule of thumb presented in (3.20), the maximum bit-rate B_0 is given by:

$$B_0 = \frac{1}{4\tau_0\sqrt{\chi_{max}}}. \tag{6.35}$$

The figure of merit is then:

$$F = \frac{1}{16\chi_{max}}. \tag{6.36}$$

The bit-rate squared product with the length of the optical fiber will be simply:

$$B_0^2 L = \frac{F}{|\beta_2|}. \tag{6.37}$$

Before looking into some numerical simulations, let us remind how we get χ_{max}. Reminding (6.23), the transition coefficient for $C = C_{cr}$ will be:

$$a_c = \frac{2\sqrt{3}}{3}[3(1 + C_{cr}^2)]^{\frac{1}{4}}. \tag{6.38}$$

Now, considering the results from (6.24), χ_{max} will be obtained by the following expressions:

$$\begin{cases} a \le a_c \rightarrow \chi_{max} = 2\sqrt{\frac{p_{cr}}{3}}\cos\left[\frac{1}{3}cos^{-1}\left(\frac{9a^2}{2}\sqrt{\frac{p_{cr}}{3}}\right)\right] \\ a \ge a_c \rightarrow \chi_{max} = 2\sqrt{\frac{p_{cr}}{3}}\cosh\left[\frac{1}{3}cosh^{-1}\left(\frac{9a^2}{2}\sqrt{\frac{p_{cr}}{3}}\right)\right] \end{cases}. \tag{6.39}$$

Of course, if we take $a = 0$ which is the same way as saying we are considering $\beta_3 = 0$, χ_{max} will be:

$$\chi_{max} = 2\sqrt{\frac{p_{cr}}{3}}\cos\left(\frac{\pi}{6}\right) = \sqrt{p_{cr}} = \frac{1}{2}\sqrt{1 + C_{cr}^2} = \frac{1}{\sqrt{3}}. \tag{6.40}$$

The last expression is similar to (6.25) but now done for $C = C_{cr}$.

As a reminder, in the expressions presented in this section until now, it is always referred χ_{max} because as seen in figure (6.21), for $C = C_{cr}$, $\chi_0^{opt} = \chi_1^{opt} = \chi_{max}$.

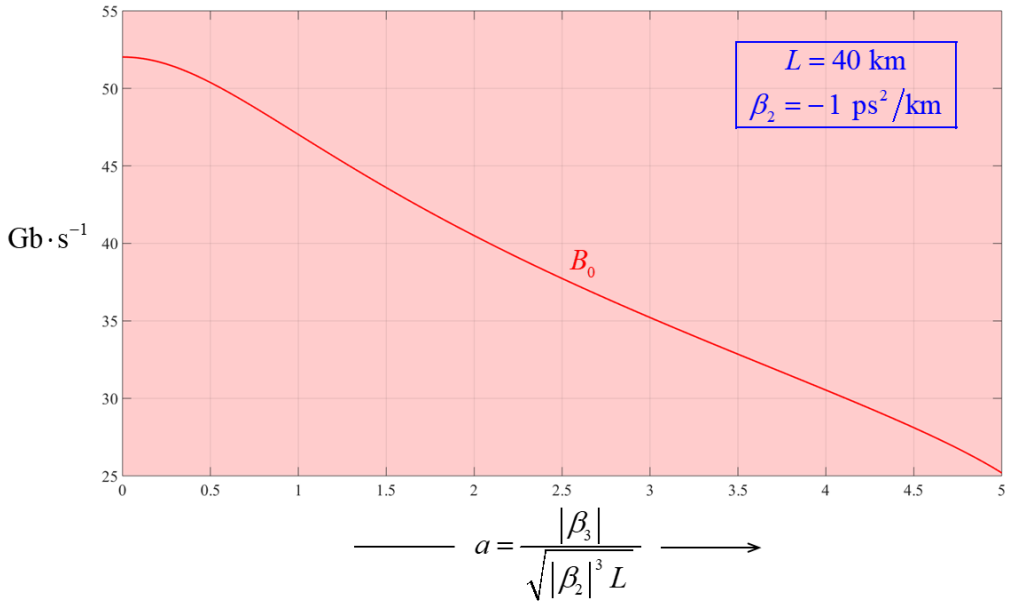

Figure 6.22 – Variation of the bit-rate B_0 with the adimensional coefficient a for $\beta_2 = -1\ ps^2/km$ and for a fiber length $L = 40\ km$. As it is possible to observe, the value of the bit-rate continuously decreases for bigger values of a.

Analyzing figure (6.22), the example shown give us an idea on how big the influence of the effects of higher-order dispersion may be. Looking attentively to the curve, we may notice percentual decrease of more than 50% for the bit-rate for $a = 5$ which is a lot. So, we may conclude from here that the presence of β_3 in fiber-optic communication systems will always be terrible for the performance of such systems.

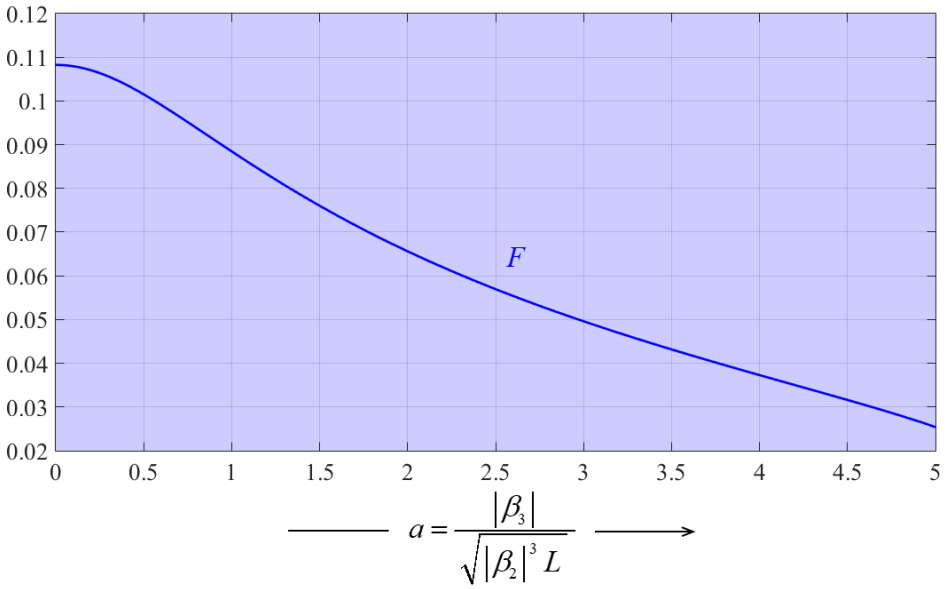

Figure 6.23 – Variation of the figure of merit F with the adimensional coefficient a. Being F a way to measure the efficiency of a fiber-optic communication system, we may notice that increasing a will make the system less efficient, meaning it gets tougher to have high bit-rates for larger distances.

Analyzing figure (6.23) and being F a way to measure the efficiency of a fiber-optic communication system, we see that as the influence of β_3 becomes greater in the channel, the efficiency of the mentioned system decreases consequently. This means that if we compare the bit-rate for a given distance where $\beta_3 = 0$ with another one on which $\beta_3 \neq 0$, from figure (6.23) we can say that the bit-rate will be lower for the case whose $\beta_3 \neq 0$ in comparison with the one whose $\beta_3 = 0$. Therefore, we conclude once more that β_3 is always not desirable in a fiber-optic communication system.

Since β_3 is always undesirable when considering fiber-optic communication systems, it will be nice to have a way to measure the error the effect of higher-order dispersion β_3 introduces in the channel. We have, already noticed that having $\beta_3 = 0$ is the best-case scenario, being the cases when $\beta_3 \neq 0$ the non-desirable ones. That way, we need the error committed in the cases where $\beta_3 \neq 0$. As such, the error is measured as follows:

$$\varepsilon = \frac{B_0(\beta_3 = 0) - B_0(\beta_3 \neq 0)}{B_0(\beta_3 = 0)}, \tag{6.41}$$

being $B_0(\beta_3 = 0)$ equal to (4.35) and $B_0(\beta_3 \neq 0)$ equal to (6.35). Therefore, the last equation may be rewritten as:

$$\varepsilon = 1 - \frac{1}{\sqrt[4]{3}\sqrt{\chi_{max}}}. \tag{6.42}$$

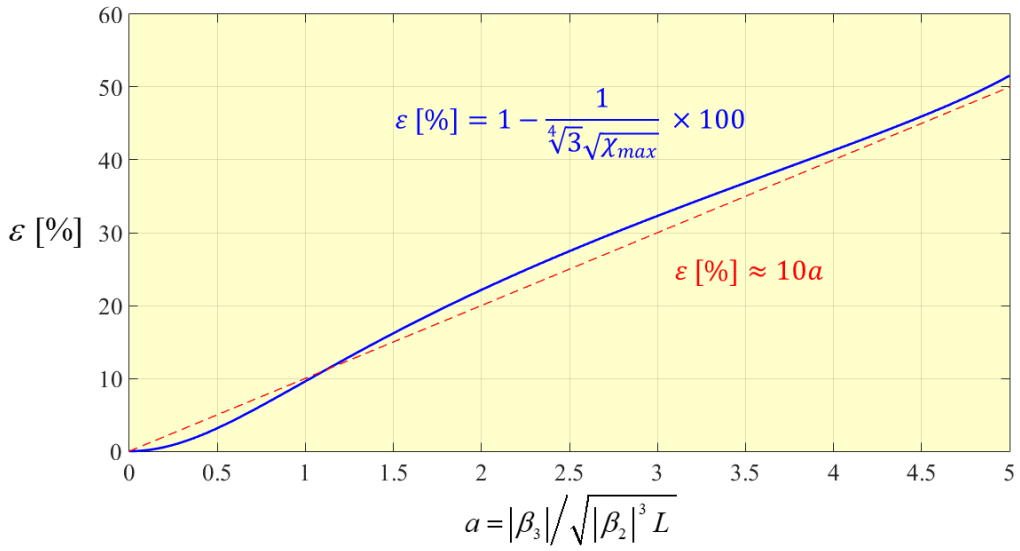

Figure 6.24 – Bit-rate percentage loss introduced by β_3 on the channel and corresponding first approximation. As it is possible to see, β_3 may have a great negative effect on the bit-rate since bit-rate losses always increase with higher presence of β_3 in fiber-optic communication systems.

Looking at figure (6.24), it is undeniable that β_3 may cause severe bit-rate losses on fiber-optic communication systems. Even more, the losses are already in the order of 10% for values of a in the order of $a = 1$. Of course, the higher a is the worse it will be the performance of the system. Furthermore, it is possible to make a first approximation on the behavior the bit-rate percentage loss curve has, by considering a linear function which is $10a$, meaning if we increase a by one unit, the bit-rate loss percentage increases by 10%. Next, we will see if this a good approximation or not.

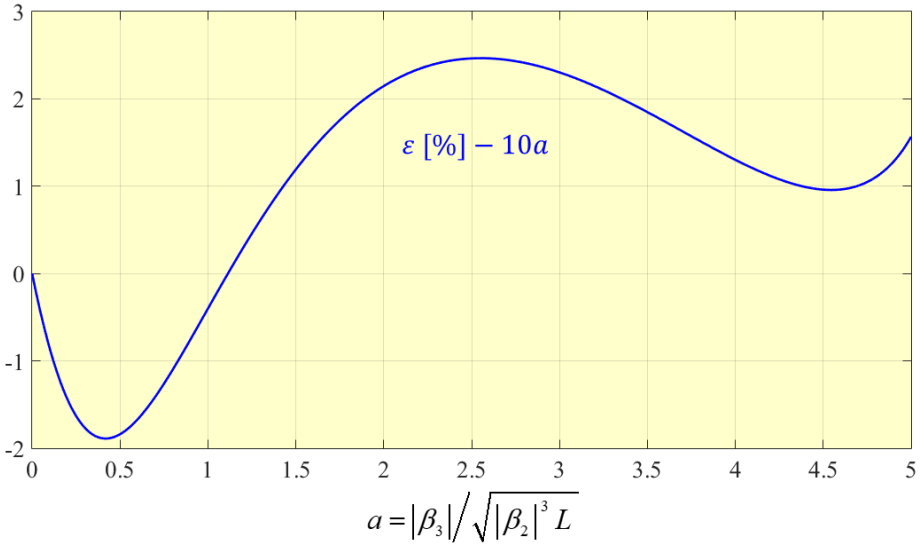

Figure 6.25 – Approximation error between the expression that gives the bit-rate loss percentage and the first approximation which is a linear curve whose expression is defined by $10a$. The interval error is $[-2; 3]\%$ which proves the chosen approximation is a good one.

Analyzing figure (6.25), since the interval error is $[-2; 3]\%$ it means that the error committed by approximating the bit-rate percentage loss with the linear expression $10a$ is good one because no matter the a value we consider, the approximation error is always much less than 10%. Even more, the error is always in order of 1% which means the chosen approximation is acceptable and gives us a simpler way to analyze the bit-rate losses in a fiber-optic communication system affected by the presence of β_3. If not considering the approximation error in percentage, the first approximation to be considered for comparison with the real one would be $\varepsilon \approx 0.a$. Of course, all the considerations done would still hold true.

7. Super-Gaussian Pulses

A pulse is said to be super-Gaussian if at the input of the fiber, $z = 0$, we have a pulse of the form [4]:

$$A(0,t) = A_0 \exp\left[-\frac{1+iC}{2}\left(\frac{t}{T_0}\right)^{2m}\right], \tag{7.1}$$

where m is the parameter that controls the degree of edge sharpness and C is the dimensionless chirp parameter. If $m = 1$, we fall into the category of chirped gaussian pulses. As m increases, the sharpness of the pulse increases accordingly.

The input pulse intensity can therefore be written as:

$$|A(0,t)|^2 = A_0^2 \exp\left[-\left(\frac{t}{T_0}\right)^{2m}\right]. \tag{7.2}$$

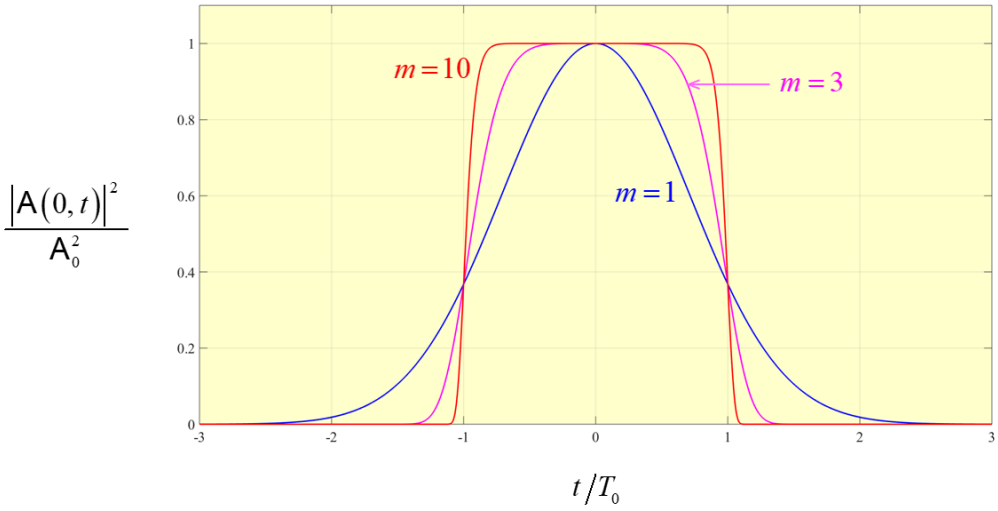

Figure 7.1 – Super-Gaussian pulse shape for $m = 1$, $m = 3$ and $m = 10$. Being m the parameter that measures the degree of edge sharpness, it is observable that a higher value of m means sharper edges than for lower values of m.

Looking at figure (7.1), we can see how the parameter m affects the shape of Gaussian pulses. For $m = 1$, we recover the case already studied in chapters 4 and 6. However, in this chapter we are going to study Gaussian pulses whose $m > 1$. Those pulses are the so called super-Gaussian pulses. As we can see in figure (7.1), the higher the value of m is, the sharper the edges will be. Throughout this chapter, we are going to see what are the consequences in terms of bit-rate and system performance of having pulses with sharper edges being used to convey information along an optical fiber.

The RMS width of a super-Gaussian pulse [5] assumes the following form:

$$\sigma_0^2 = \frac{\Gamma(3/2m)}{\Gamma(1/2m)} T_0^2 . \tag{7.3}$$

For $m = 1$, we get the RMS width of a chirped-Gaussian pulse, as it was supposed to be.

Then, for any given point z, it is possible to evaluate the broadening factor analytically for super-Gaussian pulses (if $\beta_3 = 0$, since there is no expression in the literature regarding the influence of β_3 in the pulse width) as follows [4]:

$$\frac{\sigma}{\sigma_0} = \left[1 + \frac{\Gamma(1/2m)}{\Gamma(3/2m)} \frac{C\beta_2 L}{T_0^2} \left(\frac{z}{L}\right) + m^2(1+C^2) \frac{\Gamma(2-1/2m)}{\Gamma(3/2m)} \left(\frac{\beta_2 L}{T_0^2}\right)^2 \left(\frac{z}{L}\right)^2\right]^{\frac{1}{2}}, \tag{7.4}$$

$$\frac{\sigma}{\sigma_0} = \left[1 + \frac{\Gamma(1/2m)}{\Gamma(3/2m)} \frac{C\beta_2 L}{\frac{\Gamma(1/2m)}{\Gamma(3/2m)}\sigma_0^2} \left(\frac{z}{L}\right) + m^2(1+C^2) \frac{\Gamma(2-1/2m)}{\Gamma(3/2m)} \left(\frac{\beta_2 L}{\frac{\Gamma(1/2m)}{\Gamma(3/2m)}\sigma_0^2}\right)^2 \left(\frac{z}{L}\right)^2\right]^{\frac{1}{2}}, \tag{7.5}$$

$$\sigma^2(\xi) = \sigma_0^2 + C\beta_2 L\, \xi + m^2(1+C^2) \frac{\Gamma(2-1/2m)\Gamma(3/2m)}{\Gamma^2(1/2m)} \frac{\beta_2^2 L^2}{\sigma_0^2} \xi^2, \tag{7.6}$$

$$\frac{\sigma^2(\xi)}{|\beta_2|L} = \frac{\sigma_0^2}{|\beta_2|L} + sgn(\beta_2) C\, \xi + m^2(1+C^2) \frac{\Gamma(2-1/2m)\Gamma(3/2m)}{\Gamma^2(1/2m)} \frac{|\beta_2|L}{\sigma_0^2} \xi^2. \tag{7.7}$$

Now, after introducing the following dimensionless parameters (if $\beta_2 \neq 0$):

$$\chi(\xi) = \frac{\sigma^2(\xi)}{|\beta_2|L};\ \chi_0 = \chi(\xi = 0) = \frac{\sigma_0^2}{|\beta_2|L};\ \chi_1 = \chi(\xi = 1) = \frac{\sigma_1^2}{|\beta_2|L}, \tag{7.8}$$

$$f_m = \frac{\Gamma(2-1/2m)\Gamma(3/2m)}{\Gamma^2(1/2m)}, \tag{7.9}$$

equation (7.7) may be rewritten as:

$$\chi(\xi) = \chi_0 + sgn(\beta_2) C\, \xi + m^2 f_m \left(\frac{1+C^2}{\chi_0}\right) \xi^2. \tag{7.10}$$

At this point, it is desirable to know how to obtain the optimal broadening values at each point of the optical fiber, being the input and the output of the optical of special importance. To start, expressions for the optimum value at the input and at the output of the optical fiber are going to be shown:

$$\chi_1 = \chi_0 + sgn(\beta_2) C + m^2 f_m \left(\frac{1+C^2}{\chi_0}\right), \tag{7.11}$$

$$\frac{d\chi_1}{d\chi_0} = 1 - m^2 f_m \left(\frac{1+C^2}{\chi_0^2}\right) = 0\,, \tag{7.12}$$

$$\chi_0^{opt} = m\sqrt{f_m(1+C^2)}\,, \tag{7.13}$$

$$\chi_1^{opt} = \chi_1\left(\chi_0^{opt}\right) = sgn(\beta_2) C + 2m\sqrt{f_m(1+C^2)}\,. \tag{7.14}$$

Then, for every point ξ in the optical fiber, the optimum broadening value may be obtained through the following expression:

$$\chi^{opt}(\xi) = sgn(\beta_2)C\,\xi + m\sqrt{f_m\,(1+C^2)}\,(1+\xi^2)\,. \tag{7.15}$$

To compare the width of the pulse at any given point ξ with the width at $\xi = 0$, the upcoming result arises:

$$\mu^{opt}(\xi) = \frac{\chi^{opt}(\xi)}{\chi_0^{opt}} = 1 + \frac{sgn(\beta_2)C}{m\sqrt{f_m\,(1+C^2)}}\xi + \xi^2\,. \tag{7.16}$$

Now, considering:

$$\mu_0^{opt} = \mu(0) = 1\,, \tag{7.17}$$

$$\mu_1^{opt} = \mu(1) = 2 + \frac{sgn(\beta_2)C}{m\sqrt{f_m\,(1+C^2)}}, \tag{7.18}$$

it is possible to find a value for the chirp parameter that will allow $\mu_0^{opt} = \mu_1^{opt} = 1$, that is going to be denominated as $C = C_{cr}$. Then, we get the corresponding equation:

$$\frac{sgn(\beta_2)C_{cr}}{m\sqrt{f_m\,(1+C_{cr}^2)}} = -1\,, \tag{7.19}$$

which will give us the way to obtain $C = C_{cr}$:

$$C_{cr} = -\frac{\sqrt{m^2\,f_m}}{\sqrt{1-m^2\,f_m}}sgn(\beta_2)\,. \tag{7.20}$$

However, it will only be possible to find C_{cr} for a certain range of m values. Since $1 - m^2\,f_m \geq 0$ is only verified for $1 \leq m \leq 6$, it means for $m \geq 7$ there is no critical value of the chirp parameter. If for $m \geq 7$ we cannot obtain C_{cr}, it also means it will not be possible to achieve $\chi_1^{opt} = \chi_0^{opt}$, therefore we must find another way to achieve optimization.

As it may be obvious for you at this point, the goal of this chapter is to analyze how the factor m will influence the behavior of the Gaussian pulses. Therefore, the following results that are going to be shown will focus on studying how to optimize the performance of a fiber-optic communication system in the presence of super-Gaussian pulses.

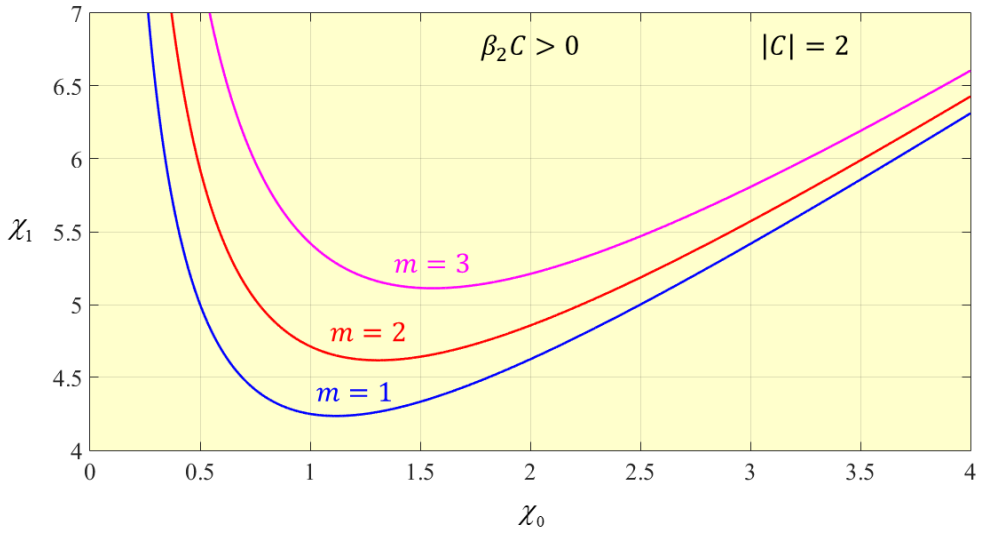

Figure 7.2 - Variation of the normalized output pulse width χ_1 with the normalized input pulse χ_0 for a super-Gaussian pulse for a chosen value of $|C| = 2$ and for $m = 1$, $m = 2$ and $m = 3$. In this example, it is also possible to state that $\beta_2 C > 0$.

Analyzing figure (7.2), the first thing worth noticing is that for $m = 1$, the curve obtained here matches the ones obtained in figures (4.4) and (4.8). In figure (4.4), the chirp parameter was $C = -2$ and in figure (4.8) the chirp parameter was $C = 2$, with both cases having β_2 with the same signal as the one of the chirp parameters. We can also see that the pulse, as in figures (4.4) and (4.8), continues to always undergo broadening since $\beta_2 C > 0$. Now, to fulfill the objective of figure (7.1), we see that a higher m value causes both χ_1 and χ_0 to be higher, which will mean a poorer performance of a fiber-optic communication system comparing to the case when $m = 1$.

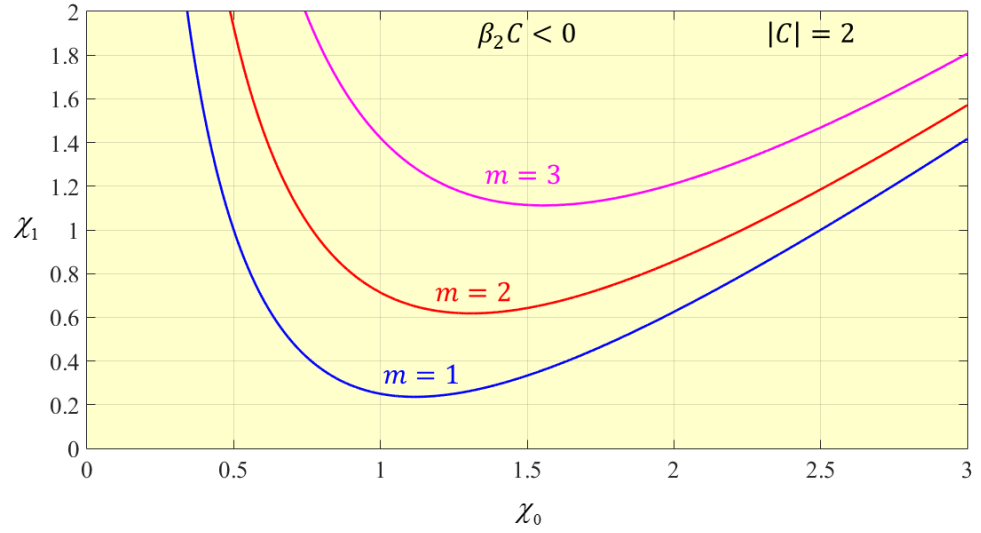

Figure 7.3 - Variation of the normalized output pulse width χ_1 with the normalized input pulse χ_0 for a super-Gaussian pulse for a chosen value of $|C| = 2$ and for $m = 1$, $m = 2$ and $m = 3$. In this example, it is also possible to state that $\beta_2 C < 0$.

Analyzing figure (7.3), the first thing worth noticing is that for $m = 1$, the curve obtained here matches the ones obtained in figures (4.5) and (4.7). In figure (4.5), the chirp parameter was $C = 2$ and in figure (4.7) the chirp parameter was $C = -2$, with both cases having β_2 with the opposite signal as the one of the chirp parameters. We can also see that the pulse, as in figures (4.5) and (4.7), may suffer compression since $\beta_2 C < 0$. Now, to fulfill the objective of figure (7.2), we see that a higher m value causes both χ_1 and χ_0 to be higher, which will mean a poorer performance of a fiber-optic communication system comparing to the case when $m = 1$.

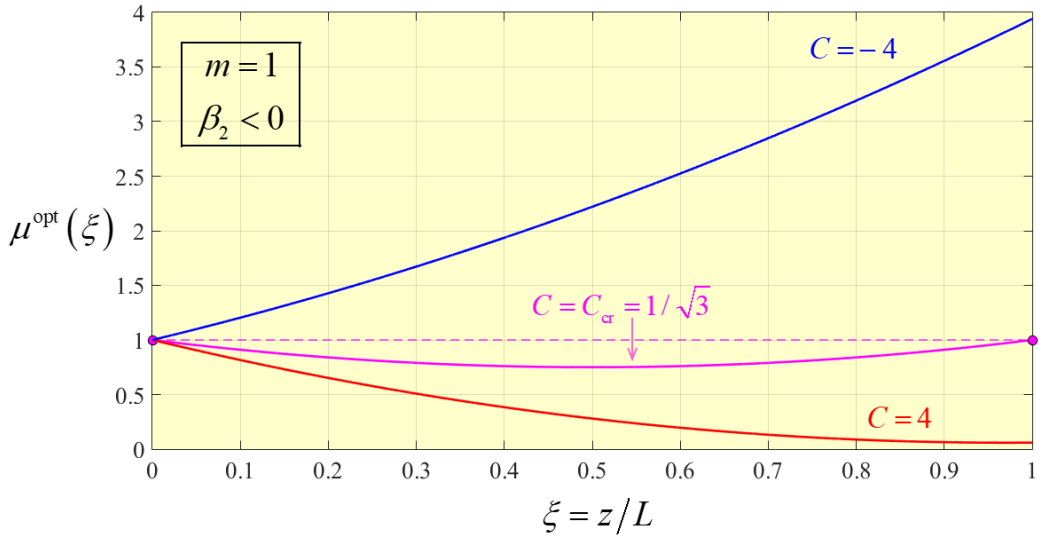

Figure 7.4 - Optimum pulse width behavior of a super-Gaussian pulse when $\beta_2 < 0$ for $C = -4$, $C = 4$ and $C = C_{cr}$ with a fixed value of $m = 1$. As predicted, when $C = C_{cr}$ the pulse width is the same at the input as it is at the output of the optical fiber. For $C = -4$, the pulse always broadens since $\beta_2 C > 0$ and for $C = 4$ the pulse experiences compression because $\beta_2 C < 0$.

Looking at figure (7.4), we see that the critical chirp parameter value that allows to have the same pulse width at the input and at the output of the optical fiber is the one obtained in figure (4.6), which is a good indicator that we are on the right-track. Also, as expected, since $\beta_2 < 0$ we experience pulse broadening for $C = -4$ because $\beta_2 C > 0$ and pulse compression for $C = 4$ because $\beta_2 C < 0$. However, as seen before, it is $C = C_{cr}$ the most useful result since it is best to have the lowest chirp parameter value possible for the sake of practical implementation. In figures (7.5) and (7.6), we will see how increasing m will affect the value of $C = C_{cr}$.

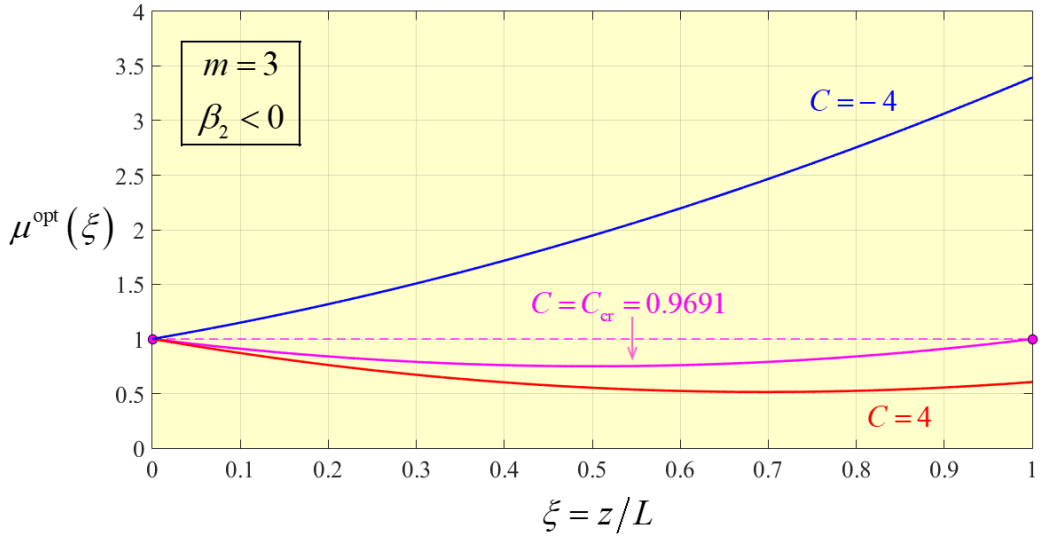

Figure 7.5 - Optimum pulse width behavior of a super-Gaussian pulse when $\beta_2 < 0$ for $C = -4$, $C = 4$ and $C = C_{cr}$ with a fixed value of $m = 3$. As predicted, when $C = C_{cr}$ the pulse width is the same at the input as it is at the output of the optical fiber. For $C = -4$, the pulse always broadens since $\beta_2 C > 0$ and for $C = 4$ the pulse experiences compression because $\beta_2 C < 0$.

Looking at figure (7.5), we see that the critical chirp parameter value obtained is higher than the one obtained in figure (7.4), which indicates it is harder to optimize super-Gaussian pulses with higher values of m. Also, as expected, since $\beta_2 < 0$ we experience pulse broadening for $C = -4$ because $\beta_2 C > 0$ and pulse compression for $C = 4$ because $\beta_2 C < 0$. However, it is still $C = C_{cr}$ the most useful result since it is best to have the lowest chirp parameter value possible for the sake of practical implementation.

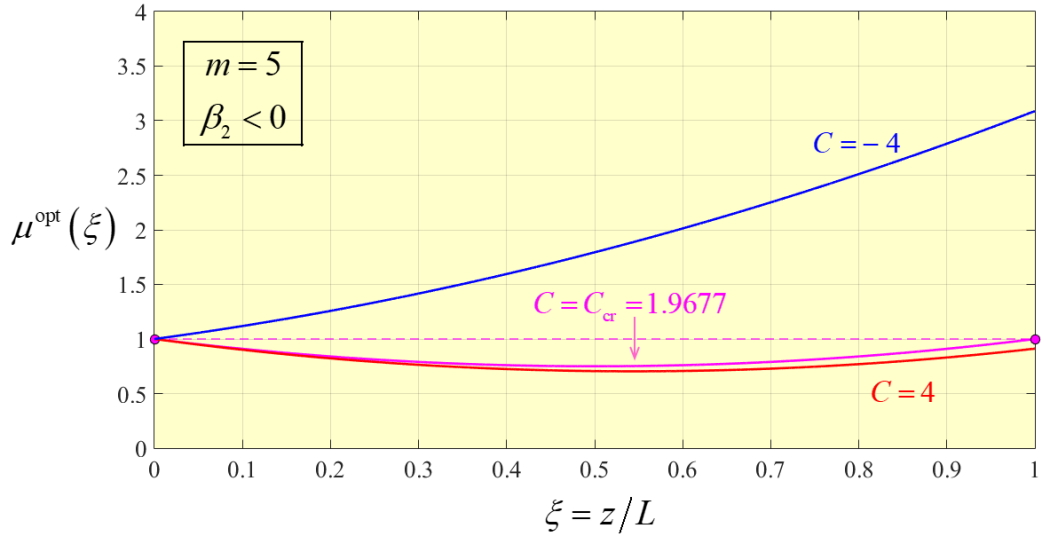

Figure 7.6 - Optimum pulse width behavior of a super-Gaussian pulse when $\beta_2 < 0$ for $C = -4$, $C = 4$ and $C = C_{cr}$ with a fixed value of $m = 5$. As predicted, when $C = C_{cr}$ the pulse width is the same at the input as it is at the output of the optical fiber. For $C = -4$, the pulse always broadens since $\beta_2 C > 0$ and for $C = 4$ the pulse experiences compression because $\beta_2 C < 0$.

Looking at figure (7.6), we see that the critical chirp parameter value obtained is higher than the one obtained in figures (7.4) and (7.5), which confirms that the higher the parameter m is, the harder will be to implement the needed optimization for a fiber-optic communication system work at its best performance possible. Once again, as expected, since $\beta_2 < 0$ we experience pulse broadening for $C = -4$ because $\beta_2 C > 0$ and pulse compression for $C = 4$ because $\beta_2 C < 0$. However, figure (7.6) is deceiving because when looking into figure (7.9), $C = C_{cr}$ will no longer be responsible for optimization which is something that will be discussed in the analysis of figures (7.9) and (7.10). A fun fact to realize is the curves corresponding to $C = -4$ and $C = 4$ converging to the curve which corresponds to $C = C_{cr}$. This means that if we kept increasing m, at some point we would get past the curve corresponding to $C = C_{cr}$, meaning with reach a point where we would no longer have a chirp parameter allowing the input pulse width being equal to the output pulse width. However, that does not interest us since such case would be extremely inefficient and impractically to implement.

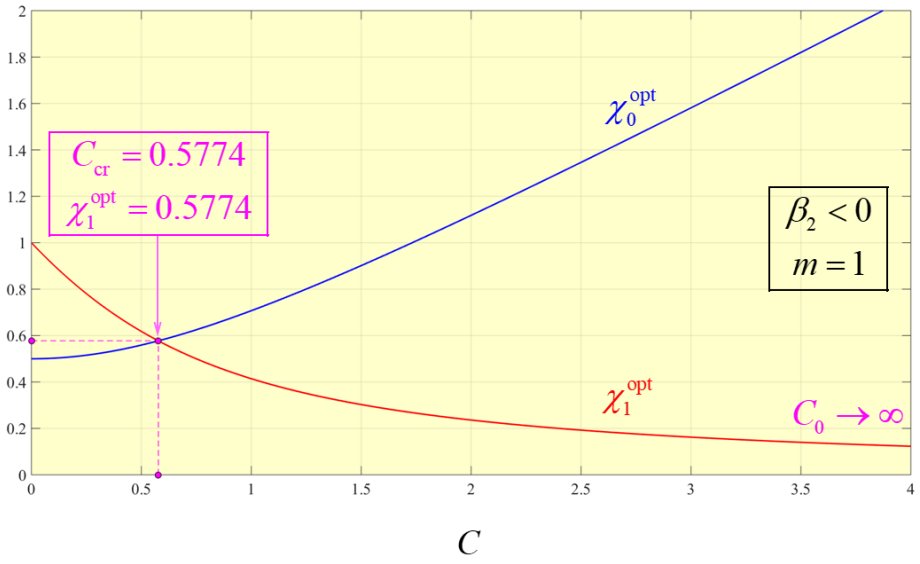

Figure 7.7 - Variation of χ_0^{opt} and χ_1^{opt} with the chirp parameter C, when $\beta_2 < 0$ for $m = 1$. As shown, the intersection of both curves gives us the critical chirp value, $C_{cr} = 1/\sqrt{3}$ for which we optimize the pulse width.

Looking at figure (7.7), it is possible to observe that we can recover the chirped Gaussian pulse analyzed in chapter 4 with $\beta_3 = 0$. We may also see that for $C_{cr} = 1/\sqrt{3}$, it exists in fact a point where χ_0^{opt} and χ_1^{opt} are equal. That point is what determines the best optimization that can be made for super-Gaussian pulses whose m value is equal to 1. It is also worth mentioning that $C_{cr} = \chi_0^{opt} = \chi_1^{opt}$, since this fact will be important to have in mind when it is time to calculate the maximum bit-rate.

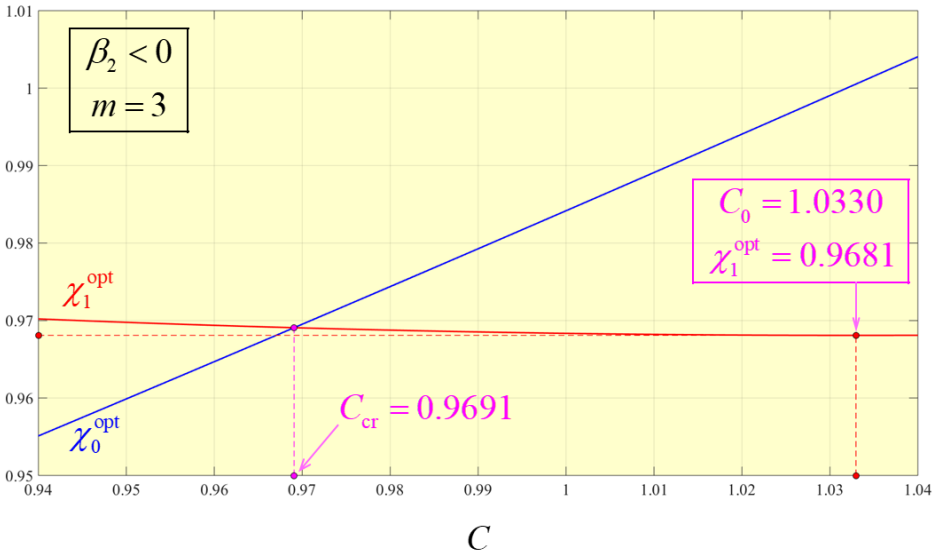

Figure 7.8 - Variation of χ_0^{opt} and χ_1^{opt} with the chirp parameter C, when $\beta_2 < 0$ for $m = 3$. As shown, the intersection of both curves gives us the critical chirp value, $C_{cr} = 0.9691$ for which we optimize the pulse width.

Analyzing figure (7.8), we see that for $C_{cr} = 0.9691$, it exists in fact a point where χ_0^{opt} and χ_1^{opt} are equal. That point is what determines the best optimization that can be made for super-Gaussian pulses whose m value is equal to 3. It is also worth mentioning that $C_{cr} = \chi_0^{opt} = \chi_1^{opt}$, since this fact will be important to have in mind when it is time to calculate the maximum bit-rate.

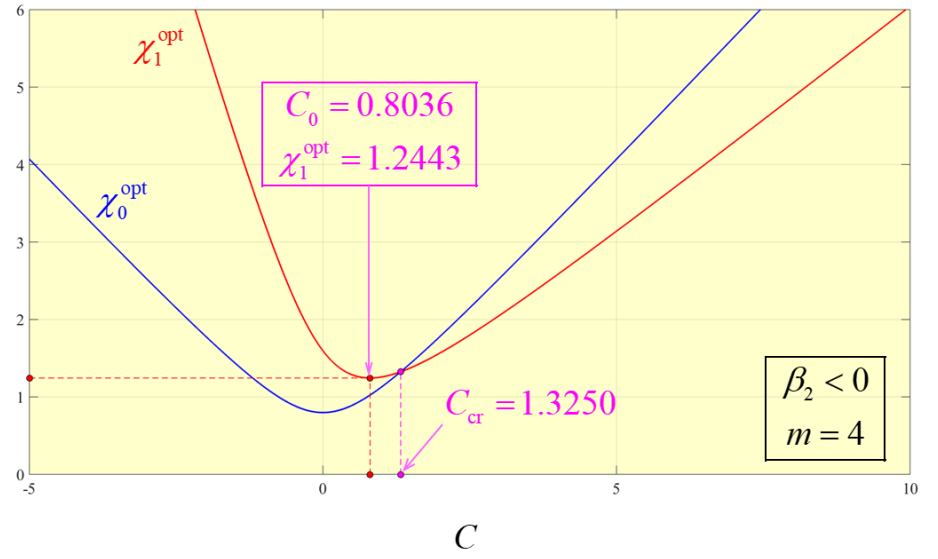

Figure 7.9 - Variation of χ_0^{opt} and χ_1^{opt} with the chirp parameter C, when $\beta_2 < 0$ for $m = 4$. As shown, the intersection of both curves gives us the critical chirp value, $C_{cr} = 1.9677$. However, C_{cr} will no longer optimize the pulse width. Now it will be the chirp parameter $C_0 = 0.8036$, for $m = 4$, that optimizes the pulse width.

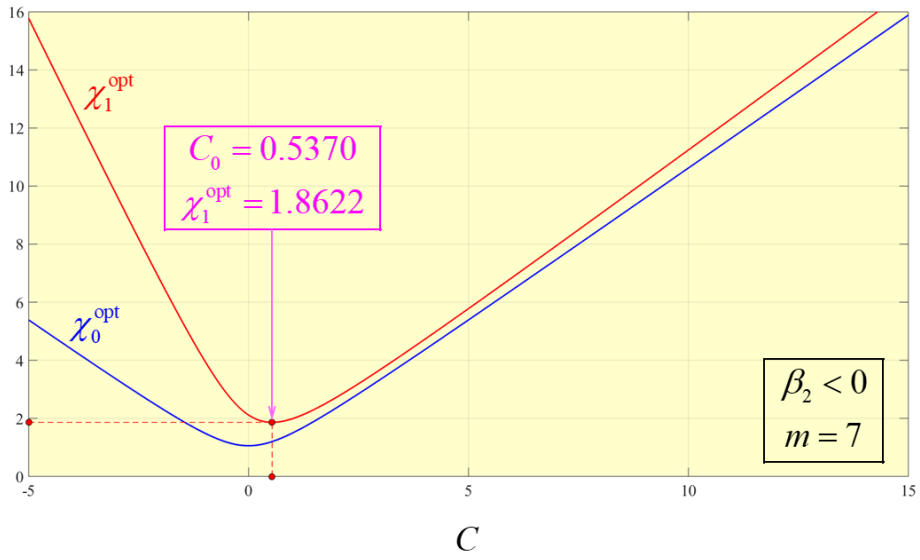

Figure 7.10 - Variation of χ_0^{opt} and χ_1^{opt} with the chirp parameter C, when $\beta_2 < 0$ for $m = 7$. As shown, both curves do not intersect each other. Therefore, it will not exist a critical chirp value for $m = 7$. Now, it will be the chirp parameter $C_0 = 0.5370$ that optimizes the pulse width for $m = 7$.

Analyzing figures (7.9) and (7.10), we see that C_{cr} is no longer the one responsible for determining χ_0^{opt} and χ_1^{opt}. Such role belongs now to C_0 which is the point where the derivative of χ_1^{opt} in relation to the chirp parameter C equals to 0. It was chosen χ_1^{opt} to calculate C_0 instead of χ_0^{opt} because as we can see in figure (7.9), before crossing the value C_{cr}, $\chi_1^{opt} > \chi_0^{opt}$. In figure (7.10), since there is no C_{cr}, i.e., no intersection in the curves corresponding to χ_1^{opt} and χ_0^{opt}, it is always verified that $\chi_1^{opt} > \chi_0^{opt}$.

Now that it is clear the relevance of C_0 for super-Gaussian pulses whose $m \geq 4$, it is time to define an expression to allow us to calculate C_0:

$$\frac{d\chi_1^{opt}}{dC} = 0\,, \tag{7.21}$$

$$C = C_0 = -\frac{sgn(\beta_2)}{\sqrt{4m^2 f_m - 1}}, \tag{7.22}$$

$$\chi_1^{opt}(C_0) = \sqrt{4m^2 f_m - 1}\,. \tag{7.23}$$

Although C_0 is only useful for $m \geq 4$, for $m = 2$ and $m = 3$ it is also possible to quantify this parameter. For $m = 1$, $C_0 \to \infty$ because $\chi_1^{opt} \to 0$ by increasing the chirp parameter of the pulse. In other words, expression (7.21) will never be verified for $m = 1$, because $d\chi_1^{opt}/dC < 0$ for every C.

Now that we know how the parameter m of a super-Gaussian pulse influences the pulse width of a signal travelling inside the optical-fiber, it is time to show what consequences it will have on the maximum bit-rate of an optical-fiber. From expression (6.8), σ_{max} may be written as follows:

$$\sigma_{max} = \sqrt{|\beta_2|L}\sqrt{\chi_{max}}\,. \tag{7.24}$$

Defining τ_0 as:

$$\tau_0 = \sqrt{|\beta_2|L}\,, \tag{7.25}$$

σ_{max} will be simply:

$$\sigma_{max} = \tau_0\sqrt{\chi_{max}}\,. \tag{7.26}$$

χ_{max} is the maximum width for any given value for the adimensional parameter m. However, to get χ_{max} we will have to consider either $C = C_{cr}$ or $C = C_0$ according to the following conditions:

$$\chi_{max} = \begin{cases} \chi_1^{opt}(C = C_{cr}), & 1 \le m \le 3 \\ \chi_1^{opt}(C = C_0), & m \ge 4 \end{cases} \tag{7.27}$$

Having in mind the rule of thumb presented in (3.20), the maximum bit-rate B_0 is given by:

$$B_0 = \frac{1}{4\tau_0\sqrt{\chi_{max}}}. \tag{7.28}$$

The figure of merit is then:

$$F = \frac{1}{16\chi_{max}}, \tag{7.29}$$

where for $m = 1$, it is recoverable the figure of merit obtained in expression (4.36), which is:

$$F = \frac{\sqrt{3}}{16}. \tag{7.30}$$

Therefore, the figure of merit for $1 \le m \le 3$ will be:

$$\Phi_m = \sqrt{\frac{1 - m^2\, f_m}{m^2\, f_m}} = \frac{1}{\chi_{max}}, \tag{7.31}$$

$$F = \frac{\Phi_m}{16}. \tag{7.32}$$

Moreover, the figure of merit for $m \ge 4$ will be:

$$\Psi_m = \frac{1}{\sqrt{4m^2 f_m - 1}} = \frac{1}{\chi_{max}}, \tag{7.33}$$

$$F = \frac{\Psi_m}{16}. \tag{7.34}$$

The bit-rate squared product with the length of the optical fiber will be simply:

$$B_0^2 L = \frac{F}{|\beta_2|}. \tag{7.35}$$

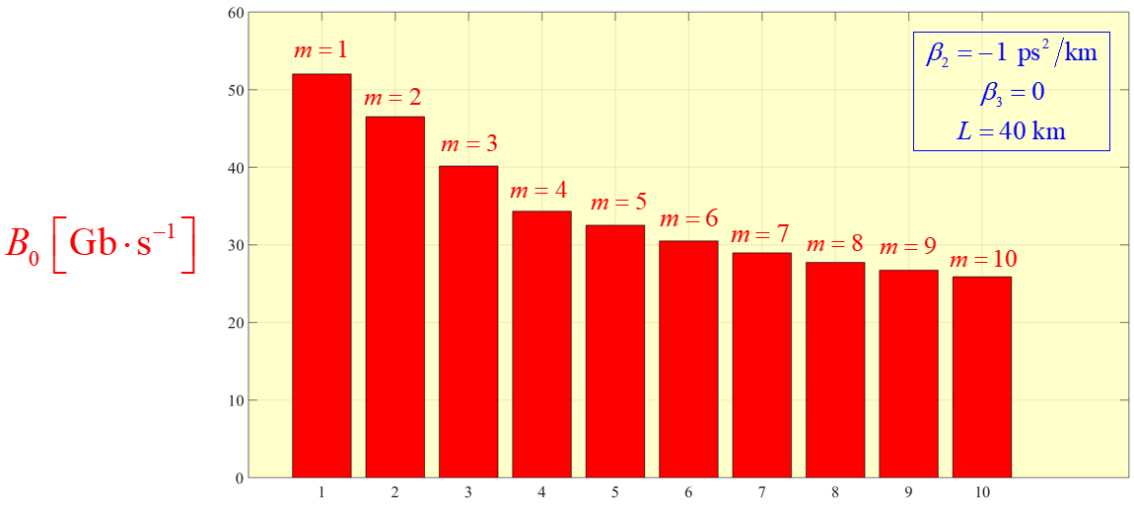

Figure 7.11 - Variation of the bit-rate B_0 with parameter m for $\beta_2 = -1\ ps^2/km$ and $\beta_3 = 0$ for an optical fiber length $L = 40\ km$. As it is possible to observe, the value of the bit-rate continuously decreases for bigger values of m.

Analyzing figure (7.11), the example shown give us an idea on how big the influence of having a higher parameter m may be. Looking attentively to the curve, we may notice percentual decrease of almost 50% in the bit-rate for $m = 10$ which is a lot. So, we may conclude from here that having impulses with a greater m parameter in fiber-optic communication systems will be worst for the performance of such systems.

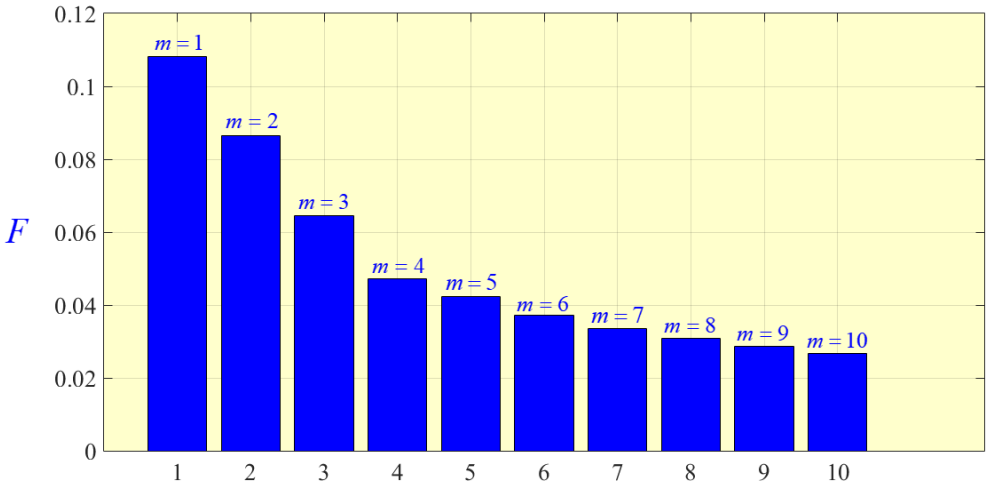

Figure 7.12 - Variation of the figure of merit F with the parameter m. Being F a way to measure the efficiency of a fiber-optic communication system, we may notice that having a higher value of m will make the system less efficient, meaning it gets tougher to have high bit-rates for larger distances.

Analyzing figure (7.12) and being F a way to measure the efficiency of a fiber-optic communication system, we see that as the influence of m becomes greater in the channel, the efficiency of the mentioned system decreases consequently. This means that if we compare the bit-rate for a given distance where $m = 1$ with another one on which $m > 1$, from figure (7.12) we can say that the bit-rate will be lower for the case whose $m > 1$ in comparison with the one whose $m = 1$. Therefore, we conclude that an impulse with higher m will be undesirable in a fiber-optic communication system.

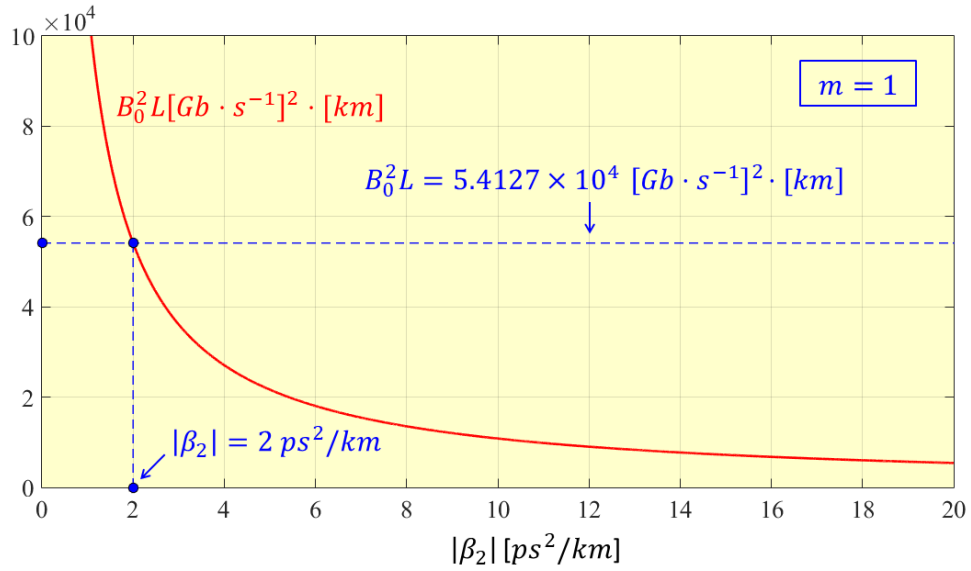

Figure 7.13 - Bit-rate squared product with the length of a given optical fiber for super-Gaussian pulses with $m = 1$, as an instrument to measure the performance of a fiber-optic communication system. It is possible to see a decay in the performance for higher β_2 values.

Looking at figure (7.13), we may see that the curve obtained corresponds to the one presented in figure (4.10) since the case when $m = 1$ corresponds to a chirped gaussian pulse and in this case when $C = C_{cr}$, which is the one we are most interested, for optimization purposes. In figures (7.14) and (7.15), we will be able to be fully aware on the impact it makes if the pulse as a higher m value.

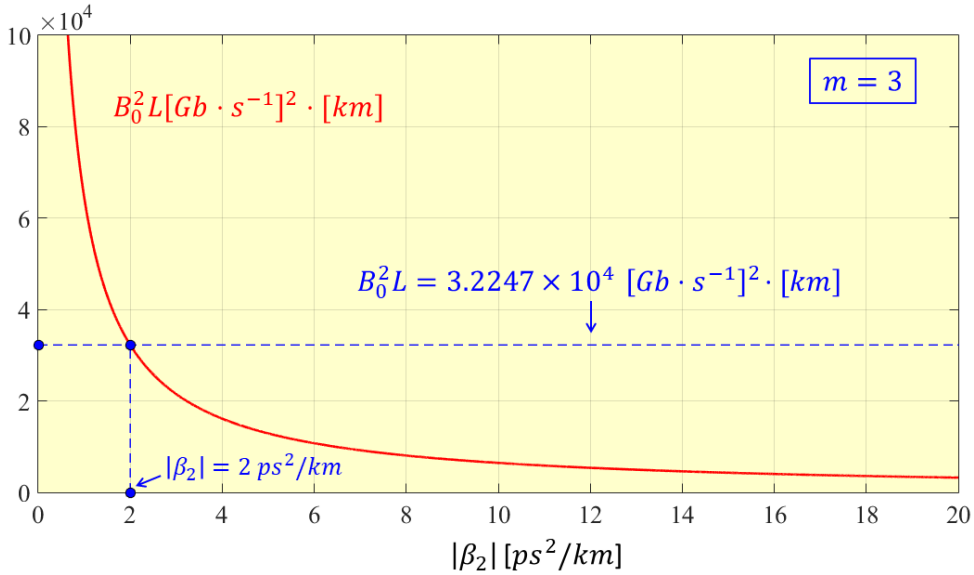

Figure 7.14 - Bit-rate squared product with the length of a given optical fiber for super-Gaussian pulses with $m = 3$, as an instrument to measure the performance of a fiber-optic communication system. It is possible to see a decay in the performance for higher β_2 values.

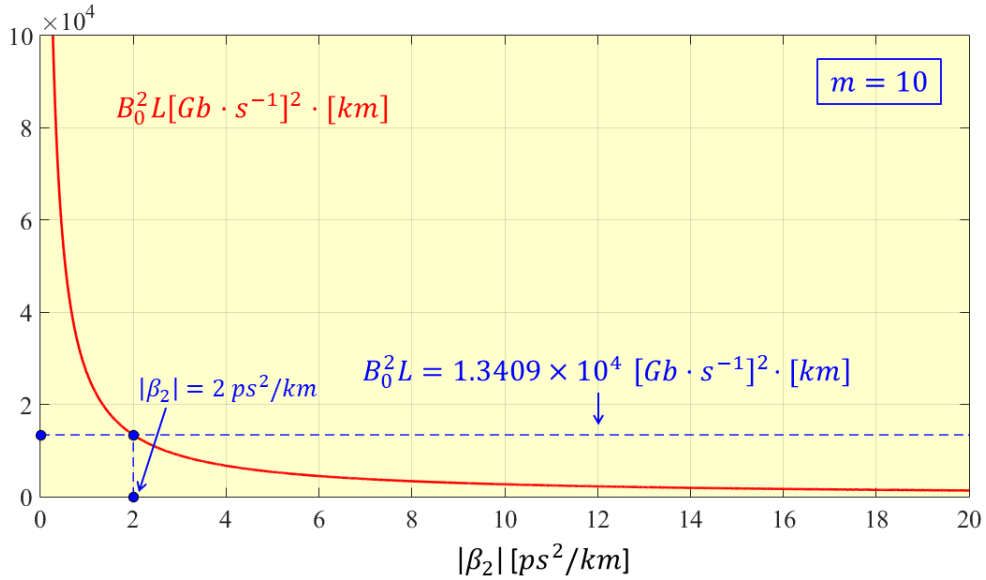

Figure 7.15 - Bit-rate squared product with the length of a given optical fiber for super-Gaussian pulses with $m = 10$, as an instrument to measure the performance of a fiber-optic communication system. It is possible to see a decay in the performance for higher β_2 values.

Analyzing figures (7.14) and (7.15), comparing with figure (7.13) we observe a decay in the performance of the fiber-optic communication system because figures (7.14) and (7.15) both correspond to super-Gaussian pulses whose $m > 1$ ($m = 3$ and $m = 10$, respectively). These results confirm what was seen in figure (7.11), which was that chirped gaussian pulses with a lower value of m allow a better performance of a fiber-optic communication system.

8. WDM Systems

Until now, we always considered an optical fiber transmitting only a single channel. Nowadays, it is already possible to transmit multiple channels within the physical structure of a single optical fiber. This is possible thanks to wavelength-division multiplexing (WDM).

Without going into full technical details (since it is out of the context of this dissertation) about WDM systems, we may consider – in WDM systems – the total bit-rate B (or capacity of the WDM system) as being the sum of all the channels individual bit-rates. It will also be assumed that this system works in the linear regime and, in that same regime, the interchannel crosstalk interference is neglected. To ensure this is feasible, it is needed that – in systems with direct detection – the spectral efficiency of the WDM system is less than one (in WDM systems with coherent detection is possible to have a spectral efficiency greater than one) [1].

Let $f_1 \leq f \leq f_2$ be the frequency range covered by the WDM system, i.e., we will have $\Delta f = f_2 - f_1$. In terms of wavelengths (measured in vacuum), this corresponds to:

$$\Delta\lambda = \lambda_1 - \lambda_2 = \frac{c}{f_1} - \frac{c}{f_2} = c\,\frac{\Delta f}{f_1 f_2}. \tag{8.1}$$

We are also going to assume, from now on, that all channels have identical spectral widths, meaning each channel will have the same Δf_{ch}. This way, being N_{ch} the total number of channels, it comes:

$$N_{ch} = \frac{\Delta f}{\Delta f_{ch}}. \tag{8.2}$$

If the bit-rate in a single channel is B_{ch} (because we are considering identical channels), the total WDM system capacity will be:

$$B = N_{ch} B_{ch}\,. \tag{8.3}$$

Then, the spectral efficiency of the WDM system, η_s, is such that:

$$\eta_s = \frac{B_{ch}}{\Delta f_{ch}}, \tag{8.4}$$

meaning the WDM system capacity may also be defined as:

$$B = \eta_s \Delta f\,. \tag{8.5}$$

Now, we are going to look at some examples for the different types of pulses studied in this work and see how optimization may impact the performance of WDM systems, by calculating its resulting capacity. First, considering we will use a dry fiber, we may eventually work with the fiber between $\lambda_1 = 1.6\ \mu m$ and $\lambda_2 = 1.3\ \mu m$. In this case, then, it will be $\Delta f = c/\lambda_0$, with $\lambda_0 = \lambda_1\lambda_2/(\lambda_1 - \lambda_2) = (104/15)\ \mu m$. Then $\Delta f = 43.25\ THz$ and, if we consider $\Delta f_{ch} = 50\ GHz$, we get a total of $N_{ch} = \Delta f/\Delta f_{ch} = 865$ channels.

In the following examples, it is considered that $\beta_2 = -1\ ps^2/km$ and $L = 40\ km$.

Example 1 – Unchirped Hyperbolic Secant Pulses:

To calculate the capacity of a WDM system, by applying the previous assumptions, considering that unchirped hyperbolic secant pulses will be the ones propagating along the channels of the WDM system, we need to recover expression (3.21) to get the maximum bit-rate for this kind of pulses and to obtain the resulting bit-rate, which is the following:

$$B_0 = \frac{1}{4}\sqrt{\frac{3}{\pi|\beta_2|L}} = 38.63\ Gb/s = B_{ch}\ . \tag{8.1}$$

Then, the capacity of the WDM system will be:

$$B = 865 \times 38.63\ Gb/s = 33.4\ Tb/s\ . \tag{8.2}$$

Example 2 – Unchirped Gaussian Pulses:

To calculate the capacity of a WDM system, by applying the previous assumptions, considering that unchirped Gaussian pulses will be the ones propagating along the channels of the WDM system, we need to recover expression (4.28) to get the maximum bit-rate for this kind of pulses and to obtain the resulting bit-rate, which is the following:

$$B_0 = \frac{1}{4\sqrt{|\beta_2|L}} = 39.53\ Gb/s = B_{ch}\ . \tag{8.3}$$

Then, the capacity of the WDM system will be:

$$B = 865 \times 39.53\ Gb/s = 34.3\ Tb/s\ . \tag{8.4}$$

Example 3 – Chirped Gaussian Pulses ($\boldsymbol{C = C_{cr}}$; $a = 0$):

To calculate the capacity of a WDM system, by applying the previous assumptions, considering that optimized chirped Gaussian pulses (with $a = 0$) will be the ones propagating along the channels of the WDM system, we need to recover expression (4.35) to get the maximum bit-rate for this kind of pulses and to obtain the resulting bit-rate, which is the following:

$$B_0 = \frac{\sqrt[4]{3}}{4}\frac{1}{\sqrt{|\beta_2|L}} = 52.02\ Gb/s = B_{ch}\ . \tag{8.5}$$

Then, the capacity of the WDM system will be:

$$B = 865 \times 52.02\ Gb/s = 45.0\ Tb/s\ . \tag{8.6}$$

Example 4 – Chirped Gaussian Pulses ($C = C_{cr};\ a = 1$):

To calculate the capacity of a WDM system, by applying the previous assumptions, considering that optimized chirped Gaussian pulses (with $a = 1$) will be the ones propagating along the channels of the WDM system, we need to recover expression (6.35) to get the maximum bit-rate for this kind of pulses and to obtain the resulting bit-rate, which is the following:

$$B_0 = \frac{1}{4\sqrt{|\beta_2|L}\sqrt{\chi_{max}}} = B_{ch}\ . \tag{8.7}$$

To get the value of χ_{max}, we first need to solve expression (6.38), which is the following:

$$a_c = \frac{2\sqrt{3}}{3}[3(1 + C_{cr}^2)]^{\frac{1}{4}}\ . \tag{8.8}$$

From figure (6.20) we know that for $a = 1$, $C_{cr} = 0.5922$. Solving expression (8.8), we now know that $a_c = 1.64 > 1 = a$. The last result determines that χ_{max} will be given by:

$$\chi_{max} = 2\sqrt{\frac{p_{cr}}{3}}\cos\left[\frac{1}{3}cos^{-1}\left(\frac{9a^2}{2}\sqrt{\frac{p_{cr}}{3}}\right)\right] \tag{8.9}$$

Finally, after solving expression (8.9), we may obtain the maximum bit-rate:

$$B_0 = \frac{1}{4\sqrt{|\beta_2|L}\sqrt{\chi_{max}}} = 47.03\ Gb/s\ . \tag{8.10}$$

Then, the capacity of the WDM system will be:

$$B = 865 \times 47.03\ Gb/s = 40.7\ Tb/s\ . \tag{8.11}$$

Example 5 – Super-Gaussian Pulses ($C = C_{cr};\ m = 3$):

To calculate the capacity of a WDM system, by applying the previous assumptions, considering that optimized super-Gaussian pulses (with $m = 3$) will be the ones propagating along the channels of the WDM system, we need to recover expressions (7.27) and (7.28) to get the maximum bit-rate for this kind of pulses and to obtain the resulting bit-rate, which is the following:

$$B_0 = \frac{1}{4\sqrt{|\beta_2|L}\sqrt{\chi_{max}}} = B_{ch}\ . \tag{8.12}$$

Knowing from figure (7.7) that $C_{cr} = 0.9691 = \chi_{max}$, the resulting maximum bit-rate will be:

$$B_0 = \frac{1}{4\sqrt{|\beta_2|L}\sqrt{C_{cr}}} = 40.15\ Gb/s\ . \tag{8.13}$$

Then, the capacity of the WDM system will be:

$$B = 865 \times 40.15\ Gb/s = 34.7\ Tb/s\ . \tag{8.14}$$

Example 6 – Super-Gaussian Pulses ($C = C_0;\ m = 4$):

To calculate the capacity of a WDM system, by applying the previous assumptions, considering that optimized super-Gaussian pulses (with $m = 4$) will be the ones propagating along the channels of the WDM system, we need to recover expressions (7.27) and (7.28) to get the maximum bit-rate for this kind of pulses and to obtain the resulting bit-rate, which is the following:

$$B_0 = \frac{1}{4\sqrt{|\beta_2|L}\sqrt{\chi_{max}}} = B_{ch}\ . \tag{8.15}$$

Knowing from figure (7.8) that $C_0 = 0.8036$ and $\chi_1^{opt}(C_0) = 1.2443 = \chi_{max}$, the resulting maximum bit-rate will be:

$$B_0 = \frac{1}{4\sqrt{|\beta_2|L}\sqrt{\chi_1^{opt}(C_0)}} = 35.44\ Gb/s\ . \tag{8.16}$$

Then, the capacity of the WDM system will be:

$$B = 865 \times 40.15\ Gb/s = 30.7\ Tb/s\ . \tag{8.17}$$

Example 7 – Super-Gaussian Pulses ($C = C_0;\ m = 7$):

To calculate the capacity of a WDM system, by applying the previous assumptions, considering that optimized super-Gaussian pulses (with $m = 7$) will be the ones propagating along the channels of the WDM system, we need to recover expressions (7.27) and (7.28) to get the maximum bit-rate for this kind of pulses and to obtain the resulting bit-rate, which is the following:

$$B_0 = \frac{1}{4\sqrt{|\beta_2|L}\sqrt{\chi_{max}}} = B_{ch}\ . \tag{8.18}$$

Knowing from figure (7.9) that $C_0 = 0.5370$ and $\chi_1^{opt}(C_0) = 1.8622 = \chi_{max}$, the resulting maximum bit-rate will be:

$$B_0 = \frac{1}{4\sqrt{|\beta_2|L}\sqrt{\chi_1^{opt}(C_0)}} = 28.97\ Gb/s\ . \tag{8.19}$$

Then, the capacity of the WDM system will be:

$$B = 865 \times 28.97\ Gb/s = 25.1\ Tb/s\ . \tag{8.20}$$

9. Conclusions and Future Work

The main goal of this work was to find an optimum chirp parameter value for a given pulse, in order to achieve the optimum input and output pulse widths which would allow fiber-optic communication systems to have the best performance possible. In other words, to optimize those systems to be able to work at the maximum bit-rate value according to the optimization performed on the pulses conveying information through the network.

In chapter 2, it was given theoretical background on the most important topics related to pulse propagation along optical fibers, as well as clarifying the dispersion phenomenon that occurs throughout the entire journey and what impact chirp has in this process. An important result to have in mind is the possibility of having pulse compression if $\beta_2 C < 0$, meaning if β_2 and C have opposite signals, the effects that both cause on the pulses will counteract each other. So, instead of having pulse broadening we would have pulse compression.

In chapter 3, unchirped hyperbolic secant pulses were analyzed and their impact performance, if used to operate in a fiber-optic communication system, was presented. Since there was no expression that gave us the broadening factor (which is the relation between the RMS pulse width at any point of an optical fiber compared with the RMS input pulse width), no optimization was possible since the performance analysis was made considering always $C = 0$. HOD effects were neglected in this chapter ($\beta_3 = 0$).

In chapter 4, chirped Gaussian pulses were analyzed for both normal ($\beta_2 > 0$) and anomalous ($\beta_2 < 0$) dispersion regimes. The conclusions for both regimes were quite similar, being the most important difference, the critical chirp value obtained for both regimes. For the normal regime the critical chirp parameter value is $C_{cr} = -1/\sqrt{3}$, whereas for the anomalous dispersion regime is $C_{cr} = 1/\sqrt{3}$. As we may notice, the value for both cases only differs in signal. It is that way because in this chapter, higher-order dispersion effects were neglected. However, since the case when $C = 0$ was also discussed here, we could confirm that a chirped Gaussian pulse with $C = C_{cr}$ delivers a better system performance compared to an unchirped Gaussian pulses. A chirped Gaussian pulse with $C = C_{cr}$ also performs better than any other chirped Gaussian pulse with $C \neq C_{cr}$.

In chapter 5, a full comparison was made between unchirped hyperbolic secant pulses and unchirped Gaussian pulses. Being compared side by side at all parameters, it turns out that the best performing type of pulse is the unchirped Gaussian pulse.

In chapter 6, higher-order dispersion effects were fully analyzed. It was clear that having $\beta_3 \neq 0$ always had a negative impact on system performance. Furthermore, increasing the HOD effects means a higher needed value for the critical chirp parameter. So, besides the need for any higher chirp parameter value to optimize system performance, the final performance achieved would always be worse than when $\beta_3 = 0$, because HOD effects contribute to higher pulse broadening, making the pulses wider and therefore resulting in lower bit-rate values. The error that β_3 introduces in the system is also presented, as well as an approximation for the error function which will allow to quickly get the percentage of bit-rate lost due to HOD effects. It is also proved that the approximation is a good one, since the error is approximately 1%.

In chapter 7, it was discussed super-Gaussian pulses. It was seen that super-Gaussian pulses with a $m > 1$ had a worse performance than a super-Gaussian pulse with $m = 1$ (have in mind $m = 1$ corresponds to the case analyzed in chapter 4). So, we concluded that the higher the value of m is, the worse it will be the system performance. With a higher m value, it also comes a higher chirp parameter value. Regarding the chirp parameter value needed to optimize system performance, it was seen that only for $1 \leq m \leq 3$ the critical chirp parameter value was the one that allowed the best optimization. However, for $m \geq 4$ it was C_0 the chirp parameter that gave the best optimization. HOD effects were also neglected in this chapter.

In chapter 8, WDM systems are introduced in a simplified manner allowing us to have an idea on how the various kinds of pulses analyzed in the former chapters perform in such systems. Practical examples were presented and, in the end, the pulse that maximizes the capacity of a WDM system is a chirped Gaussian pulse whose $C = C_{cr}$.

With all we have learned from the mentioned chapters, we may now conclude with confidence that the best pulse to achieve optimization in a fiber-optic communication system is a chirped Gaussian pulse, whose parameters are: $m = 1$ and $C_{cr} = -1/\sqrt{3}$ (if $\beta_2 > 0$) or $C_{cr} = 1/\sqrt{3}$ (if $\beta_2 < 0$). From all the pulses analyzed throughout this work, those are the ones that ensure we have the maximum bit-rate achievable by optimization. However, some final notes must be made.

For hyperbolic secant pulses, the broadening factor is only valid if these pulses have no chirp since there was no expression for the broadening factor regarding hyperbolic secant pulses with chirp. Also, the higher-order dispersion term is also not included in that same broadening factor expression used to define the performance of such pulses. Therefore, if we want to know how a fiber-optic communication system performs in the presence of hyperbolic secant pulses with chirp and/or affected by HOD effects, the only way would be by running numerical simulations for each case at hand, since there is no way of doing it by analytical approach.

For super-Gaussian pulses, although the chirp parameter is accounted for in the broadening factor expression used to make the analysis on the behavior these pulses have regarding the performance of a fiber-optic communication system, there is no analytical expression for the broadening factor having into account the effects of higher-order dispersion. Once more, if we wanted to quantify the impact of such effects in pulse behavior, we would have to do it by running numerical simulations for each single case, without the support that the analytical approach provides.

Finally, it is now undeniable the presence of chirp is not always a bad thing. It is now proved chirp, possessing the opposite signal of β_2, counteracts the GVD effects and therefore allows the possibility of having fiber-optic communication systems with higher bit-rates, rather than the ones with no chirp at all, as it was proved in the course of this work.

From this point, future work perspectives may now be pointed. Deducting a broadening factor expression for hyperbolic secant pulses which includes the chirp parameter (or even more demanding, one that includes the HOD effects), in order to quantify the performance impact such pulses would have on fiber-optic communication systems. Regarding the super-Gaussian pulses, getting an expression for the broadening factor which includes the HOD effects. Although it is obvious the performance is always worst having β_3 in play, being able to analyze such case by means of analytical approach is always better than having to run different simulations for every single case we might find relevant. One final suggestion, being this the most challenging one, would be to include the non-linear effects on pulse behavior.

A. Modal Analysis

A.1 Closed-Form Analytical Expressions

In this section, we are going to make a modal analysis of an optical fiber, using closed-form analytical expressions. However, instead of making a rigorous analysis, it will be presented an approximate analysis which is, nonetheless, valid for almost every practical case. Let us first consider step-index fibers, where the refractive index $n(r)$ is given by:

$$n(r) = \begin{cases} n_1, & r \leq a, \\ n_2, & r > a, \end{cases} \tag{A.1}$$

where

$$n_2 = n_1\sqrt{1 - 2\Delta} < n_1 \tag{A.2}$$

being Δ the dielectric constant, which may be obtain by:

$$\Delta = \frac{n_1^2 - n_2^2}{2n_1^2} \ll 1. \tag{A.3}$$

Every component of the electromagnetic field as the following form:

$$\Psi(r, \theta, z, t) = F(r, \theta)\exp[i(\beta z - \omega t)]. \tag{A.4}$$

Since we are not focusing on the study of impulse propagation, we may consider monochromatic waves whose temporal variation is exclusively given by $\exp(-i\omega t)$. Besides, $\Psi(r, \theta, z, t)$ verifies the following propagation equation [1]:

$$\nabla^2\Psi - \frac{1}{v_p^2}\frac{\partial^2\Psi}{\partial t^2} = 0, \quad v_p = \frac{c}{n(r)}. \tag{A.5}$$

Then, Helmholtz equation is obtained:

$$\nabla^2\Psi + n^2(r)k_0^2\Psi = 0, \quad k_0 = \frac{\omega}{c} = \frac{2\pi f}{c} = \frac{2\pi}{\lambda}. \tag{A.6}$$

In cylindrical coordinates, it comes:

$$\nabla^2\Psi = \frac{\partial^2\Psi}{\partial r^2} + \frac{1}{r}\frac{\partial\Psi}{\partial r} + \frac{1}{r^2}\frac{\partial^2\Psi}{\partial\theta^2} + \frac{\partial^2\Psi}{\partial z^2}. \tag{A.7}$$

This way, we may conclude that:

$$\frac{\partial^2 F}{\partial r^2} + \frac{1}{r}\frac{\partial F}{\partial r} + \frac{1}{r^2}\frac{\partial^2 F}{\partial\theta^2} + [n^2(r)k_0^2 - \beta^2]F(r, \theta) = 0. \tag{A.8}$$

From here, it is considered that the azimuthal variation has the form of $\exp(i\ell\theta)$.

But then, assuming:

$$F(r, \theta) = \Xi(r)\exp(i\ell\theta), \tag{A.9}$$

we obtain the following differential equation:

$$\frac{\partial^2\xi}{\partial r^2} + \frac{1}{r}\frac{\partial\xi}{\partial r} + \left[n^2(r)k_0^2 - \beta^2 - \frac{\ell^2}{r^2}\right]\Xi(r) = 0. \tag{A.10}$$

Let us define:

$$\begin{cases} h^2 = n_1^2 k_0^2 - \beta^2, \\ \alpha^2 = \beta^2 - n_2^2 k_0^2. \end{cases} \rightarrow \begin{cases} u = ha \\ w = \alpha a \end{cases} \tag{A.11}$$

The previous differential equation, in these conditions, assumes the form of a Bessel differential equation:

$$r < a \rightarrow \frac{\partial^2 \xi}{\partial r^2} + \frac{1}{r}\frac{\partial \xi}{\partial r} + \left(h^2 - \frac{\ell^2}{r^2}\right)\Xi(r) = 0, \tag{A.12}$$

in the core and the form of a modified Bessel equation:

$$r > a \rightarrow \frac{\partial^2 \xi}{\partial r^2} + \frac{1}{r}\frac{\partial \xi}{\partial r} + \left(\alpha^2 + \frac{\ell^2}{r^2}\right)\Xi(r) = 0, \tag{A.13}$$

in the cladding. The corresponding surface solutions are [1]:

$$\Xi(r) = \begin{cases} \dfrac{A}{J_\ell(u)} J_\ell\left(\dfrac{r}{a}u\right), & r \le a, \\ \dfrac{A}{K_\ell(w)} K_\ell\left(\dfrac{r}{a}w\right), & r \ge a, \end{cases} \rightarrow \Xi(a) = A, \tag{A.14}$$

where $J_\ell(x)$ is the Bessel function of the first kind and order ℓ and $K_\ell(x)$ is the modified Bessel function of the second kind and order ℓ.

Introducing the effective refractive index:

$$n_{eff} = \frac{\beta}{k_0}, \tag{A.15}$$

it comes,

$$\begin{cases} u^2 = (k_0 a)^2 (n_1^2 - n_{eff}^2) \\ w^2 = (k_0 a)^2 (n_{eff}^2 - n_2^2) \end{cases} \rightarrow u^2 + w^2 = v^2. \tag{A.16}$$

To obtain the last equation, the definition of normalized frequency for an optical fiber was used:

$$v = k_0 a \sqrt{n_1^2 - n_2^2} = 2\pi \frac{a}{\lambda} \sqrt{n_1^2 - n_2^2} = 2\pi \frac{a}{\lambda} n_1 \sqrt{2\Delta}\,. \tag{A.17}$$

One can also introduce a normalized longitudinal wavenumber b given by:

$$b = 1 - \frac{u^2}{v^2} = \frac{w^2}{v^2} = \frac{n_{eff}^2 - n_2^2}{n_1^2 - n_2^2} \rightarrow \begin{cases} u = v\sqrt{1-b} \\ w = v\sqrt{b} \end{cases}. \tag{A.18}$$

So, at cutoff, $n_{eff} = n_2$ e $b = 0$. On the other hand,

$$\lim_{v \to \infty} b = 1 \rightarrow \lim_{v \to \infty} n_{eff} = n_1. \tag{A.19}$$

Therefore, a higher frequency causes the electromagnetic field to be stronger in the zone corresponding to the axis of the optical fiber. So, for a given *superficial mode*, we have (for a given optical fiber operating in a given normalized frequency v):

$$\begin{cases} n_2 k_0 \le \beta < n_1 k_0 \\ n_2 \le n_{eff} < n_1 \\ 0 \le b < 1 \end{cases} \rightarrow \begin{cases} v \ge u > 0 \\ 0 \le w < v \end{cases}. \tag{A.20}$$

As it is possible to verify, the wavenumber β comes from the expression:

$$\beta = \frac{1}{a}\sqrt{\frac{v^2}{2\Delta} - u^2} = \frac{v}{a}\sqrt{\frac{1-2(1-b)\Delta}{2\Delta}}. \tag{A.21}$$

The modal equation of the superficial guide is obtained by applying the second condition over the core-cladding interface which has not been applied yet: the $\frac{d\xi}{dr}$ continuity in $r = a$. This way, it comes:

$$uJ_\ell'(u)K_\ell(w) = wJ_\ell(u)K_\ell'(w), \tag{A.22}$$

which is the modal equation of the superficial modes of the optical fiber in the small dielectric contrast approximation. Knowing that:

$$J_\ell'(u) = \pm J_{\ell\pm1}(u) \pm \frac{\ell}{u}J_\ell(u), \tag{A.23}$$

$$K_\ell'(w) = -K_{\ell\pm1}(w) \pm \frac{\ell}{w}K_\ell(w), \tag{A.24}$$

it is possible to rewrite the modal equation [1]:

$$u\frac{J_{\ell\pm1}(u)}{J_\ell(u)} = \pm\, w\frac{K_{\ell\pm1}(w)}{K_\ell(w)}. \tag{A.25}$$

The last equation is the characteristic equation for any $LP_{\ell m}$ mode. In the notation $LP_{\ell m}$, indexes ℓ and m characterize the azimuthal and radial distribution of the spatial profile of the electromagnetic field. However, for the fundamental LP_{01} mode, the modal solution will be:

$$u\frac{J_1(u)}{J_0(u)} = w\frac{K_1(w)}{K_0(w)}. \tag{A.26}$$

In single-mode optical fibers only the fundamental mode can propagate. This corresponds to the requirement that the fiber parameter (or normalized frequency) is:

$$v < 2.4048\,. \tag{A.27}$$

In fact, in the linearly polarized mode approximation, the second mode is the LP_{11} mode having a normalized cutoff frequency v_c that corresponds to the lowest real non-negative solution of the equation:

$$J_0(v_c) = 0 \rightarrow v_c = 2.40482555769577\ldots\,. \tag{A.28}$$

We conclude, therefore, that the maximum value a_{max} for the core radius, in single-mode operation, is given by:

$$a_{max} = \frac{2.4048\lambda}{2\pi n_1\sqrt{2\Delta}}. \tag{A.29}$$

We may also realize that, for single-mode operation, $f < f_c$ or $\lambda > \lambda_c$ (with $c = \lambda_c f_c$), it comes:

$$[f_c]_{LP_{11}} = \frac{2.4048}{2\pi n_1\sqrt{2\Delta}}\frac{c}{a}, \tag{A.30}$$

$$[\lambda_c]_{LP_{11}} = \frac{2\pi n_1\sqrt{2\Delta}}{2.4048}a\,. \tag{A.31}$$

Finally, the following expression may also be obtained from the previous ones:

$$\Delta = \frac{1}{2}\left(\frac{2.4048\lambda_c}{2\pi n_1 a}\right)^2. \tag{A.32}$$

A.2 Numerical Results

This section is intended, through numerical simulations, to give a more in-depth understanding on the influence the conditions presented in section A.1 will have to able to obtain single-mode fibers (the ones considered throughout the entire work), so it is possible to get rid of the intermodal dispersion present in multimode fibers.

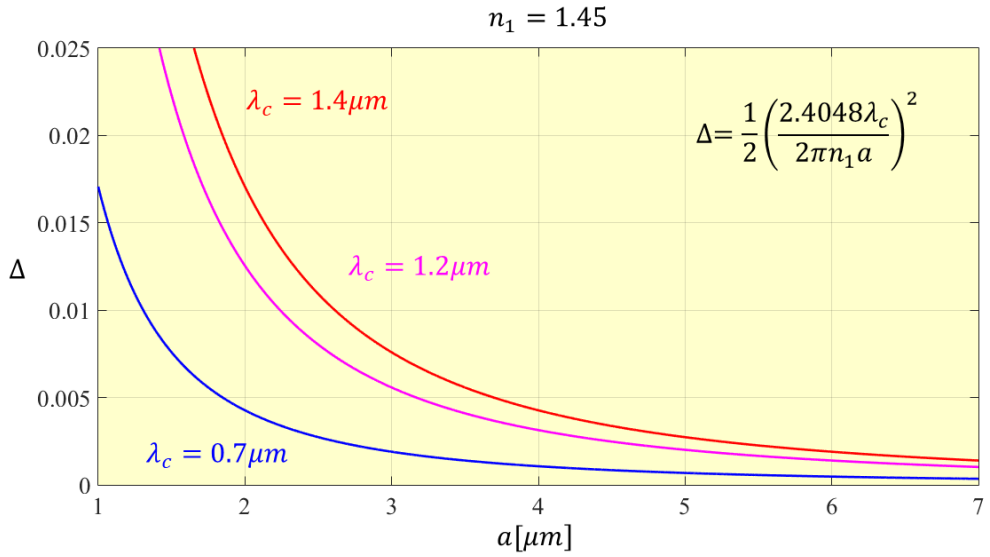

Figure A.1 - Dielectric contrast as a function of the core radius for a fixed refractive index core value, being $n_1 = 1.45$ and for fixed cutoff wavelength values of $\lambda_c = 1.4\ \mu m$, $\lambda_c = 1.2\ \mu m$, $\lambda_c = 0.7\ \mu m$.

Analyzing figure (A.1), we can see that the dependence of the dielectric contrast with the size of the core radius is quadratic. As it is possible to see, the lower the core diameter the higher the dielectric contrast. This is important to have in consideration since the value of the dielectric contrast must be much lower than 1, i.e, at least one order of magnitude. This means that it is not possible to have much lower values for the core radius of the fiber than the ones shown in the graph. Another conclusion that can be made is that the lower the frequency, the higher it as to be the core radius of the fiber to fulfill the condition. All this is valid while keeping the refractive index of the fiber constant.

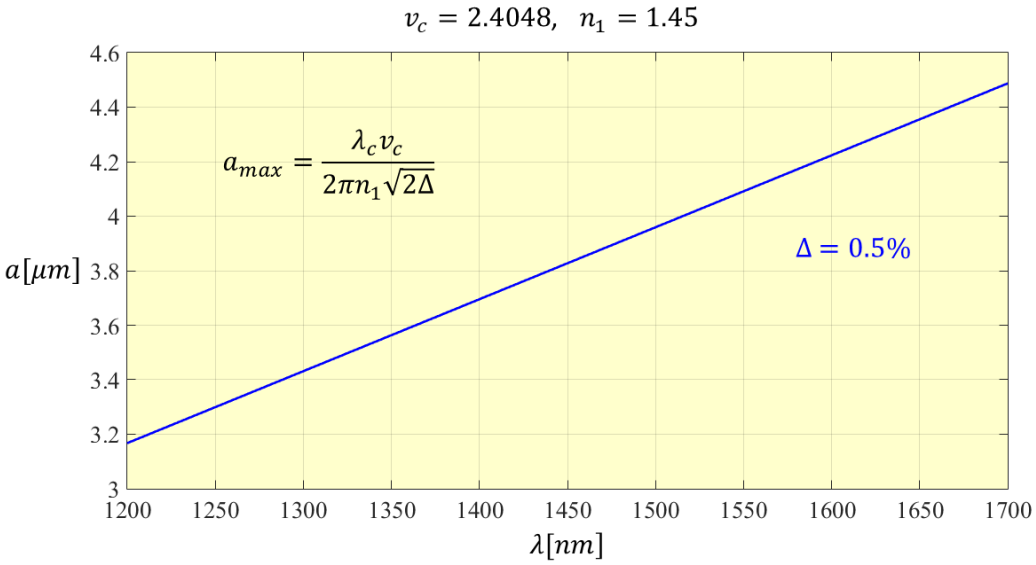

Figure A.2 - Maximum core radius for wavelengths inside the interval $\lambda = [1200; 1700]\ nm$. The refractive core index value is $n_1 = 1.45$, the normalized cutoff frequency is $v_c = 2.4048$ and $\Delta = 0.5\%$.

Looking at figure (A.2), keeping the dielectric contrast constant, being the fiber parameter at its maximum value ($v_c = 2.4048$) to have single-mode operation and keeping the index reflection of the core radius constant, it is possible to see a linear dependence of the maximum value of the core radius depending on the wavelength of the carrier signal. As it is shown in the graph, the higher the carrier wavelength the higher it can be the core radius of the fiber. This is also important to have into account, because depending on the band we want to operate, we need to keep sure that the core radius is not too large for the band of frequencies we want to transmit along the fiber.

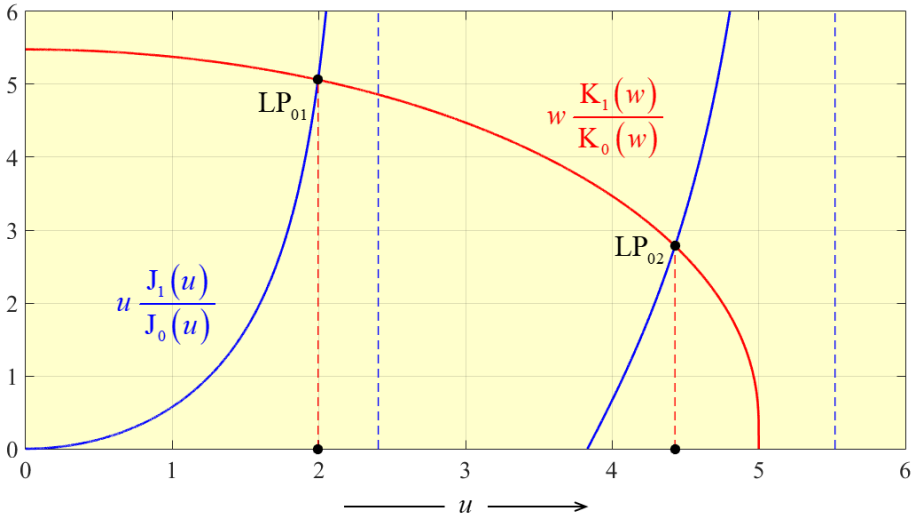

Figure A.3 – Propagation modes for $v = 5$.

Looking at figure (A.3), the curve representing the right-hand side of the equation (A.26) has a value equal to 0 for $v = 5$. This means that the right-hand side will only intercept the curves corresponding to the left-hand side of the equation (A.26) two times. The consequence of such outcome is that the equation will have only two solutions for $v = 5$. Those solutions are the LP_{01} propagation mode and the LP_{02} propagation mode, i.e, the first two LP modes. From this graph, we can conclude that the smaller the value for the normalized frequency is, the fewer the modes that can propagate along an optical fiber.

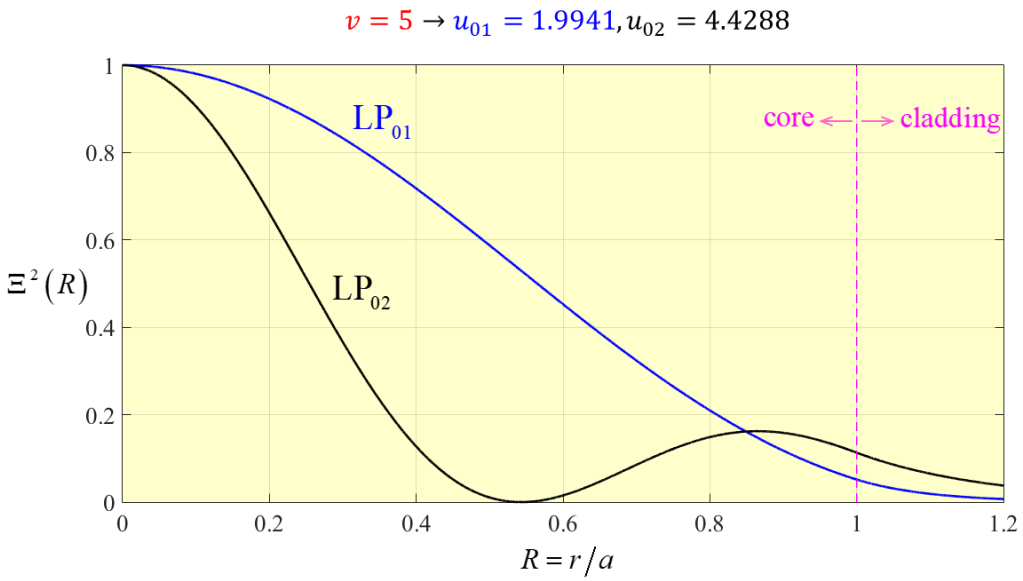

Figure A.4 - Radial distribution of the intensity profile for the propagation modes when $v = 5$.

Analyzing figure (A.4), it is shown that the two propagations modes considered earlier in figure (A.3) have different intensity profile according to the distance they are from the center of the optical fiber. Both have maximum intensity at the center. But then, as the distance to the core increases, their intensity profiles vary differently from each other. For the first propagation mode (LP_{01}), the intensity due to the distance from the center decreases almost linearly as it approaches the cladding of the fiber. For the second propagation mode (LP_{02}), the intensity decreases with the distance to the center reaching a minimum that is practically zero; then, it starts to increase a bit until it reaches a maximum value; passing that value it will always continue to decrease as it is reaching the cladding of the fiber, having this mode a slightly higher intensity than the first mode.

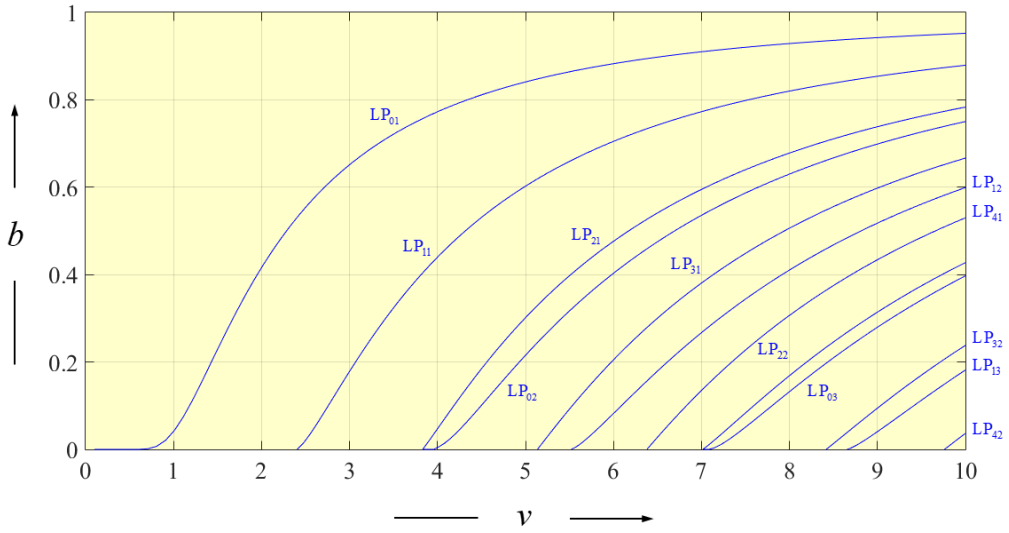

Figure A.5 - Propagation modes for $v \leq 10$.

Analyzing figure (A.5), it is shown that for higher values of the normalized frequency v, the higher the number of modes that can propagate along an optical fiber. However, what is intended to achieve is that the value of the normalized frequency is equal or less than 2,4048. Why? Because the objective is to have single-mode fibers and figure (A.5) confirms it must be that way. And why is that better? Because this kind of fiber does not introduce intermodal dispersion, since only one propagation mode is allowed.

B. Chirped Gaussian Pulses ($\beta_2 = 0, \beta_3 \neq 0$)

In this section, it is going to be study the pulse width behavior for chirped Gaussian pulses. However, it is going to be neglected the effects of GVD in this analysis and we will focus on the effects of HOD. It is going to be seen how the upcoming behavior will affect the bit-rate in a fiber-optic communication system.

To start, we need to remind the broadening factor given in [2] for chirped Gaussian pulses:

$$\left(\frac{\sigma}{\sigma_0}\right)^2 = \left[1 + C\left(\frac{\beta_2 L}{2\sigma_0^2}\right)\right]^2 + \left(\frac{\beta_2 L}{2\sigma_0^2}\right)^2 + (1 + C^2)^2 \left(\frac{\beta_3 L}{4\sqrt{2}\sigma_0^3}\right)^2. \tag{B.1}$$

Then, if we make $\beta_2 = 0$ we will obtain:

$$\left(\frac{\sigma}{\sigma_0}\right)^2 = 1 + (1 + C^2)^2 \left(\frac{\beta_3 L}{4\sqrt{2}\sigma_0^3}\right)^2. \tag{B.2}$$

Introducing the following dimensionless parameters:

$$P(\xi) = \frac{\sigma^2(\xi)}{\beta_3^{2/3} L^{2/3}}, \tag{B.3}$$

$$r = P(\xi = 0), \tag{B.4}$$

$$\varrho = P(\xi = 1), \tag{B.5}$$

equation (B.2) can be rewritten in the form:

$$P(\xi) = r + \frac{p^2}{2r^2}\xi^2, \tag{B.6}$$

from which we may obtain:

$$\varrho = P(1) = r + \frac{p^2}{2r^2}. \tag{B.7}$$

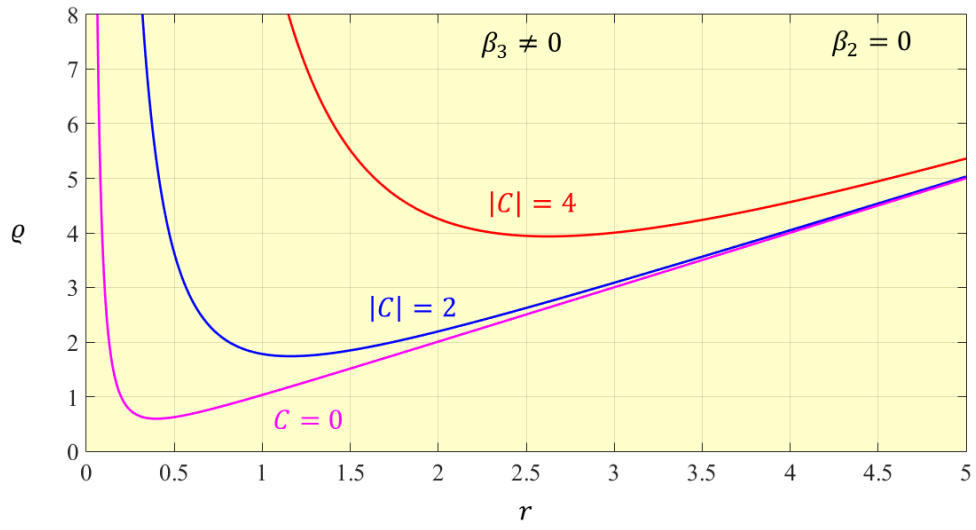

Figure B.1 - Variation of the normalized output pulse width ϱ with the normalized input pulse r for a chirped Gaussian pulse for $\beta_2 = 0$ and $\beta_3 \neq 0$. The chosen values for the chirp parameter are $C = 0$, $|C| = 2$ and $|C| = 4$.

Analyzing figure (B.1), it is possible to see that we obtain the best performance for $C = 0$, i.e., the smallest values for both the input and output pulse width are obtained when there is no chirp. This means that regardless of the chirp signal, if the chirp value is greater than zero in module, the optimum values for ϱ and r will be higher than the ones obtained for $C = 0$.

Therefore, it would be nice to be able to quantify these optimum values for the input pulse width and for the output pulse width. To do so, we start by doing the following calculation:

$$\frac{d\varrho}{dr} = 1 - \frac{p^2}{r^3} = 0 \rightarrow r_{opt} = p^{2/3} \rightarrow \varrho_{opt} = \frac{3}{2}p^{2/3} \ . \tag{B.8}$$

From this point we may get:

$$P_{opt}(\xi) = p^{2/3}\left(1 + \frac{1}{2}\xi^2\right). \tag{B.9}$$

It is now possible to conclude that the following expression will always be true, regardless of what the C value may be:

$$\gamma(\xi) = \frac{P_{opt}(\xi)}{r_{opt}} = 1 + \frac{1}{2}\xi^2 \, . \tag{B.10}$$

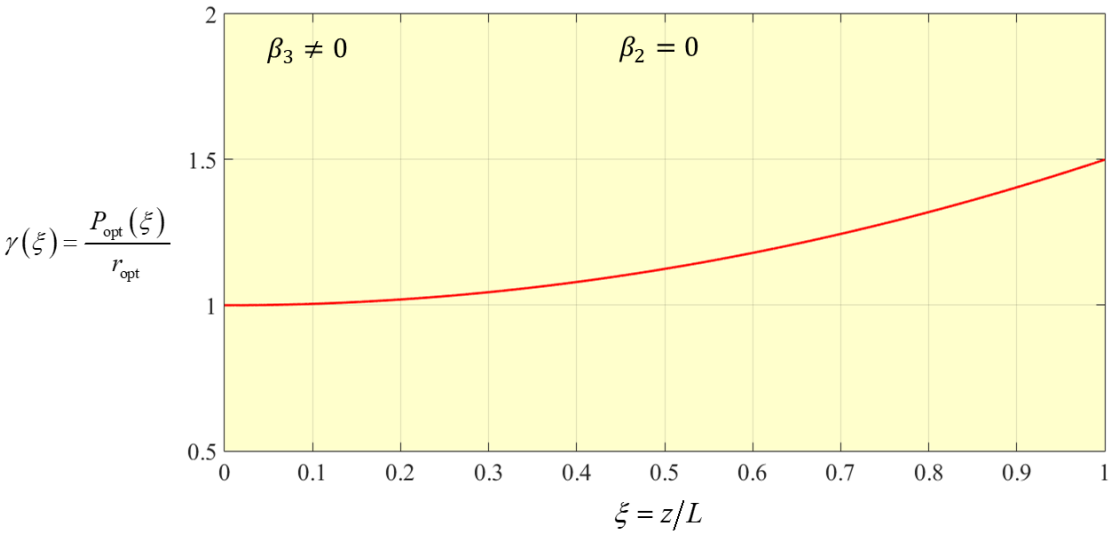

Figure B.2 - Behavior of the pulse width along an optical fiber for $\beta_3 \neq 0$ and $\beta_2 = 0$.

Looking at figure (B.2), it is possible to observe that the pulse width grows monotonically through the entire journey inside the optical fiber. Even more, the growth rate of the pulse width increases with the distance traveled inside the optical fiber. We can also state that the pulse width has a size which is exactly one and a half at the output in comparison with the pulse width at the input of the optical fiber, which is exactly what the analytical expressions predicted.

Gathering what we know from analyzing both figures (B.1) and (B.2), we found that we get the best performance if $C = 0$ (because $\beta_2 = 0$ and therefore it will never be possible to have $\beta_2 C < 0$, which is the condition that ensures pulse compression and would allow pulse chirp optimization) and that the bit-rate is going to be determined by the pulse width at the output of the optical fiber. Then, in the next section, it is going to be shown how to quantify the bit-rate value considering $\beta_2 = 0$ and $\beta_3 \neq 0$. It is also going to be shown how to measure system performance.

B.1 Maximum Bit-Rate Value

In this section, it is going to be shown how to get the maximum bit-rate possible for chirped Gaussian pulses when $\beta_2 = 0$ and $\beta_3 \neq 0$. First, we need to remember the common rule of thumb applied in fiber-optic communication systems [1]:

$$\sigma_{max} \leq \frac{T_b}{4} = \frac{1}{4B} \rightarrow B \leq B_0 = \frac{1}{4\sigma_{max}}. \tag{B.11}$$

If $\beta_2 = 0$ and $\beta_3 \neq 0$, σ_{max} will be simply given by:

$$\sigma_{max} = \sigma_1 = \sqrt{\varrho_{opt}}|\beta_3|^{1/3}L^{1/3}, \tag{B.12}$$

where B_0 will be:

$$B_0 = \frac{1}{4\sigma_{max}} = 4^{-2/3}\sqrt{\frac{2}{3}}\frac{1}{[(1+C^2)|\beta_3|L]^{1/3}}. \tag{B.13}$$

The system performance may be measured by knowing $B_0^3 L$, which is defined as:

$$B_0^3 L = \frac{F'}{|\beta_3|}. \tag{B.14}$$

The figure of merit F' is given by:

$$F' = \frac{1}{24(1+C^2)}. \tag{B.15}$$

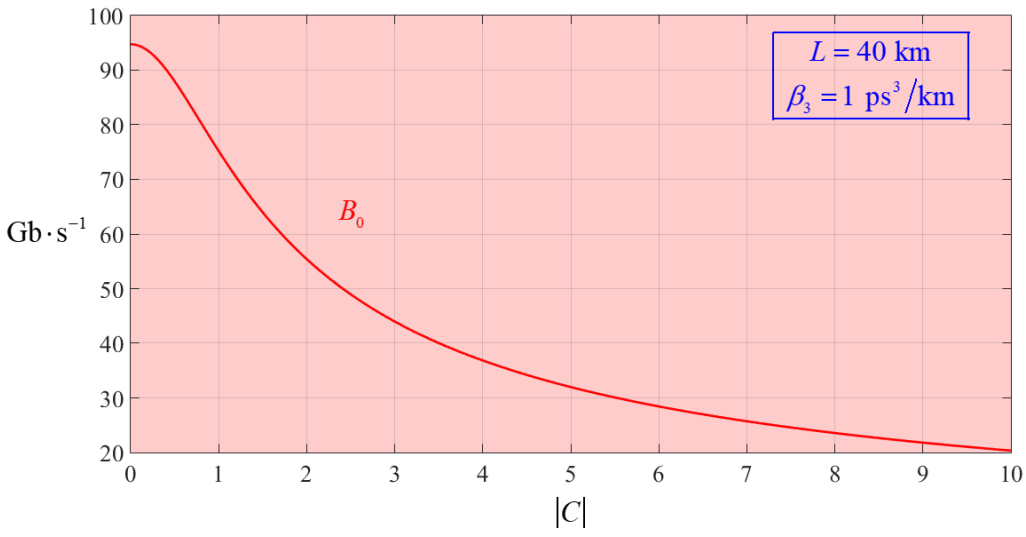

Figure B.3 - Variation of the bit-rate B_0 with the chirp parameter C for $\beta_3 = 1\, ps^3/km$ and $\beta_2 = 0$ for an optical fiber with length $L = 40\, km$. As it is possible to observe, the value of the bit-rate continuously decreases for bigger values of $|C|$.

Looking at figure (B.3), it is possible to see a decrease of the bit-rate value for higher C values. Even more, it is possible to see that if $\beta_2 = 0$, increasing C will only contribute to have less bit-rate on the channel and therefore decrease the performance of a fiber-optic communication system.

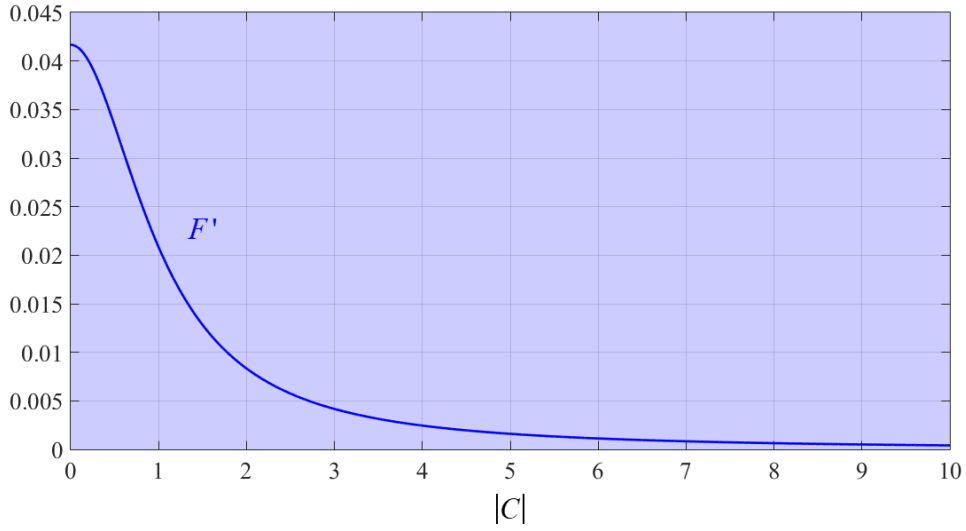

Figure B.4 - Variation of the figure of merit F' with the parameter C. Being F' a way to measure the efficiency of a fiber-optic communication system, we may notice that having a higher value of C will make the system less efficient, meaning it gets tougher to have high bit-rates for larger distances.

Analyzing figure (B.4) and being F' a way to measure the efficiency of a fiber-optic communication system, we see that as the influence of C becomes greater in the channel, the efficiency of the mentioned system decreases drastically. This means that if we compare the bit-rate for a given distance where $C = 0$ with another one on which $|C| > 0$, from figure (B.4) we can say that the bit-rate will be lower for the case whose $|C| > 0$ in comparison with the one whose $C = 0$. Therefore, we conclude that an impulse with higher C will be undesirable in a fiber-optic communication system.

However, our analysis would not be complete without analyzing the product $B_0^3 L$. In figures (B.5) and (B.6), we will see how the chirp parameter influences the performance of a fiber-optic communication system and of course, what impact β_3 will have as well.

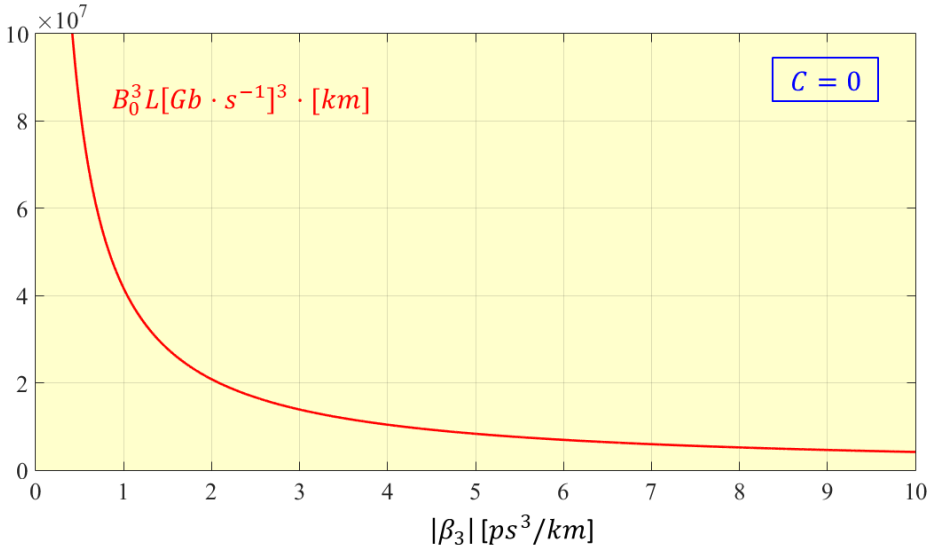

Figure B.5 - Bit-rate cubic product with the length of a given optical fiber for chirped Gaussian pulses with $C = 0$, as an instrument to measure the performance of a fiber-optic communication system considering $\beta_2 = 0$. It is possible to see a decay in the performance for higher β_3 values.

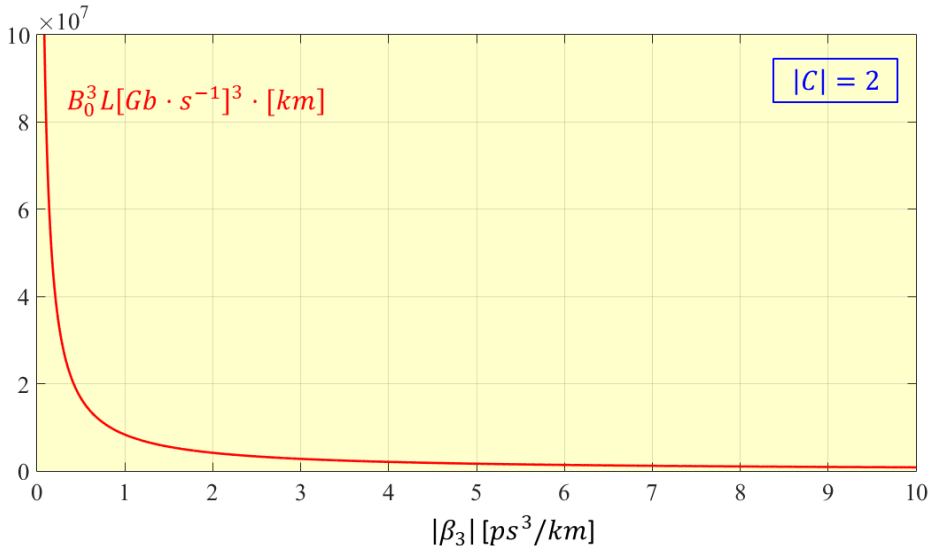

Figure B.6 - Bit-rate cubic product with the length of a given optical fiber for chirped Gaussian pulses with $|C| = 2$, as an instrument to measure the performance of a fiber-optic communication system considering $\beta_2 = 0$. It is possible to see a decay in the performance for higher β_3 values.

Comparing figures (B.5) and (B.6), we observe a decay in the performance of a fiber-optic communication system for the case where $|C| = 2$ in relation to the one where $C = 0$. These figures confirm what we were expecting, which was a better performance for chirped Gaussian pulses whose chirp is null because in the situation of figures (B.5) and (B.6), $\beta_2 = 0$. This is important to have in mind because if $\beta_2 = 0$, it means there is no way to counteract the effects of chirp in the pulse. Since we would need $\beta_2 C < 0$ in order to experience pulse compression, knowing that $\beta_2 = 0$, the chirp that exists in the case of figure (B.6) will mean the pulse will broaden wider throughout its journey inside an optical fiber than the one analyzed in figure (B.5). Once again, we conclude that if $\beta_2 = 0$, using a Gaussian pulse with no chirp to convey information inside an optical fiber will be the best choice. Then, in this case, the common belief would be true which means that having pulses with no chirp would be better.

References

[1] C. R. Paiva, *Fibras Ópticas*, IST, 2016.

[2] G. P. Agrawal, *Fiber-Optic Communication Systems*, 4th Ed. New York: Wiley, 2010.

[3] C. R. Paiva, *Project 2019*, Photonics. IST, 2019.

[4] G. P. Agrawal, *Nonlinear Fiber Optics*, 4th Ed. Boston: Academic Press, 2007.

[5] D. Anderson and M. Lisak, "Propagation characteristics of frequency-chirped super-Gaussian optical pulses", *Optics Letters*, Vol. 11, No. 9, pp. 569-571, September 1986.